Enhancement of HIV vaccine efficacy via lipid nanoparticle-based adjuvants

Melissa C. Hanson
Bachelor of Science, Biomedical Engineering
University of Utah, Salt Lake City, Utah, 2009

Submitted to the Department of Biological Engineering
In Partial Fulfillment of the Requirements for the Degree of

Doctor of Philosophy
at the

Massachusetts Institute of Technology

December 2014 [February 2015]

Signature of Author: Signature redacted
Melissa C. Hanson
Department of Biological Engineering

Certified by: Signature redacted
Professor Darrell J. Irvine
Department of Biological Engineering and Materials Science
Thesis Supervisor

Accepted by: Signature redacted
Forest M. White
Associate Professor of Biological Engineering
Chairman, Graduate Program Committee for Biological Engineering

Members of Thesis Committee

Darrell J. Irvine

Professor of Biological Engineering and Materials Science & Engineering
Massachusetts Institute of Technology
Thesis Advisor

Jianzhu Chen

Professor of Biology
Massachusetts Institute of Technology

K. Dane Wittrup

Professor of Biological Engineering and Chemical Engineering
Massachusetts Institute of Technology
Thesis Committee Chair

Enhancement of HIV vaccine efficacy via lipid nanoparticle-based adjuvants

by
Melissa Hanson

Submitted to the Department of Biological Engineering
On January 8, 2014 in partial fulfillment of the requirements for the degree of
Doctor of Philosophy in Biological Engineering

Adjuvants are immunomodulators and/or formulations/delivery vehicles which enhance immune responses to vaccines. The lack of progress in the development of an HIV humoral vaccine is due, in part, to the absence of available adjuvants which can be sufficiently potent with minimal adverse side effects. The main goal of this thesis was to develop nanoparticles as HIV vaccine adjuvants. Building upon previous work in the Irvine lab, we determined the potency of lipid-coated microparticles was due in part to the *in situ* generation of antigen-displaying liposomes. Synthetic liposomes were nearly as potent as lipid-coated microparticles, but with a 10-fold greater antigen conjugation efficiency. We subsequently optimized unilamellar liposomes as delivery vehicles for surface-displayed HIV antigens. For vaccines with a recombinant gp120 monomer (part of the HIV envelope trimer), immunization at 0 and 6 weeks with 65 nm or 150 nm diameter liposomes with 7.5 pmol gp120 was found to induce strong anti-gp120 titers which competed with the broadly-neutralizing antibody VRC01. The second HIV antigen used was a peptide derived from the membrane proximal external region (MPER) of the gp41 protein. High-titer IgG responses to MPER required the presentation of MPER on liposomes and the inclusion of molecular adjuvants such as monophosphoryl lipid A. Anti-MPER humoral responses were further enhanced optimizing the MPER density to a mean distance of ~10-15 nm between peptides on the liposomes surfaces. Lastly, we explored the adjuvant potential of cyclic dinucleotides (CDNs) with MPER liposome vaccines. Encapsulation of CDN in PEGylated liposomes enhanced its accumulation in draining lymph nodes (dLNs) 15-fold compared to unformulated cyclic dinucleotide. Liposomal CDN robustly induced type I interferon in dLNs, and promoted durable antibody titers comparable to a 30-fold larger dose of unformulated CDN without the systemic toxicity of the latter. This work defines several key properties of liposome formulations that promote durable, high-titer antibody responses against HIV antigens and demonstrates the humoral immunity efficacy of nanoparticulate delivery of cyclic dinucleotides, which is an approach broadly applicable to small molecule immunomodulators of interest for vaccines and immunotherapy.

Thesis Supervisor: Darrell J. Irvine
Title: Professor of Biological Engineering and Materials Science & Engineering

Acknowledgements

It's hard to believe that five years have flown by and that I'm at the end of my graduate work; many people have helped and encouraged me, both scientifically and personally. It is a deep pleasure of mine to be able to acknowledge these contributions here in permanent form.

First and foremost, I would like to thank my thesis advisor, Dr. Darrell Irvine, for your constant support of this work and for your immeasurable patience with me and optimism for my results. I would also like to thank you for doing the hard work of writing grants and managing the laboratory funds. It was a luxury to be able to concentrate solely on the science. By working in your lab, I fulfilled my goal for my PhD, which was to learn how to be a scientist while working to develop an HIV vaccine; thank you for taking me onboard!

Secondly, I would like to thank my committee members, Dr. Jianzhu Chen and Dr. K. Dane Wittrup. You both helped me "see the forest through the trees", so to speak, and your insights and perspectives helped direct my project and prioritize the research goals. In addition, I'd like to thank Dr. Wittrup for your role as my academic advisor in my first year at MIT. Your honesty and openness were of great help as I was looking for an advisor and trying to navigate my first year classes.

I want to extend a huge thank you to Dr. Anna Bershteyn, who supervised my first six months in the Irvine lab and has continued to provide mentorship ever since. I really don't know how to convey how much I appreciate your patience, your teaching, and your kindness. Thank you. I would also like to thank Dr. Jordi Mata-Fink from the Wittrup lab. Your cheerful optimism and thoughtful scientific analysis were huge assets to our project and your encouragement in my early graduate school years were immensely helpful.

There are so many current and former members of the Irvine lab to thank, I could write a thesis alone on all of it. First and foremost, thank you all for your friendship. You've made the Irvine lab a great place to work. Dr. Talar Tokatlian, Chyan-Ying Ke and Dr. Tyson Moyer: thanks for being my liposome vaccine buddies and for having sympathetic ears to my griping and worries. Dr. Greg Szeto: thank you for all of the scientific help and personal advice. Dr. Bonnie Huang: thank you so much for your mentorship. More than anyone, you've challenged me to critically review my own work and your advice at the end of my PhD was invaluable. Dr. Matthias Stephan: Thank you for looking out for me, in your own way.

I also need to thank four key people from the University of Utah. Dr. Patrick Kiser, thank you so very much for you constant support. Dr. Meredith Clark, thank you for all of the scientific training, for encouraging me to go to graduate school, and for your cheerful friendship. Azadeh Poursaid, thank you for being my sister-in-engineering, for remembering

when homework was due, and for going canyoneering! Dr. Greg Owens, thank you for challenging me about my medical school plans and for encouraging me to try out research.

To all of my friends, thank you so much for the encouragement, for listening to tales of bleeding mice, and for tons of fun and laughter over the years. BE-2009, Simmons GRTs, and Martha House – Thank you! Dr. Dana Foarta, Carrie Margulies, and Rebecca Lescarbeau: thank you so much for going through grad school with me and for always lending your ears.

It's impossible to fully thank my family for all of their love and support of the years which helped me get to and then through graduate school. But I will try. Mom, you deserve my first thank you. Thank you for always expecting the best out of me, for teaching me little arithmetic tricks in 2nd grade (I still use them), for answering when I call, and so many more things. Dad, thank you for your steadfast belief in me, for encouraging me to try bioengineering, and for life lessons on long skiing road trips. Uncle Steve, thank you for always making me laugh. To my brothers, Matthew, Garrett, and Alex: thank you for protecting me, for challenging me, and for allowing me to find my own way.

Nicolas, thank you for your love. Thank you for Café 6 teas, for my bike fenders, for correcting my mispronunciations (in French and English), for taking the time to understand my science, for listening to me and for chasing away my doubts. Thank you.

Now finally, I want to say thank you to my team, who has been there "in the trenches" with me day after day: Stephanie Chen, Wuhbet Abraham and Dr. Monica Crespo. Steph, thank you for your cheerful willingness to help, even with the gross stuff. Monica, thank you for being there at the beginning, working on the lipid-coated microparticles. But thank you even more for coming back at the end, and helping us to develop and complete the complicated experiments of the last chapter of this thesis. Most importantly, thank you for your constant friendship throughout the whole process. Wuhbet, you have become a second mother to me. Thank you for questioning me, for your absolute faith in me, and for the years of hard work that are now summed up as chapters 3 and 4.

Table of Contents

List of Figures

1. Background and scope of thesis

1.1. Necessity of HIV vaccine adjuvant development

In 2012, it was estimated that 35.3 million people were living with HIV, 2.3 million people became newly infected, and 1.6 million people died of HIV[1,2]. Although antiretroviral therapy has significantly extended the life expectancy of HIV-infected individuals, it is prohibitively expensive in sub-Saharan Africa and other developing regions. Despite the increased availability of antiretroviral therapy in developing countries in the last decade, only 7.6 million of the 21.2 million of those in need of antiretroviral therapy are actually are receiving antiretroviral therapy in Africa[3]. The lack of curative treatment options and the economic, societal, and personal destruction caused by the HIV epidemic makes it imperative that a prophylactic method to prevent HIV infection be developed.

Since the development of the smallpox vaccine by Edward Jenner in the 1790s, vaccines have revolutionized global health, decreasing infant and childhood mortality from diseases such as smallpox, polio, measles, and diphtheria. The large-scale development and implementation of vaccines is considered by the US Center for Disease Control to be the greatest public health achievement of the twentieth century[4]. In addition, the cost-effectiveness of vaccination is indisputable[5,6]. In comparison to other HIV prophylactics such as microbicides, abstinence & monogamy, or condoms, vaccines also do not require any long-term user adherence or lifestyle change in order to be effective. Hence, development of an HIV vaccine is a major goal of the global health community[7].

Although HIV vaccine research has been ongoing for more than 25 years, the scientific community has failed thus far to develop a protective vaccine due to several biological hurdles unique to HIV[7–9]. These factors include the high mutation rate of HIV replication, which results in extraordinary antigenic diversity, as well as the rapid development of a latent reservoir of HIV-infected cells and the fact that HIV infects $CD4^+$ T-cells, which are critical for development of adaptive immune responses[10,11]. HIV vaccine concepts typically fall into one of two approaches, with goals of generating either cytotoxic T lymphocytes (CTLs) or neutralizing antibodies against HIV[10]. Hypothetically, in a CTL-based approach, memory T-cells induced by vaccination rapidly expand after HIV infection and the subsequently produced CTLs kill virus-infected cells. Although a CTL based vaccine could kill infected cells, it wouldn't prevent the initial infection. Complete protection from viral infection is mediated by the elicitation of neutralizing antibodies; these antibodies are the body's primary defense against an infection. Neutralizing antibodies act by opsonizing viral particles and inducing complement activation and viral clearance before cellular infection can be established. In addition, at mucosal surfaces, neutralizing antibodies block entry of the virus into the tissue.

Based on studies in large animal models, induction of high and durable levels of broadly neutralizing antibody (BNAbs) should provide sterilizing immunity against HIV[12], although thus far, strategies to induce such antibodies by vaccination remain elusive[13].

Antibodies that neutralize a diverse array of HIV-1 strains, known as broadly neutralizing Abs (BNAbs), are very rare, but have been isolated from HIV-1 infected patients. These antibodies react against the HIV envelope at the membrane proximal external region (MPER) of gp41 (2F5, 4E10, Z13E1), the gp120 CD4-binding site (B12, VRC01, VRC02), a complex of glycans on the surface of gp120 (2G12), or a set of variable loops of gp120 trimer (PG9 and PG16)[14–21]. A successful humoral vaccine against HIV will need to generate antibodies similar to these patient-isolated antibodies, and therefore, both gp41 and gp120 have been the subjects of considerable study as model antigens for an HIV vaccine. Unfortunately, a BNAb-inducing antigen has not been elucidated due to several factors, including the highly variable nature of HIV, low density of Env protein trimers on each viral particle, the heavy glycosylation of the HIV envelope, and the masking of vulnerable epitopes either by glycosylation, virion lipids, or by conformation[11,22]. All currently identified broadly neutralizing antibodies arise only after several years of infection and are typically highly mutated from germline antibodies; this is indicative of the highly variant nature of the virus, forcing the immune system to constantly try and develop new antibodies against the viral escape mutants[21,23–25]. These findings suggest that a vaccine platform which encourages somatic hypermutation may be critical for the development of antibodies capable of neutralizing the HIV virus.

As a member of both the Ragon Institute and the Collaboration for AIDS Vaccine Discovery, the Irvine lab is fortunate to have access to some of the most-promising gp120 and gp41-based antigens currently in development. However, it is becoming apparent that even the most sophisticated HIV envelope protein antigen designs will be unable to generate sufficiently high titers of neutralizing antibodies and memory B-cell levels. All of the HIV vaccines tested thus far in humans elicit only short-lived antibody responses, exhibiting half-lives of roughly eight weeks[23]. Therefore, it is imperative that vaccine platforms be developed to help translate the antigenicity of current protein constructs into immunogenicity which results in long-lasting titers of neutralizing antibodies.

1.2. Conventional vaccines and adjuvants

The development of structure-based vaccinology employing well-defined subunit antigens has enabled the development of vaccines with excellent safety profiles, but this increase in safety has been accompanied by a decrease in immunogenicity compared to traditional live attenuated vaccines. This lack of immunogenicity is mainly because induction of the adaptive immune response is dependent on the initial activation of the innate immune system, which is triggered by danger signals not present on engineered antigens. These signal include pathogen-

associated molecular patterns (PAMPs) which are recognized by the pattern-recognition receptors (PRRs) of innate immune cells, however the links between innate and adaptive immunity are still not fully understood[26–28]. An adjuvant can be defined as a substance that enhances the body's immune response to an antigen; adjuvants have become critical components of subunit vaccines.

Traditionally, adjuvants were broadly separated into immunopotentiators (agonists of PRRs, saponins, cytokines, bacterial toxins) and vehicles/delivery systems (aluminum salts, oil-in-water emulsions, virus-like particles (VLPs), and liposomes)[29–31]. As our understanding of the mechanisms of action for adjuvants has expanded, this separation has merged into spectrum, varying from purely delivery-based adjuvants to purely immunostimulatory adjuvants, as summarized in schematic 1-1[32].

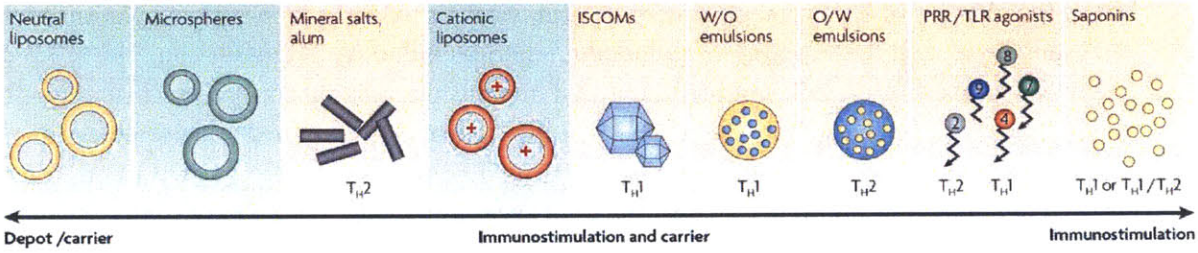

Schematic 1-1. Classification of adjuvants with respect to their depot/carrier and immunostimulatory properties.

ISCOMs: immunostimulating complexes; W/O: water-in-oil emulsion; O/W: oil-in-water emulsion; PRR: Pattern-recognition receptor; TLR: Toll-like recptor; T_H1/T_H2: T helper 1- or 2- biased responses. Adapted from [32].

Traditional adjuvants such as aluminum salts and water/oil emulsions have set the standard for safety and efficacy in vaccine development but fail to elicit effective immune responses to many candidate antigens, and diverse new adjuvant formulations have been pursued in both academic and industrial vaccine research[33]. Alum is an aluminum salt-based adjuvant currently in use for human vaccines against diphtheria, tetanus, Hepatitis B and Hepatitis A, to name a few[29]. Unfortunately, it is incapable of inducing long-lived humoral responses against HIV envelope antigens[34]. While water-in-oil emulsions are considered too toxic for prophylactic use in humans[35], oil-in-water emulsion have a better safety profile and have been licensed for several vaccines (MF59 by Novartis and AS03 by GSK)[36].

Toll-like receptors (TLRs) were the first set of PRRs to be identified and they are subsequently the most well characterized set as well. Currently, 10 functional human and 12 functional mouse TLRs have been identified in total. TLRs are transmembrane proteins, expressed by innate immune cells, which contain an ectodomain to recognize PAMPs as well as a cytosolic Toll-IL-1 receptor (TIR) domain to initiate downstream signaling. TLRs

recognize a variety of PAMPs from bacteria, mycobacteria, parasites, fungi, and viruses. PAMPs recognized by TLRs include lipopolysaccharide (TLR-4), flagellin (TLR-5), cytosine-guanine dinucleotide DNA (TLR-9), single-stranded RNA (TLR-7,-8), double stranded RNA (TLR-3), and lipopeptides (TLR-1,-2,-6)[37]. After recognition of their respective PAMPS, TLRs initiate signaling cascades through TIR-containing adaptor proteins such as MyD88 and TRIF. These signaling cascases, as summarized in schematic 1-2, result in the secretion of inflammatory cytokines and type 1 interferon, which induces innate immune responses such as neutrophil recruitment and macrophage activation as well as the maturation of dendritic cells (which is a key step in initiating adaptive immunity)[37].

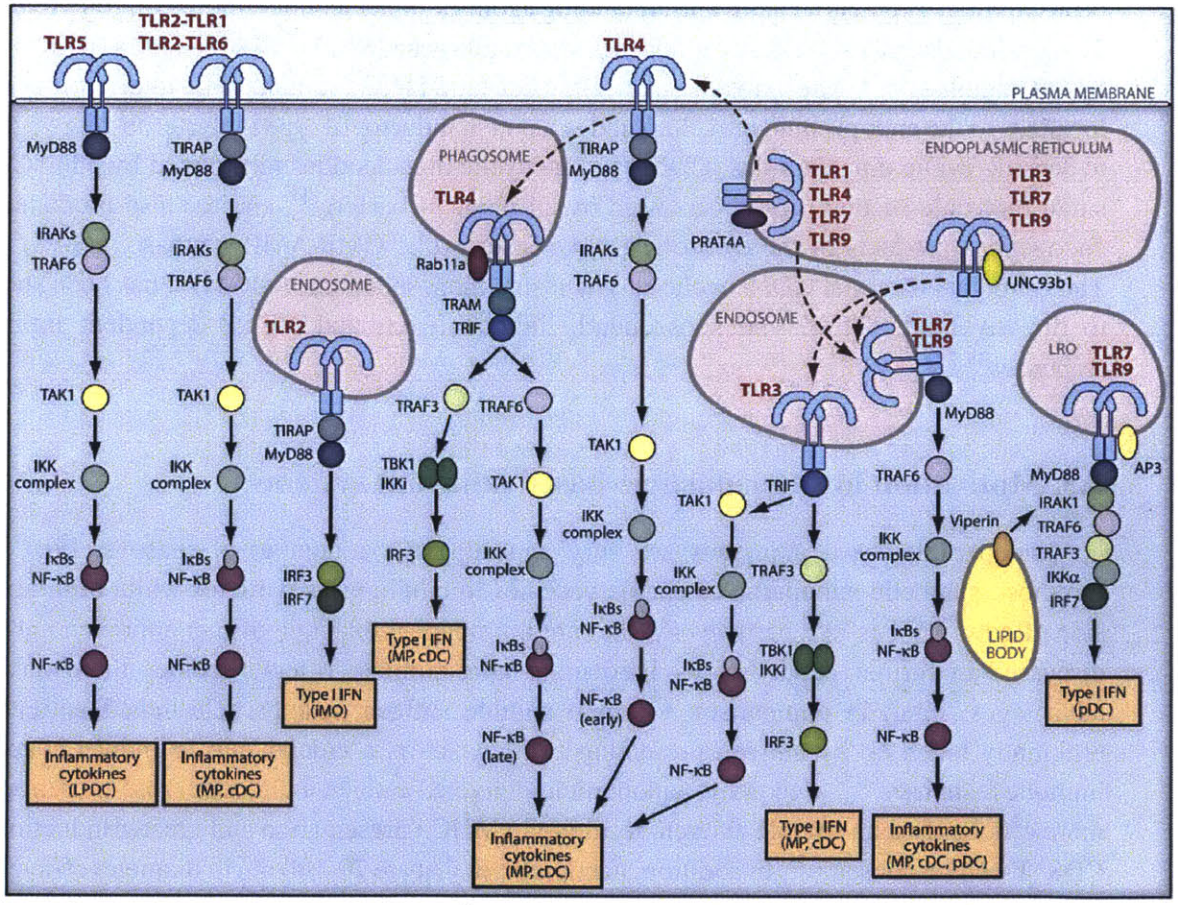

Schematic 1-2. TLR trafficking and signaling.

Illustration of the location of TLR receptors and their signaling pathways. TLRs 1, 2, 4, 5 & 6 are expressed on the cell-surface while TLRs 3, 7, 8, & 9 are localized to intracellular vesicles. Recognition of respective PAMP by a TLR induces TIR-dependent signaling cascades which culminate in type 1 interferon expression (TLRs 2, 3, 4, 7, 8 & 9) and/or inflammatory cytokine secretion (TLRs 1, 2, 4, 5, 6, 7, 8 & 9.) Adapted from [37].

Adjuvants developed for TLRs include monophosphoryl lipid A (MPLA), CpG ODN, R848, Poly I:C, and Pam3Cys; these are agonists to TLR 4, 9, 7 and 8, and 1,2 and 6, respectively[38]. At present, MPLA is the only agonist licensed for human use[39]. TLR adjuvants have been applied to HIV vaccine development in mice and non-human primate studies, with an improvement in immune responses over non-adjuvanted controls, however they will probably require additional adjuvant help via a delivery system[38]. Indeed, in the Irvine lab, TLR-agonists with soluble antigen generate very weak immune responses in comparison to TLR-agonists loaded onto particulate delivery systems[40,41].

In addition to TLR agonists, in recent years other small molecule immunomodulators have been explored as potential adjuvants, including agonists of nucleotide-binding oligomerization domain-like receptors (NLRs), retinoic acid-inducible gene (RIG)-1-like receptors (RLRs) and STING agonists[42,43]. The cytosolic nucleotide sensor STING (stimulator of interferon genes) localizes to the endoplasmic reticulum and is a potent inductor of type I interferons in response to sensing cyclic dinucleotides (CDNs)[42]. The cyclic dinucleotides recognized by STING are small molecule second messengers used by all phyla of bacteria[44], and are also produced as endogenous products of the cytosolic DNA sensor cyclic GMP-AMP synthase (cGAS)[45–47]. The canonical bacterial CDN, cyclic-di-guanosine monosphophate (cdGMP), has been shown to directly bind STING and subsequently initiate IRF3- and NF-κB-dependent immune responses[48–50].

1.3. Motivation for nanoparticle-based adjuvant systems

Nanoparticle-based adjuvants are very appealing for a number of reasons. First and foremost, synthetic nanoparticles enable vaccines to mimic virus particles while minimizing side effects[51]. Virus-like particles (VLPs) are a prominent example of this approach and are discussed in further depth below. Particulate viral-mimicry offers vaccines three distinct advantages. First, in comparison to small soluble antigen, nanoparticle-linked antigen is efficiently taken up by antigen presenting cells, which is a crucial step to induce adaptive immune responses[51,52]. Secondly, nanoparticle-delivered antigen undergoes cross-presentation more efficiently than soluble antigen, resulting in MHC I presentation and greater induction of $CD8^+$ T-cell responses[52,53]. In addition, nanoparticles that are 20-100 nm in diameter efficiently enter the lymphatic system in free form, without requiring specialized transportation via dendritic cells [54]. Free draining of vaccine to the lymph node enables antigen to directly interact with B-cells, which generates potent immune responses[51]. In addition, by surface-displaying antigens on the surfaces of particulate carriers such as liposomes or polymer particles, antigen delivery can be modulated at the single-cell level. Surface display has been shown to enhance immune responses, likely by increasing the degree of B-cell receptor crosslinking and subsequent B-cell activation[55–61].

In addition to the viral mimicry benefits, there are several additional motivations that nanoparticles offer. In particular, nanoparticles serve not only as adjuvants, but as platforms which can be further engineered. The prime example of this is the inclusion of TLR-agonist adjuvants on nanoparticles to additionally enhance the immune responses[40,41,62]. Secondly, certain nanoparticle formulations, such as lipid-coated PLGA particles, generate sustained levels of serum IgG antibodies at very low doses (10 ng of ovalbumin) of antigen[40]. Conversely, vaccines adjuvanted with TLR agonist and alum at such low antigen doses fail to generate immune responses. Potency at such low doses strongly suggests the potential of nanoparticles as vaccine adjuvants.

Virus-like particles, as mentioned above, are an excellent example of the viral mimicry benefits that nanoparticles may offer. VLPs consist of antigen-functionalized viral capsid components which self-assemble into nanoparticles that induce both innate and adaptive immune responses[63]. Virosomes—which are semi-synthetic virus-like particles—are in use in several non-American markets for hepatitis A and influenza vaccines and the VLP-based vaccine Gardasil® is FDA-approved for prevention of human papillomavirus infection[64,65]. In addition to their uptake by APCs and efficient drainage to lymph nodes, surface display of antigen on VLPs is attributed to greater degrees of B-cell receptor crosslinking and subsequent B-cell activation[55]. Virus-like particles have been developed for delivery of gp120 antigens, albeit without sufficient immunogenicity, which may be attributed to the low rate of gp120 incorporation into VLPs and thus work is ongoing to increase this incorporation efficiency[66,67]. In addition to the low immunogenicity of VLPs for HIV antigens, designing VLPs is a non-trivial process which can make varying the antigen-of-study cumbersome.

Although many different nanoparticles have been developed for drug and vaccine delivery, liposomes are a particularly attractive option. Effective yet safe, liposomes have been recognized for more than 35 years for their potential as immunological adjuvants[68]. Non-toxic themselves, liposomes are efficacious by presenting antigen in particulate form, which prolongs antigen half life[69]. In addition, small unilamellar liposomes (40-150 nm) are excellent virus-mimics in terms of APC uptake, cross-presentation, and lymphatic draining. Liposomal antigen may either be encapsulated or surface-displayed, the latter of which is achieved either by specific chemical linkage, non-specific adsorption by electrostatic interactions, or the inclusion of a hydrophilic tail. During liposome formation, antigen with a hydrophilic tail will insert itself into the phospholipid bilayer. Cell-targeting of lipids can be achieved by inclusion in the lipid bilayer of antibodies to specific cell receptors[70]. Liposomes also confer the ability to deliver both hydrophobic molecules (in the lipid bilayer) and hydrophilic molecules (encapsulated or surface-displayed). A major benefit of liposomes is their elimination of MPLA's solubility issues. MPLA is a lipopolysaccharide-derived TLR-4 agonist and a potent inducer of both humoral and cellular immunity, however, it is prone to aggregation with

decreases its bioavailability. Inclusion of MPLA in the lipid bilayer of liposomes eliminates aggregation events while maintaining its adjuvant abilities[29].

There are several liposomal vaccines currently approved or in development. A lyophilized liposomal formulation, Stimuvax®, is currently being investigated for treatment of non-small cell lung cancer[64]. The liposomal adjuvant AS01, developed by GlaxoSmithKline, consists of liposomes with MPLA and QS21 (a saponin) and is in development as an adjuvant for a malaria vaccine. In Phase III trials, AS01 elicited high antibody titers and prevented a substantial number of malaria cases[71,72]. AS01 is also in development as an HIV vaccine adjuvant. A phase I clinical trial indicated superior $CD4^+$ T-cell activation in the AS01 group over the two other adjuvants used, $AS02_V$ and $AS02_A$ (oil-in-water emulsions)[73].

As discussed in Chapter 1.1, the membrane proximal external region of gp41 (MPER) is actively being pursued as a possible HIV antigen because of the isolation of broadly neutralizing antibodies which bind to it. A key element to consider when designing MPER-based vaccines is that MPER is closely associated with the HIV virion lipid membrane and this lipid membrane association holds MPER in a conformation which may be essential to elicit broadly neutralizing antibodies like 2F5 and 4E10[74]. Surface display of MPER on liposomes is a simple and effective method to maintain the lipid-specific confirmation of 2F5/4E10-binding liposomes.

Stealth liposomes are liposomes whose surfaces are shielded by poly(ethylene glycol); they were originally developed to extend the half-life of drug-loaded liposomes after intravenous injection to improve drug delivery to tumor sites[69]. Application of PEGylated liposomes as vaccine adjuvants is less common. For CTL-based vaccine approaches, stealth liposomes with encapsulated antigen have been shown to both decrease and enhance $CD8^+$ T-cell activation in comparison to non-PEGylated liposomes[75–77]. In a humoral-based vaccine study, 20kDa PEGylated liposomes were used for delivery of surface-displayed gp41 and induced higher immune responses than non-PEGylated liposomes, although this was not maintained over time[78]. The effect of PEGylation on humoral immune responses against MPER is explored in Chapter 4.

Despite the well-established adjuvant properties of liposomes, there is no clearly defined optimal liposome composition. This lack of clarity is due in part to the vast array of liposomal vaccine strategies. Indeed, the numerous options in lipid composition, size, membrane fluidity and surface charge, immunization route, immunization schedule, adjuvant/small molecule inclusion, and antigen loading strategies, as well as the choice of antigen itself, manifests in the limitation that currently only general assumptions can be inferred from the literature. To mitigate these current limitations, chapters 3 and 4 systematically study liposomes to design the optimal liposome-based HIV vaccine

adjuvant/delivery vehicle for both a model HIV peptide antigen (MPER) and a model HIV protein antigen (gp120).

1.4.Scope and outline of thesis

In this thesis, we designed lipid particles loaded with immunomodulators as adjuvant/delivery systems for surface-displayed HIV antigens. After a comparison of synthetic unilamellar liposomes with lipid-coated microparticles which generate liposomes *in situ*, synthesis liposomes were chosen as the delivery vehicle of two HIV immunogens: a peptide (MPER) derived from the gp41 protein and an engineered recombinant gp120 protein. The adjuvant capabilities of nanoparticle-loaded immunomodulators was explored, particularly with the STING agonist cyclic-di-GMP.

Chapter 2 describes the work with lipid-coated microparticles from which the rest of this thesis evolved from. Lipid-coated poly(lactide-*co*-glycolide) microparticles (LCMPs) consist of a solid polymer core wrapped by a surface lipid bilayer and previous studies demonstrated LCMPs elicit potent humoral immune responses in mice. Here we characterized the spontaneous delamination of the lipid envelope and subsequent *in situ* production of antigen-displaying liposomes. We then compared the immunogenicity profiles of LCMPs, bilayer-stabilized LCMPs and synthetic liposomes.

Chapter 3 was done in collaboration of Dr. Jordi Mata-Fink, who designed a recombinant gp120 monomer as an HIV antigen. In this chapter, we explored the immunogenicity profile of this gp120 construct with respect to display on liposomes or formulated in aluminum salt- or emulsion-based adjuvants. Furthermore, we optimized formulation and vaccination parameters to enhance anti-gp120 antibody responses.

In Chapter 4 we systematically explored how the structure and composition of liposomes displaying MPER peptides impacts the strength and durability of humoral responses to this antigen as well as helper T-cell responses in mice. We compared liposomes to traditional adjuvant delivery systems. To characterize the impact of density of a surface-displayed antigen, we determined anti-vaccine responses as a function of the number of MPER peptides per liposome. We then explored the how size, PEGylation, and composition of liposomes impacts immunogenicity. $CD4^+$ T-helper peptides were included in the vaccines to provide $CD4^+$ T-cell help and we thus systematically explored how various methods of T-helper peptide delivery impacted humoral immunogenicity.

Chapter 5 explores the adjuvant capability of STING agonists (cyclic dinucleotides (CDNs)) when encapsulated in PEGylated liposomes and co-delivered with MPER liposomes.

We determined the kinetics of drainage to the lymphatic system or blood stream, the kinetics of activation of lymph node antigen-presenting cells, and the impact on humoral immune responses for both soluble and nanoparticulate CDN. Furthermore, we explored the dependence of CDN-induced responses on the presence of plasmacytoid dendritic cells, TNF-α signaling, and type I interferon signaling.

Chapter 6 provides an overall summary and the broad conclusions of this thesis work as well as possible future directions. Chapter 7 details several key methods which were developed in for this work, as well as supplemental data. Chapter 8 is a bibliography of the literature cited in this thesis.

2. *In situ* vesicle shedding mediates antigen delivery by lipid-coated

2.1. Introduction

Subunit antigen vaccines have increased safety but decreased potency profiles in comparison to traditional live attenuated microbe vaccines. To increase the immunogenicity of subunit vaccines, adjuvants thus play an important role in vaccine development. As discussed in Chapter 1.2, adjuvants are materials that enhance immune responses elicited by vaccines either by providing inflammatory signals (e.g., ligands for Toll-like receptors[79]), modulating the delivery of antigen to immune cells, or both[32]. For example, antigen delivery can be altered by providing a depot for long-term antigen release from a vaccination site. Long-term biomolecule release is often achieved by encapsulation of the cargo into a biodegradable polymer matrix, such as poly(lactide-co-glycolide) (PLGA), which is often employed due to its history of safe use in humans, efficient encapsulation of hydrophobic materials and tunable drug release behavior[80]. However, delivery of protein antigens encapsulated in PLGA micro- or nano-particles is challenging due to low antigen encapsulation efficiency and denaturation/aggregation of proteins during encapsulation and release[81–83]. Surface-display of antigen on a lipid bilayer is an attractive alternative to encapsulation PLGA as it enhances immune responses and can be readily achieved by chemically linking the antigen to lipids containing reactive groups. For example, phospholipid headgroups functionalized with maleimide can readily link to cysteine-containing antigens. Furthermore, incorporation into lipid particles has previously been shown to be an effective delivery method of lipophilic adjuvants such as MPLA[84,85]. Despite the disadvantages of degradable polymers for use with protein antigen, these polymers remain attractive for the slow-release co-delivery of inflammatory adjuvant compounds that could shape the immune response over time[86–89].

In order to combine surface-display of antigen with a biodegradable core in which we could ultimately co-deliver additional adjuvant molecules, in work led by Dr. Anna Bershteyn, we previously described an approach for synthesis of lipid-enveloped polymer microparticles and nanoparticles that present antigen bound to a surface lipid bilayer[90]. A self-assembled lipid-bilayer coat surrounding a PLGA core was achieved by using lipids as the surfactant component of an emulsion/solvent evaporation-based PLGA particle synthesis. The lipid bilayer was observed to be a two-dimensionally fluid surface that tightly envelops the polymer core. We employed these lipid-coated microparticles (LCMPs) as vaccine delivery agents by conjugating protein antigens to PEGylated lipids anchored in the bilayer coating, and co-incorporating adjuvant compounds such as the TLR agonist monophosphoryl lipid A (MPLA) or α-galactosyl ceramide in the particles, LCMPs elicited high, durable humoral immune responses in response to injection of as little as 2.5 ng of the model antigen ovalbumin (OVA) surfaced-displayed on LCMPs[40]. In addition, these particles triggered antigen-specific

proliferation of both $CD4^+$ and $CD8^+$ T-cells and production of Th1-biased cytokines from T-cells *in vivo*[40]. When formulated as nanoparticles and functionalized with a candidate malaria antigen VMP0001 and MPLA, LCMPs were shown to induce germinal center formation and elicited higher, more durable antigen-specific titers IgG antibodies of diverse isotypes compared to vaccination with soluble VMP001 and MPLA[91].

Despite the efficacious nature of these lipid-coated particles, it was unclear how they presented antigen to the immune system, particularly in the case of LCMPs, because these microparticles (diameter: 2.6 ± 1.2 μm) did not freely drain to lymph nodes [92]. However, during initial cryo-TEM characterization studies on the LCMPs, we observed that over time, lipid bilayers at the surface of the biodegradable particles begin to delaminate from the polymer core[90]. This observation of delamination suggested that the lipid bilayer might not be stable on the PLGA particle cores over time. Since antigen was conjugated to the lipid bilayer, we hypothesized that delamination of the lipid envelope could play a role in the adjuvant characteristics of LCMPs.

In this chapter, we directly evaluated the stability of the bilayer coating of LCMPs and examined the role of bilayer delamination in the immunogenicity of this particulate vaccine system. We found that under physiological conditions, LCMPs exhibit rapid bilayer delamination, leading to the release of antigen-bearing lipid vesicles. We evaluated the kinetics of bilayer shedding and the resulting effects on the immunogenicity of LCMPs *in vivo*. In addition, we explored the kinetic dependence of lipid delamination on the presence of lipid/serum in the surrounding environment. To test the hypothesis that delamination impacts immunogenicity, stabilized-bilayer LCMPs were developed either by the inclusion in the lipid bilayer of cholesterol or lipids with saturated carbon chains. Mice immunized with OVA-LCMPs generated higher anti-OVA titers than mice immunized with stabilized-bilayer OVA-LCMPs or OVA on delaminated lipid vesicles (DLVs) alone. These results suggest that the *in situ* release of delaminated lipid vesicles enhances humoral immune responses to surface-displayed antigen, with LCMPs acting as a source of *in situ*-generated antigen-bearing liposomes following injection. The majority of this work has been published in a first author publication, *Biomacromolecules (2014);15(7):2475-81*[93].

2.2. Materials and Methods

2.2.1. Materials

All lipids—1,2-dioleoyl-sn-glycero-3-phosphocholine (DOPC), 1,2-dioleoyl-sn-glycero-3-phoshpo-(1'-rac-gylcerol) (DOPG), 1,2, distearoyl-sn-glycero-3-phosphocholine (DSPC), 1,2 distearoyl-sn-glycero-3-phosphoethanolamine-N-[maleimide(polyethylene glycol)2000]

(DSPE-PEG2K-maleimide), 1,2-dioleoyl-sn-glycero-3-phosphoethanolamine-N-(lissamine rhodamine B sulfonyl) (14:0 Liss-Rhod-DOPE), 1,2-distearoyl-sn-glycero-3-phospohethanolamine-N-(7-nitro-2-1,3-benzoxadiazol-4-yl) (NBD-DSPE) and cholesterol—were purchased from Avanti Polar Lipids (Alabaster, Alabama). Poly(lactic-co-glycolic acid) (PLGA) with a 50:50 ratio of lactic acid and glycolic acid and an inherent viscosity of 0.42 dL/G was purchased from Evonik Corporation (Birmingham, Alabama). Monophosphoryl lipid A (MPLA,from *Salmonella enterica* serotype minnesota Re 595 cat. no. L6895) and solvents were purchased from Sigma Aldrich (St. Louis, Missouri). n-succinimidyl s-acetyl(thiotetraethylene glycol) (SAT(PEG)$_4$) was purchased from Pierce Biotechnology (Rockford, Illinois). Purified ovalbumin (OVA) was purchased from Worthington Biochemical (Lakewood, New Jersey) and subsequently passed through detoxi-gel endotoxin removing columns (Pierce Biotechnology, Rockford, Illinois) to remove any trace endotoxin.

2.2.2. Synthesis of lipid-coated particles and liposomes

Microparticles consisting of a PLGA core and lipid bilayer envelope were synthesized as previously reported.[40,90] Briefly, 5mg of lipid in a 72:18:10 DOPC:DOPG:DSPE-PEG2K-maleimide molar ratio (for DOPC-LCMPs) or a 75:16:9 DSPC:DOPG:DSPE-PEG2K-maleimide molar ratio (for DSPC-LCMPs) was dried under nitrogen followed by incubation under vacuum at 25°C for 18 hr. The resulting lipid film was dissolved in dichloromethane (DCM) containing PLGA for a final polymer:lipid weight ratio of 16:1. This organic solution was emulsified into distilled deionized ultrapure water by homogenization at a ratio of 8:1 aqueous phase:organic phase and stirred for 12 hr at 25°C to remove DCM by evaporation and passed through a 40 μm filter. Microparticles were isolated from the resulting polydisperse samples by two centrifugation steps at 1,100 RCF for 1 min each, with removal of the supernatant and resuspension into pH 7.4 PBS following each centrifugation step. Particle size distributions were determined using the Horiba Partica LA-950V2 Laser Diffraction Particle Size Analysis System.

Liposomes prepared with a 72:18:10 molar ratio of DOPC:DOPG:DSPE-PEG2K-maleimide were used for immunization studies and vesicles with an 80:20 molar ratio of DOPC:DOPG were used for *in vitro* lipid delamination studies. Lipid films dried as described above were resuspended in pH 7.4 PBS, vortexed for 30 seconds every 10 min for 1 hr, subjected to 6 freeze-thaw cycles in liquid nitrogen and a 37°C water bath, and extruded for 21 passes through a 200 nm pore polycarbonate membrane (Whatman Inc, Sanford, Maine). Vesicle sizes were determined by dynamic light scattering. (Brookhavenn 90Plus Particle Size Analyzer, Worcetershire, UK). Liposomes were stored at 4°C until use.

2.2.3. Antigen conjugation onto lipid-enveloped particles and liposomes

Thiolated ovalbumin was conjugated to the surface of maleimide-functionalized lipid-enveloped particles or liposomes as previously described[40]. In brief, endotoxin-free ovalbumin

was functionalized with the heterobifunctional cross-linker $SAT(PEG)_4$ (Pierce Biotechnology, Rockford, Illinois), which was then deacetylated to expose sulfhydryl groups following the manufacturer's instructions. Following buffer exchange into 10 mM EDTA (pH=7.4), via 7000 mwco Zeba spin desalting columns (Pierce Biotechnology, Rockford, Illinois), thiolated OVA (5 mg/mL) was incubated with particles (70 mg/mL) or liposomes (3 mg/mL) at 25°C for 4 hr (for particles) or overnight (for liposomes). To remove unbound antigen, particles were washed three times by centrifugation for 5 min at 10,000 rcf with pH 7.4 PBS and liposomes were washed three times by centrifugation in 30 KDa MWCO Vivaspin columns (Vivaproducts, Littleton, Massachusetts). The amount of OVA coupled was determined by solubilizing lipids from the particles/vesicles in 30 mM Triton-X100 and measuring the quantity of OVA by enzyme-linked immunosorbent assay (ELISA). Particles and liposomes were stored at 4°C until use, which was within 4 hours for immunization experiments and 48 hours for *in vitro* experiments.

2.2.4. Analysis of lipid delamination from LCMPs

Particles were synthesized as described above, incorporating 2 mole % of 14:0 Rhod-DOPE (for DOPC-LCMPs) or NBD-DSPE (for DSPC-LCMPs) in the lipid composition. For characterization of the delamination of protein antigen displayed on the lipid envelope, OVA was conjugated to lipid-enveloped particles as described above. Post-synthesis, particles were washed 3 times by centrifugation at 5,000 r.c.f. for 5 minutes and subsequent suspension in pH 7.4 PBS. After the third wash, particles were suspended at 12 mg/mL in pH 7.4 PBS, fetal bovine serum, or 10 mM 80:20 DOPC:DOPG liposomes in pH 7.4 PBS, divided into 150 uL aliquots in separate eppendorf tubes for each time point/replicate and incubated with rotation at 37°C. At each time point, replicate aliquots were centrifuged for 20 min at 16,100 r.c.f. and the resulting supernatant collected for analysis. Lipid release from the LCMPs was determined by adding 30 mM Triton-X100 to the supernatants, measuring rhod-DOPE fluorescence in a fluorescence plate reader (Tecan Infinite M200 Pro, Männedorf, Switzerland), and normalized to the total amount of fluorescent lipid present. OVA released from particles was determined by anti-ovalbumin ELISA on the supernatants of the particle aliquots and normalized to the total amount of OVA-lipid present. This total amount of lipid per aliquot was determined in fluorescently-tagged samples by addition of Triton to three or four standard aliquots, incubated at 55°C and subsequently vortexed and sonicated for 1 min each prior to centrifugation for 15 min at 16,100 r.c.f. and fluorescent-based quantification of the supernatant. To determine the total amount of the antigen, ovalbumin, released from DOPC-LCMPs particles, the same procedure as above was employed minus the 55°C incubation step and with ELISA-based quantification. The 55°C incubation step is unnecessary for lipid delamination from DOPC-LCMPs and therefore was omitted to prevent any degradation of the ovalbumin protein.

2.2.5. Size characterization of delaminated lipid vesicles

DOPC-LCMPs were prepared and incubated at 37°C in pH 7.4 PBS for 7 days, after which the microparticles were pelleted via a 30 minute centrifugation step at 16,100 r.c.f. The size distribution of DLVs in the supernatant was determined by laser diffraction as described above.

2.2.6. In vivo immunization studies

All animal experiments were conducted under an IUCAC-approved protocol in accordance with local, state, and NIH animal care and use guidelines. Immunizations were carried out on female BALB/c mice, 6-7 weeks of age, purchased from Jackson Laboratories. Immediately prior to immunization, 1.3 μg of the TLR-4 agonist MPLA per 50 μL was mixed with 10 ng OVA conjugated to LCMPs, DLVs, or liposomes in sterile pH 7.4 PBS, following post-synthesis insertion techniques described previously [40,94]. Mice were immunized by injection of 50 μL solutions s.c. at the tail base, and boosted 14 days later. Serum samples were collected on a weekly basis for analysis of serum antibody titers.

2.2.7. Antibody titer analysis

Serum total IgG titers, isotype IgG_1 and IgG_{2A} titers, and avidity indices were determined as previously described.[40] Briefly, 96-well plates were coated with OVA and blocked with bovine serum albumin, then incubated with serially diluted serum and detected with HRP-labeled anti-mouse IgG, IgG_1 or IgG_{2A} (Bio-Rad), followed by development and measurement of optical absorbance at 450 nm. Antibody titer is reported as reciprocal serum dilution at an absorbance of 0.5. For avidity indices, duplicate serum dilutions were prepared for each sample and for one set of dilutions, wells were incubated for 10 min with 6 M urea prior to detection with the respective anti-mouse secondary antibody. The avidity index is reported as the ratio of the titers of the urea treated sample to the non-urea treated sample.

2.2.8. Statistical analysis

Statistical analyses were performed using GraphPad Prism software. Comparisons of formulations over time were performed using two-way ANOVA tests and comparisons of multiple formulations at a single time point were performed using one-way ANOVA tests. Two-tailed unpaired t-tests were used to determine statistical significance between two experimental groups for all other data.

2.3. Results and Discussion

2.3.1. Delamination kinetics of lipid-coated microparticles

We previously reported that phospholipids incorporated into PLGA particles during an emulsion/solvent evaporation synthesis segregate to the surface of nascent particles, self-assembling into a lipid envelope surrounding the polymer core (Fig. 2-1A). When these particles were incubated in pH 7.4 PBS at 37°C for 7 days to permit partial hydrolysis of the biodegradable particle core, cryoTEM imaging revealed evidence of delamination of lipid bilayers from the particle surfaces, which was observed even in the absence of added MPLA, suggesting that adjuvant incorporation did not induce this effect[90]. This finding suggested that lipids might be shed from LCMPs by "budding" of lipid bilayers from the particles over time (Fig. 2-1A). This might be particularly promoted *in vivo*, since serum albumin and lipoproteins are known to extract lipid from fluid bilayers[95–97]. To directly test this hypothesis, LCMPs with a diameter of 2.54±0.95 μm (Fig. 2-1B) were incubated in PBS at 37°C for one week. After this incubation time, the PLGA particle cores were still macroscopically intact[90], and the size distribution of the particles recovered by centrifugation were essentially unchanged from the starting material (data not shown). However, analysis of the supernatant by laser diffraction to detect released lipid vesicles revealed nanoparticles with a mean size of 176±6 nm in the LCMP supernatants (Fig. 2-1C). These particles were not PLGA fragments, as neat PLGA nanoparticles of this size prepared independently were pelleted by the centrifugation step used to remove LCMPs from the sups in this experiment. To verify that these nanoparticles in the LCMP supernatant were in fact lipid vesicles, we prepared particles containing a rhodamine-tagged lipid tracer in the bilayer coating. Fluorescence measurements on the supernatant collected from LCMPs incubated 7 days in PBS at 37°C showed the release of 54±11% of the total lipid tracer into the supernatant, confirming the release of delaminated lipid vesicles (DLVs) from the microparticles over time.

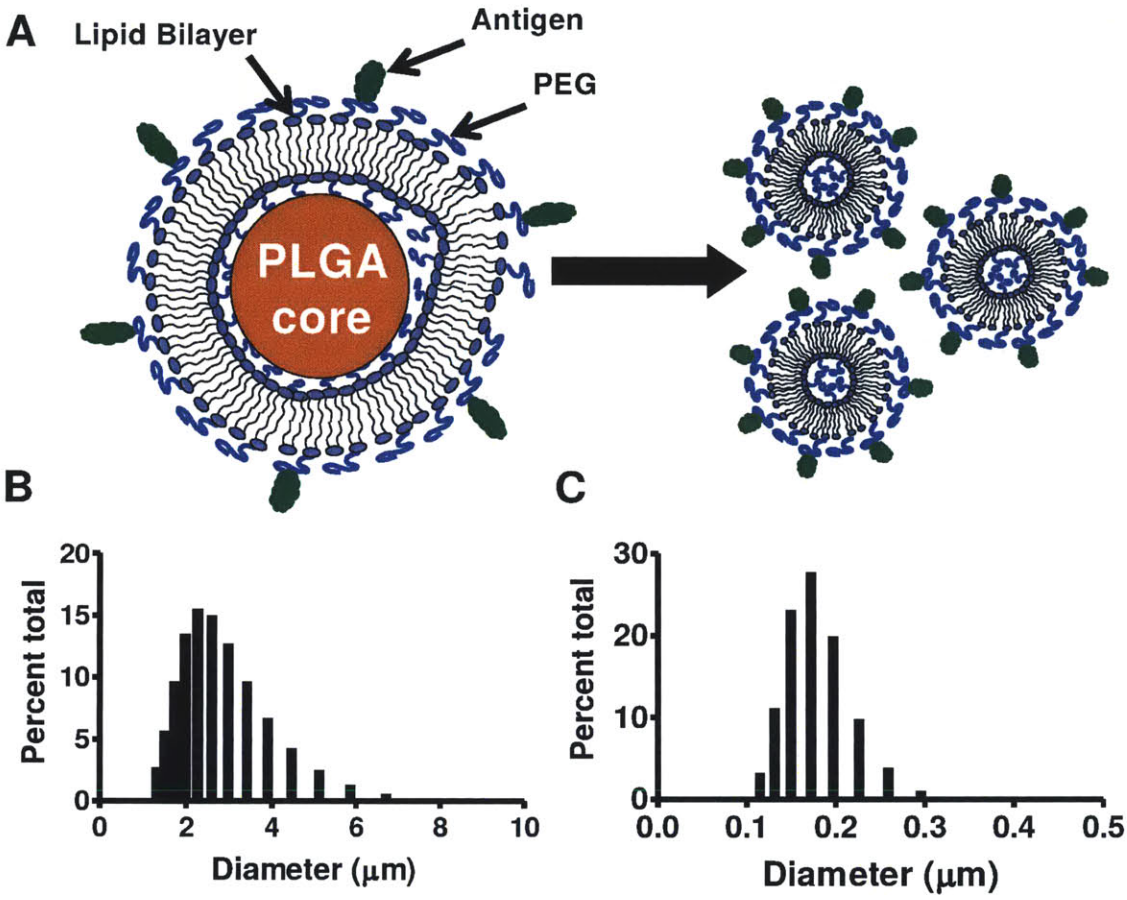

Figure 2-1. Delamination of lipid vesicles from lipid-coated nanoparticles.

(A) Schematic structure of as-synthesized LCMPS with surface-conjugated protein antigen and vesicles "budded" from PLGA polymer core, forming delaminated-lipid vesicles (DLVs). (B) Size distribution of freshly synthesized microparticles post-wash steps determined by laser diffraction. (C) Size distribution of delaminated vesicles released from LCMPs after 7 days in PBS at 37°C determined by laser diffraction.

We next characterized the kinetics of DLV shedding from LCMPs. Microparticles containing rhodamine-labeled lipid were incubated in PBS and DLVs released into the supernatants over time were detected by fluorescence spectroscopy. As shown in Fig. 2-2A, although lipids remained stably associated with LCMPs at 4°C, vesicles were rapidly shed from the particles at 37°C in PBS, with delamination reaching a plateau after 24 hrs. To test the effect of serum on lipid delamination kinetics, LCMPs containing rhodamine-conjugated

lipid were incubated in either serum or PBS and delamination was quantified as before. Fig. 2-2A shows that serum increased the fraction of delaminated lipid by 1.6-fold, with substantial vesicle shedding within 4 hours that continued slowly through 48 hours. We hypothesized that interactions of the lipid surface layers with lipid droplets in serum may be a major contributor to vesicle delamination, as the adsorption of lipids by serum lipoprotein particles is essential for lipid transport in vivo [98]. Previous studies have shown that liposomes are destabilized in the presence of serum due to the transfer of phospholipids to lipoproteins[95,96,99]. To model interactions of LCMPs with lipids in serum, a group of microparticles was incubated in PBS containing 10 mM of 200 nm-diameter synthetic 4:1 DOPC:DOPG liposomes. The results indicate that the inclusion of liposomes in the aqueous buffer replicates the kinetics of lipid delamination in serum (Fig. 2-2B), thus suggesting the presence of environmental lipid promotes DLV delamination from LCMPs.

LCMPs carrying protein antigen covalently linked to the membrane (e.g., as illustrated in Fig. 2-1A) elicit robust humoral immune responses in vivo[40,91]. To test whether antigen conjugated to the lipid coat is transferred to delaminating vesicles, thiol-functionalized ovalbumin (OVA) was conjugated to maleimide-functionalized PEG chains incorporated into the particle bilayer coating, and its release over time into serum at 37°C was quantified by ELISA. As expected, lipid-conjugated OVA was shed from the LCMPs with kinetics matching rhodamine-labeled lipid delamination (Fig. 2-2C). Altogether, these data suggest that LCMPs rapidly shed submicron liposomes in conditions mimicking interstitial fluid to which the particles would be exposed to in vivo during immunization.

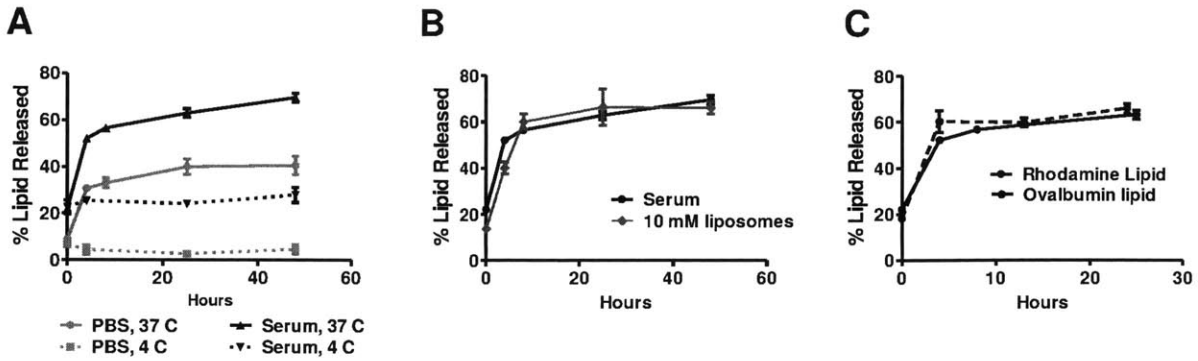

Figure 2-2. Kinetics of lipid delamination from lipid-coated microparticles.

Kinetics of lipid delamination from LCMPs in vitro determined by monitoring release of fluorescently-labeled lipid tracer (A-C) or PEG-lipid-conjugated OVA (C) into the supernatants of particles over time. (A) Release of rhodamine-lipid into the supernatant of LCMP particles was assessed as a function of temperature in pH 7.4 PBS or 100% fetal bovine serum. ($p < 0.0001$ comparing 37°C serum to 37°C PBS, 4°C serum to 4°C PBS, 37°C serum to 4°C serum, and 37°C PBS to 4°C PBS. (B) Lipid release kinetics for rhodamine-lipid-labeled LCMPs incubated in PBS containing 10 mM unlabeled DOPC/DOPG liposomes at 37°C. (C) LCMPs conjugated with OVA protein were incubated in 100% fetal bovine serum at 37°C and OVA accumulation in the supernatant was assessed over time by ELISA analysis of LCMP supernatants.

2.3.2. Immunogenicity of delaminated vesicles and lipid-coated microparticles

Given the rapid shedding of liposomes from LCMPs in the presence of serum, we hypothesized that vesicles spontaneously released from the microparticles following injection could play an important role in the immunogenicity of LCMP vaccines. To explore this possibility, we prepared OVA-conjugated LCMPs and incubated a fraction of the particles at 37°C in PBS to induce delamination, followed by collection of the supernatant containing shed vesicles. The concentration of antigen in the shed vesicle preparation was measured by ELISA, and mice were then immunized with MPLA mixed with 10 ng OVA carried by purified delaminated vesicles or the parent (non-delaminated) particle fraction. In addition, a third group of mice were immunized with OVA-conjugated pure liposomes prepared with the same lipid composition as the LCMPs, to control for possible changes in the lipid structure or composition occurring during "budding" of vesicles from the PLGA-core particles. Each group of mice was boosted on day 14 with identical formulations, and serum was collected over time for analysis of titers of anti-ovalbumin IgG. As shown in Figs. 2-3A and B, DLVs and the control synthetic liposomes elicited essentially identical OVA-specific IgG responses. Both liposomal vaccines were somewhat less immunogenic than intact LCMPs, eliciting average

antibody titers 2-fold lower than LCMPs. However, DLVs were still capable of priming a strong immune response to this low dose of OVA, which elicited undetectable anti-OVA titers in 3 out of 4 animals when administered as a soluble vaccine mixed with MPLA (Figure 2-3A). Titers in all 3 particle immunization groups were maintained over at least 70 days post priming (Fig. 2-3B). Although DLVs elicited weaker OVA-specific IgG_1 and IgG_{2A} antibodies than parent LCMPs (Fig. 2-3C), both groups exhibited identical IgG_{2A}/IgG_1 ratios (Fig. 2-3D). As IgG_{2A} is considered indicative of "Th1-like" responses and IgG_1 "Th2-like" responses, this result suggests both the lipid-coated microparticles and shed liposomes primed balanced Th1/Th2 responses, and that the small difference in titers comparing LCMPs and shed vesicles reflects a difference in strength of priming rather than different Th-biasing of the antibody response. Altogether, these data suggest that delamination of antigen-bearing liposomes plays a critical role in the immune response primed by LCMPs carrying surface-bound antigens.

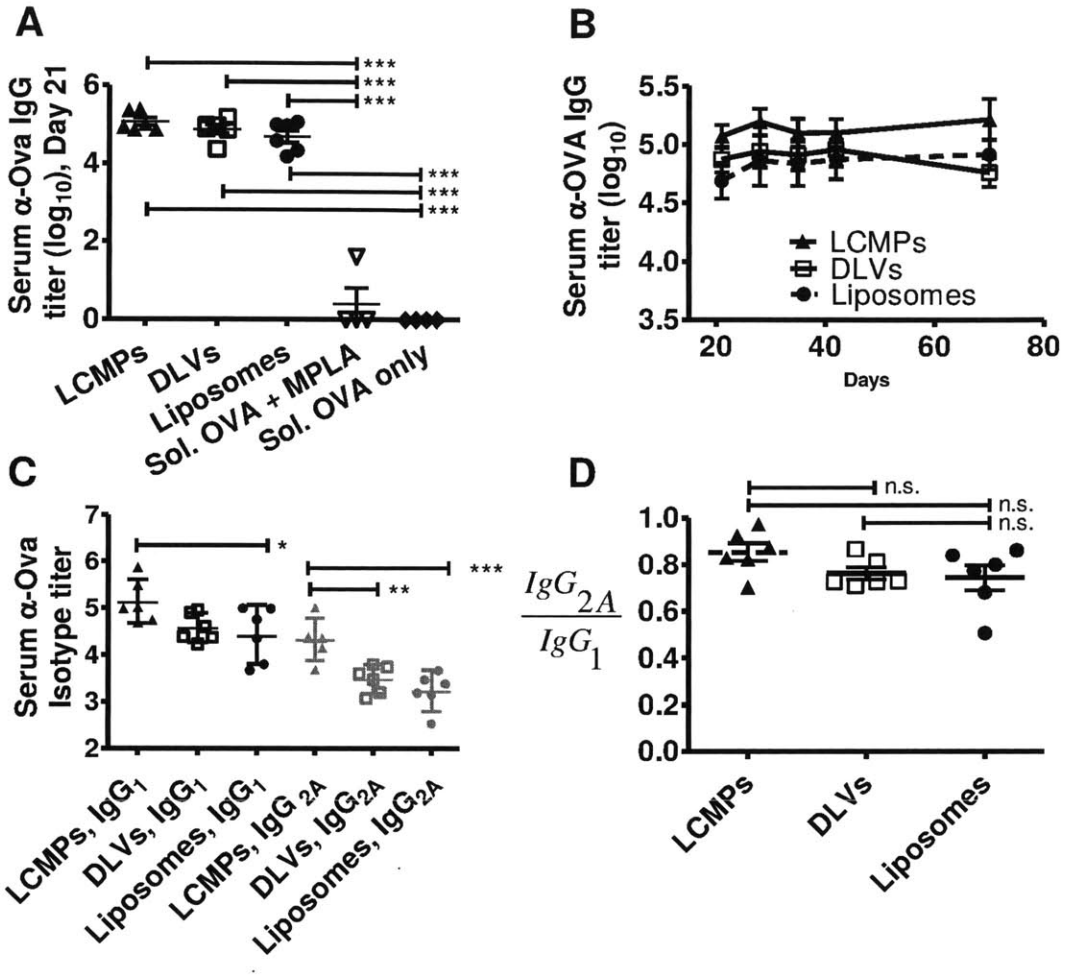

Figure 2-3. Immunogenicity of lipid coated microparticles and delaminated lipid vesicles

*(A-D) Balb/c mice (n = 6/group) were immunized s.c. with 10 ng of ovalbumin displayed on lipid-enveloped microparticles (LCMPs), delaminated lipid vesicles (DLVs) collected from LCMPs, or pure liposomes, and boosted with identical formulations on day 14. Liposomal vaccines are compared to control immunizations with soluble OVA. In all particle formulations, 1.3 ug of MPLA per injection was included. (A) Mean endpoint OVA-specific IgG serum titers on day 21. (***, $p < 0.001$) (B) Mean endpoint OVA-specific IgG serum titers over time. ($p = 0.006$ for formulation over time) (C) OVA-specific IgG_1 and IgG_{2A} isotype serum titers at day 21 (*, $p < 0.05$; **, $p < 0.01$; ***, $p < 0.001$) (D) Ratio of post-boost peak (day 28) endpoint ova-specific IgG_{2A} to IgG_1 serum titers.*

2.3.3. Immunogenicity of lipid-stabilized microparticles

Although Fig. 3 demonstrates that *in vitro*-generated DLVs induced slightly lower antibody titers than parental LCMPs, it remained unclear whether *in vivo* budding of antigen-carrying vesicles from the microparticles was necessary for the high immunogenicity of the lipid-coated microparticles. If *in vivo* delamination were essential, then LCMPs that failed to undergo lipid delamination would be expected to prime weaker immune responses. To test this hypothesis, we sought to prepare LCMPs with lipid envelopes stabilized against delamination. We tested two strategies to create such stabilized-envelope particles: incorporation of high-T_M lipid and incorporation of cholesterol into the lipid coating.

Phospholipids with high melting temperatures have few/no unsaturated bonds in their acyl tails, allowing the lipids to pack tightly and favoring formation of liquid crystalline gel phases. In addition, the removal of double bonds in the acyl chains of phospholipids in vesicles reduces the rates of lipid transfer from liposomes to serum lipoproteins by four fold[100]. Therefore, DSPC (T_M = 55°C) was used in place of DOPC (T_M = -20°C), to generate "high-T_M" DSPC-LCMPs. *In vitro*, inclusion of high-T_M lipid did not block vesicle shedding completely but did lower the fraction of lipid lost from the particles in the presence of serum by 33%, as shown in Fig. 2-4A. We tested whether the reduced shedding of vesicles would impact the immunogenicity of these particles compared to DOPC-based LCMPs. Balb/c mice were immunized s.c. on day 0 and day 14 with MPLA mixed with DOPC-LCMPs or DSPC-LCMPs each carrying 10 ng OVA. As shown in Fig. 2-4B, despite the modest reduction in lipid shedding exhibited by DSPC-LCMPs, the immunogenicity of these particles was significantly altered, as mice immunized with DSPC-LCMPs showed a 3.5-fold reduction in titers of OVA-specific antibodies compared to DOPC-LCMPs at one week post-boost (Fig. 2-4B). Futhermore, DSPC-LCMPs elicited 64±10% lower total OVA-specific IgG titers ($p = 0.0023$, Fig. 2-4C) and lower serum IgG_1 titers at the post-boost peak on day 21 ($p = 0.0067$, Fig. 2-4D) when compared to DOPC-LCMPs. Interestingly, the avidity index of the antibody response elicited by DSPC-LCMPs was higher than that of the response primed by to DOPC-LCMPs from day 28 onward ($p = 0.0491$ comparing the two groups over time). However, the overall strength of the antibody response elicited by LCMPs was reduced when vesicle shedding was impeded by incorporation of high-T_M lipids.

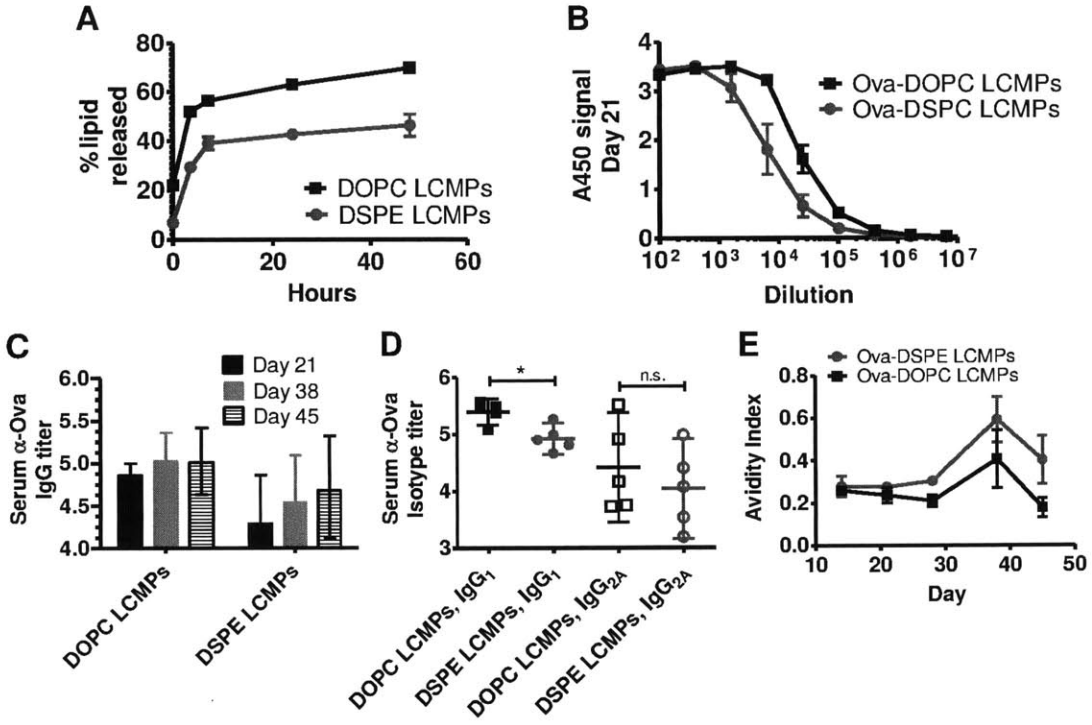

Figure 2-4. LCMPs prepared with high-T_M lipids show reduced vesicle shedding and weaker antibody responses *in vivo*.

*(A) Kinetics of in vitro lipid release from high-T_M lipid-enveloped microparticles (DSPC-LCMPs) or regular, low-T_M lipid microparticles (DOPC-LCMPs) in serum, determined by following fluorescent lipid tracer released into particle supernatants upon incubation with FBS at 37°C ($p < 0.0001$). (B-E) Balb/c mice ($n = 5$) were immunized on days 0 and 14 with 1.3 μg MPLA mixed with DOPC-LCMPs or DSPC-LCMPs, each conjugated with 10 ng OVA. (B) OVA-specific antibodies detected by ELISA as a function of serum dilution at the post-boost peak, day 21. ($p < 0.0001$) (C) Mean OVA-specific IgG serum titers on days 21, 38 and 45. (DOPC LCMPs vs DSPE LCMPs over time, $p = .0023$) (D) OVA-specific IgG_1 and IgG_{2A} isotype serum titers at day 21. (DOPC IgG_1 vs. DSPE IgG_1, * = p value of 0.0067) (E) Mean OVA-specific IgG avidity indices as a function of time. ($p = 0.0491$)*

To further test the idea that vesicle "budding" from antigen-conjugated LCMPs is important for their immunogenicity, we also tested a second strategy for inhibiting liposome shedding from the microparticles. Cholesterol is a major component of cell membranes and is often used as a stabilizing agent in lipid vesicle preparations because it orders and condenses fluid-phase bilayers[101–103]. Thus, we hypothesized that cholesterol, like high T_M lipids, could also act to stabilize the lipid bilayer of LCMPs. We prepared DOPC-LCMPs incorporating 0, 1, or 10 mg cholesterol per 80 mg PLGA. *In vitro*, DLV formation was not inhibited completely

by the inclusion of cholesterol but delamination did decrease with increasing cholesterol quantity. As shown in Figs. 2-5A and B, increasing the amount of cholesterol incorporated in the particles lowered the fraction of lipid shed into solution from LCMPs, although the effect was less pronounced in serum than in PBS, perhaps due to cholesterol absorption by lipoprotein particles in serum. As with the high-T_M lipid LCMPs, we tested the immunogenicity of LCMPs with cholesterol by vaccinating balb/c mice. A plot of mean ova-specific IgG endpoint titers shows decreased immunogenicity (up to a 2.5-fold average drop in titers) with increasing cholesterol content (Fig. 2-5C) (Comparison of 10 mg vs 1 mg titer over time, $p<0.001$). An analysis of IgG_1 and IgG_{2A} isotype titers at the post-boost peak indicate that IgG_1 titers are also inversely dependent on cholesterol quantity; however IgG_{2A} isotype titers remained relatively independent of cholesterol presence (Fig. 2-5D). Interestingly, avidity indices were independent of cholesterol incorporation in the particles (data not shown). Thus, using a second strategy to stabilize the lipid bilayer of LCMPs by altering its composition, we found a similar reduction in antibody responses when vesicle shedding was inhibited.

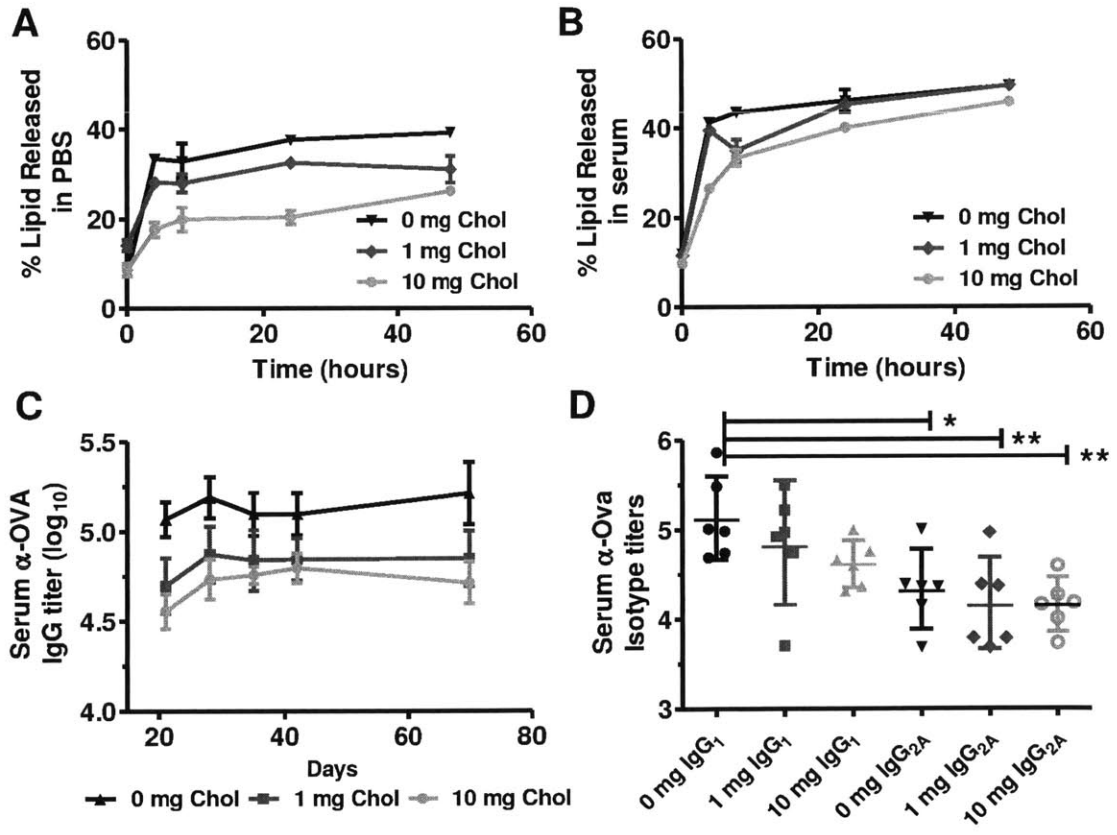

Figure 2-5. Cholesterol was included in the lipid bilayer of LCMPs to decrease delamination of the envelope.

(A-B) The kinetics of lipid release—in PBS (A) or fetal bovine serum (B)—of LCMPs, which were synthesized with 0 mg, 1 mg or 10 mg of cholesterol (per standard 80 mg PLGA batch). Delamination was quantified by the fluorescent detection of rhodamine lipid in the supernatant of aliquots of pelleted microparticles. (A: $p < 0.0001$; B: $p < 0.0001$ for effect of cholesterol over time.) (C-D) Balb/c mice (n=5) were immunized and boosted 14 days later with 10 ng of ovalbumin conjugated to the surface of LCMPs containing 0 mg, 1 mg, of 10 mg of cholesterol per batch. In all formulations, 1.3 ug of MPLA per mouse was incorporated into the lipid bilayer. (C) Mean endpoint ELISA-based ova-specific IgG serum titers over time. (Comparison of 10 mg vs 1 mg titer over time, $p < 0.0001$) (D) Endpoint OVA-specific IgG_1 and IgG_{2A} isotype serum titers at day 28, the post-boost peak (= $p < 0.05$, ** = $p < 0.01$).*

The agreement in results obtained by these two different strategies for physically stabilizing the bilayer suggests that the reduced immunogenicity observed with DSPC-LCMPs or chol/DOPC-LCMPs when compared to DOPC-LCMPs is not due to the chemical alterations in the bilayer composition. The antibody response to LCMPs was not entirely ablated by inhibiting vesicle delamination, but the reduced response is all the more striking given the fact that the lipid bilayer composition-based strategies we tested here for blocking DLV release from the particles were at best only ~30% effective under conditions mimicking exposure to serum components. Furthermore, the immunogenicity of liposomes is inversely proportional to membrane fluidity and it has been specifically shown that inclusion of cholesterol or high-T_M lipid in liposome vaccine formulations increases immunogenicity[104]. Thus, an enhancement derived from decreased membrane fluidity of shedded liposomes may be masking the full impact that decreased delamination from LCMPs has on humoral antibody responses. Altogether, these results are consistent with vesicle shedding from LCMPs playing an important role in the priming of humoral responses by these microparticle vaccines. An advantage of this system is the 180 nm diameter of DLVs, as nanoparticles in this size range are well suited for delivery to lymph nodes via subcutaneous injection and direct draining into the lymphatic system [54]. Furthermore, antigen that drains freely to lymph nodes can interact directly with B cells, which generates optimal humoral immune responses[51].

Coupling the observed reduction in immunogenicity from lipid-stabilized LCMPs with the *in vitro* observation of identical delamination kinetics of LCMPs in serum or in 10 mM liposome buffer leads to the possibility that antigen conjugated to lipid on LCMPs may be taken up by lipoprotein particles *in vivo*. This uptake and subsequent circulation throughout the lymphatic system could account for the enhanced immunogenicity of LCMPs over stabilized-lipid bilayer MPs or synthetic liposomes. Prior work characterizing the lipid transfer between liposomes and lipoproteins further supports this concept, especially as inclusion of

cholesterol in liposome formulations was shown to decrease the rate of lipid transfer to lipoproteins[99]. These results are consistent with our observation of decreased immunogenicity of LCMPs with increasing cholesterol inclusion.

2.4. Conclusions

Here we have explored the mechanisms underlying the potent immunogenicity of lipid-coated biodegradable microparticles in vaccine delivery. We found that although these particles are too large to efficiently drain from subcutaneous injection sites to lymph nodes, they are still very effective in antigen delivery due to spontaneous shedding of antigen-bearing lipid vesicles from the particle surfaces, which occurs rapidly under physiological conditions. Changes in lipid composition that reduce microparticle surface vesicle "budding" lowered the immunogenicity of the particles *in vivo*, suggesting this mechanism is important for the effectiveness of these antigen delivery vehicles. This antigen-bearing vesicle release combined with molecular adjuvants either incorporated in the membranes (as shown here) or encapsulated in the PLGA particle core and slow-released at the injection site to drain to local lymph nodes[86–89] could provide an effective strategy for enhancing the immunogenicity of subunit vaccines.

3. Exploration of liposomes with surface-displayed HIV protein as vaccines

3.1. Introduction

The HIV-1 envelope trimer consists of three heterodimers, each consisting of one gp41 monomer and one gp120 monomer. Gp120 contains the site by which HIV-1 binds to the CD4 receptor. Binding to the CD4 receptor is a key initial step in viral entry of HIV into host $CD4^+$ cells. This CD4 binding site is a highly conserved epitope, to which several broadly neutralizing antibodies (BNAbs) have been isolated. These CD4-binding site antibodies include B12, VRC01, and VRC02[18–21]. Eliciting neutralizing antibodies against the CD4-binding site via vaccination has proven difficult due to the immunodominance of variable regions of the HIV envelope trimer, and the masking of the CD4 binding site by glycosylation and steric hindrance[11,22].

Efforts to develop vaccines to induce antibodies which bind the CD4 binding site have traditionally either utilized monomeric gp120 or the complete envelope trimer. Although timeric envelope is an attractive antigen now that the production of stable trimer has been achieved[105,106], the production of large quantities of stable and purified trimer is still an ongoing process[107]. In contrast, gp120 monomer is more tolerant of modifications and more efficient to produce[108].

In order to methodically yet rapidly engineer a gp120 monomer to be a potent immunogen which elicits BNAb-like antibody responses, Jordi Mata-Fink of the Wittrup lab developed yeast surface display method to methodically characterize gp120 variants[108,109]. Briefly, the gp120 gene was subcloned into a yeast display vector, which resulted in display of gp120 on the yeast surface. This surface-displayed gp120 can then be tested for ability to bind the BNABs VRC01 or B12 (with flow cytometry-based detection). Through rational design (e.g. removal of sterically-hindering epitopes or glycosylation to make off-target epitopes), a "stripped-core" gp120 monomor, referred to as 4G, which had a high affinity binding to the BNAbs VRC01, PGV04, and b12, was developed[108]. This representation of 4G is shown in schematic 3-1.

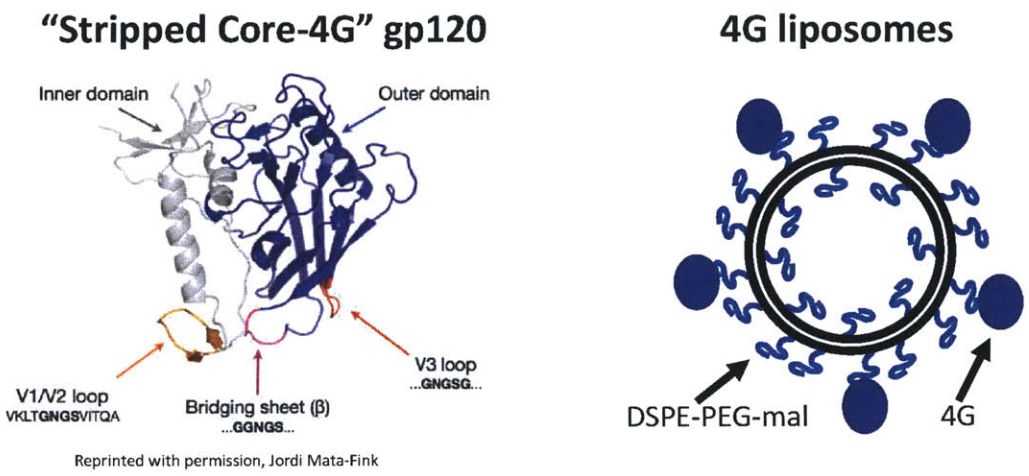

Schematic 3-1: Representation of 4G gp120 protein and 4G liposomes.

We sought to test the potential of 4G as an HIV immunogen. In order to mimic display of gp120 on HIV virions, we developed utilized unilamellar liposomes to surface display the 4G protein. In Chapter 2, we reported that lipid-coated microparticles were slightly more potent than synthetic liposomes when using the model antigen ovalbumin. Due to the 10-fold higher antigen conjugation efficiency to liposomes than to LCMPs and the finite supply of 4G, the decision was made to utilize liposomes rather than LCMPs as the vaccine delivery system. As shown in Schematic 3-1, 4G was linked via its terminal cysteine to liposomes containing the lipid DSPE-PEG-maleimide. This approach is similar to the method of ovalbumin conjugation to lipid-coated microparticles or liposomes discussed in chapter 2. This chapter presents the work done to assess the immunogenicity of 4G liposomes in comparison to traditional adjuvants such as alum and furthermore to identify the optimal immunization and liposome parameters to elicit strong humoral responses against the 4G immunogen.

3.2.Materials and Methods

3.2.1. Materials

All lipids—1,2-dioleoyl-sn-glycero-3-phosphocholine (DOPC), 1,2-dioleoyl-sn-glycero-3-phoshpo-(1'-rac-gylcerol) (DOPG), and 1,2 distearoyl-sn-glycero-3-phosphoethanolamine-N-[maleimide(polyethylene glycol)2000] (DSPE-PEG2K-maleimide)—were purchased from Avanti Polar Lipids (Alabaster, Alabama). Monophosphoryl lipid A (MPLA,from *Salmonella enterica* serotype minnesota Re 595 cat. no. L6895) and solvents were purchased from Sigma Aldrich (St. Louis, Missouri). n-succinimidyl s-acetyl(thiotetraethylene glycol) (SAT(PEG)$_4$) was purchased from Pierce Biotechnology (Rockford, Illinois). Recombinant "stripped-core"

gp120 protein, version "4G", was provided by Jordi Mata-Fink, produced in the laboratory of Dane Wittrup.

3.2.2. Synthesis of gp120 antigen-displaying liposomes

A 4:1 molar ratio of DOPC:DOPG (for DOPC liposomes) in chloroform with 10 mol% of DSPE-PEG2k-maleimide was dried under nitrogen followed by incubation under vacuum at 25°C for 18 hr. Liposomes incorporating MPLA were prepared by including these components in the organic solution prior to drying lipid films. Lipids were hydrated with pH 7.4 PBS and vortexed 30 seconds every 10 minutes for an hour. For 150 nm diameter liposomes, the resulting vesicles were passed through six freeze-thaw cycles between liquid nitrogen and a 37°C water bath followed by extrusion 21 times through 0.2 μm or 0.4 μm pore polycarbonate membranes (Whatman Inc, Sanford, ME), respectively. For 65 nm diameter liposomes, the lipid resuspension was subjected to 5 minutes of sonication alternating for 30 second periods between 10 watts and 3 watts output power on a Misonix XL-2000 probe sonicator.

4G constructs were conjugated to the surface of maleimide-functionalized liposomes via a terminal cysteine on the 4G protein. In brief, purified gp120 was incubated with liposomes at 25°C for 18 hrs. To remove unbound antigen, liposomes were purified via FPLC in the Wittrup lab. The amount of gp120 coupled to liposomes was determined by enzyme-linked immunosorbent assay (ELISA), as described in Appendix B. Particles and liposomes were stored at 4°C until use, which was within 4 hours for immunization experiments and 48 hours for *in vitro* experiments.

3.2.3. In vivo immunization studies

Female BALB/c mice 6-7 weeks of age were purchased from Jackson Laboratories for all immunizations, and handled under federal, state, and local guidelines. Immediately prior to immunization, 1.3 μg of the TLR-4 agonist MPLA per 100 μL was mixed with gp120 liposomes in sterile pH 7.4 PBS, following post-synthesis insertion techniques described previously [40,94]. Mice were immunized by injection of 100 μL gp120 liposome solutions s.c. at the tail base, 50 μL on each flank, and boosted on days 14 and 28 with the same formulations. Serum was collected weekly via retro-orbital bleeding for subsequent ELISA-based titer analyses.

3.2.4. Antibody titer analysis

A gp120-specific enzyme-linked immunosorbant assay (ELISA) was developed in order to determine serum total IgG titers, isotype IgG_1 and IgG_{2A} titers, IgM titers and avidity indices. The full protocol can be found in Appendix B. Briefly, 96-well MAXIsorp plates (Nunc) were coated with poly-L-Lysine (Sigma-Aldrich), blocked with 1% BSA in PBS, and then incubated with 50 nM 4G in 1% BSA in PBS for 2 hours. Plates were then washed and incubated with

serially diluted serum and detected with HRP-labeled anti-mouse IgG, IgG_1, IgG_{2A}, (BioRad) or IgM (AbCam) followed by development and measurement of optical absorbance at 450 nm. Antibody titer is reported as reciprocal serum dilution at an absorbance of 0.5. Fraction of VRC01-comptitive antibody was determined via VRC01 competition ELISA, as described in Appendix B.

3.2.5. Statistical analysis

Statistical analyses were performed using GraphPad Prism software. Comparisons of formulations over time employed two-way ANOVA tests and comparisons of multiple formulations at a single time point were performed using one-way ANOVA and Tukey's tests. Two-tailed unpaired t-tests were used to determine statistical significance between two experimental groups for all other data unless otherwise noted.

3.3. Results and Discussion

3.3.1. Immunogenicity of gp120 liposomes in comparison to traditional vaccine formulations

In order to assess the potency of liposomes with surface-displayed gp120 as an adjuvant formulation, we compared gp120 liposomes to traditional adjuvant formulations. Imject Alum (ThermoScientific), is an aluminum hydroxide/magnesium hydroxide adjuvant and Montanide ISA 51 (Seppic)—also known as Incomplete Freund's Adjuvant—is a water-in-oil emulsion adjuvant. Both adjuvants are widely-used in vaccine research[36] and alum is the most-common form of adjuvant for human vaccines[110] but montanide is too toxic for use in human prophylactic vaccines[111]. Balb/c mice were immunized on days 0 and 42 with 3.75 pmoles of Fc-4G displayed on liposomes or delivered in soluble form mixed with plan liposomes or mixed with alum or montanide. Analysis of serum 4G-specific IgG antibody titers on day 49 revealed that empty liposomes with soluble Fc-4G induced no IgG response, alum with Fc-4G elicited weak IgG responses, and Fc-4G displayed on liposomes elicited strong IgG antibody titers that were 80-fold greater than the alum-induced responses and equivalent to mountain-induced responses (Fig. 3-1A). Analysis of the serum 4G-specific IgM antibody levels revealed a strong trend of class-switching from IgM to IgG; alum-adjuvanted vaccines had 6-fold and 4-fold higher levels of IgM than Fc-4G in montanide or Fc-4G on liposomes (Fig. 3-1B). Soluble Fc-4G with empty liposomes elicited moderate IgM titers but no IgG titers, indicating that the response was entirely non-class-switched. Isotype class-switching from IgM to IgG is dependent upon CD40 ligand signaling from $CD4^+$ T cells to the CD40 receptor on B cells and therefore these results suggest that the antibody responses elicited from Fc-4G liposomes is a $CD4^+$ T cell-dependent phenomenon[112]. CD40/CD40L signaling also promotes the formulation

of germinal centers and antibody affinity maturation which are critical steps in the generation of memory B cells and long-lived plasma cells.

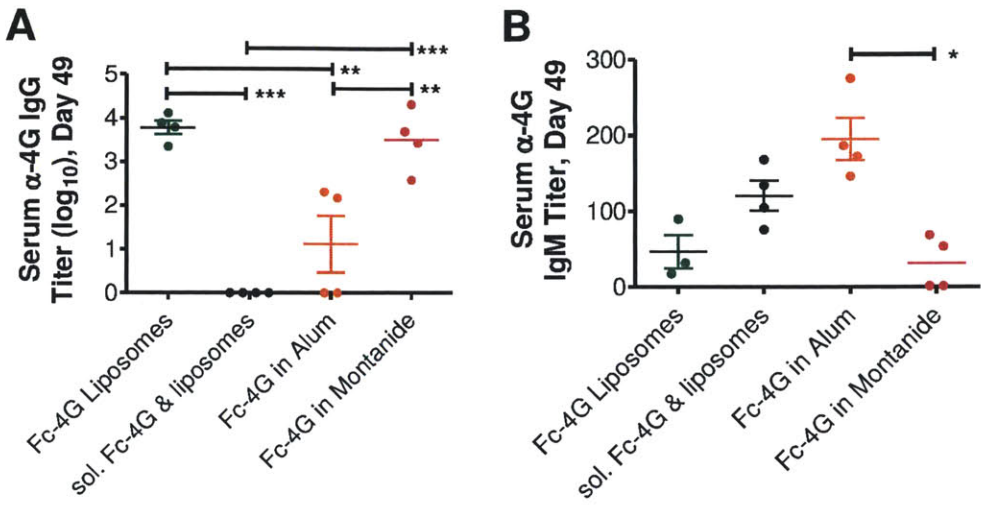

Figure 3-1. Liposomes induce strong, class-switched gp120-specific antibody responses

*(A-B) Balb/c mice (*n=*4/group) were immunized on days 0 and 42 with FC-4G delivered on liposomes, in soluble form with empty liposomes, or in soluble form mixed with alum or montanide together. All immunizations contained 1.3 μg MPLA per injection. (A) Anti-4G serum IgG titers. (B) Anti-4G serum IgM titers. *, $p < 0.05$; **, $p < 0.01$; ***, $p < 0.001$ as determined by ANOVA followed by Tukey's multiple comparison test.*

3.3.2. Optimization of liposome formulation and immunization parameters

Encouraged by the ability of liposomes to induce serum IgG responses as potent as montanide-adjuvanted vaccines, we set out to optimize the parameters of immunization and liposome formulation, such as dosage, liposome size, timing of boost injection and protein form. Fc-4G consists of two gp120 "stripped core" proteins (4G) linked at their C-termini to a mouse IgG_{2A} Fc fragment[108]. In order to determine whether the Fc region played a role in the immunogenicity of Fc-4G liposomes, balb/c mice were immunized with liposomes displaying either 7.5 pmol of 4G or 3.75 pmol of Fc-4G (which has two 4G proteins per molecule) and adjuvanted with 1.3 μg MPLA. As shown in Figure 3-2A, the difference in 4G-specific IgG titer was negligible between the two groups. Therefore further studies were continued with Fc-4G because the Fc region enabled simple and efficient purification of Fc-4G via protein A chromatography post-synthesis.

Particle size plays a key role in vaccine responses, though optimal dimensions are likely dependent on particle composition and the type of immune responses desired[113]. To investigate the role of liposome size in Fc-4G vaccine formulations, balb/c mice were immunized with Fc-4G displayed on 150 nm diameter or 65 nm diameter liposomes. Interestingly, diameter of liposomes played no role in determining the immunogenicity of Fc-4G liposome vaccines (Figure 3-2B).

Length of time between prime and boost immunizations is typically an empirically-determined parameter of vaccine development. In previous works, an extended period between prime and boost induced higher antibody responses[114,115], but it's often desirable to find the minimal length of time between boosts in order to minimize the length of experiments. In order to asses this in our system, balb/c mice were immunized on day 0 with 3.75 pmol Fc-4G on liposomes with 1.3 μg MPLA and boosted at 2, 4 or 6 weeks. Analysis of antibodies over time revealed that while all immunization schemes induced 4G-specific IgG titers, a 6 week interval induced the highest antibody titer which was well maintained over time. At day 69, the titer from the 6 week interval group was 2-fold and 3.2-fold higher than the 4 week and 2 week intervals, respectively (Figure 3-2C).

Although a 6 week interval maximized humoral responses, a 4 week interval also induced detectable immune responses. We hypothesized that a higher dose of antigen immunized on the 4 week interval schedule could strengthen anti-4G antibody titers. To test this hypothesis, balb/c mice were immunized at days 0 and 28 with the standard 1x Fc-4G (3.75 pmol) or 5x Fc-4G (18.75 pmol) on liposomes. Interestingly, 4G-specific antibody titers at day 49 were independent of Fc-4G dose (Figure 3-2D). This observation of the gp120 dose-sparing capabilities of liposomes pairs well with previously-observed dose-sparing of ovalbumin when presented on liposomes (data not shown) and suggests that at these dosage levels, presentation on nanoparticles, rather than antigen dose, is a key mediator of anti-4G immunogenicity. Altogether, these observations suggest that 3.75 pmol of antigen (either Fc-4G or 4G) displayed on liposomes (150 nm or 65 nm) administered at days 0 and 42 induce optimal 4G-specific IgG antibody responses.

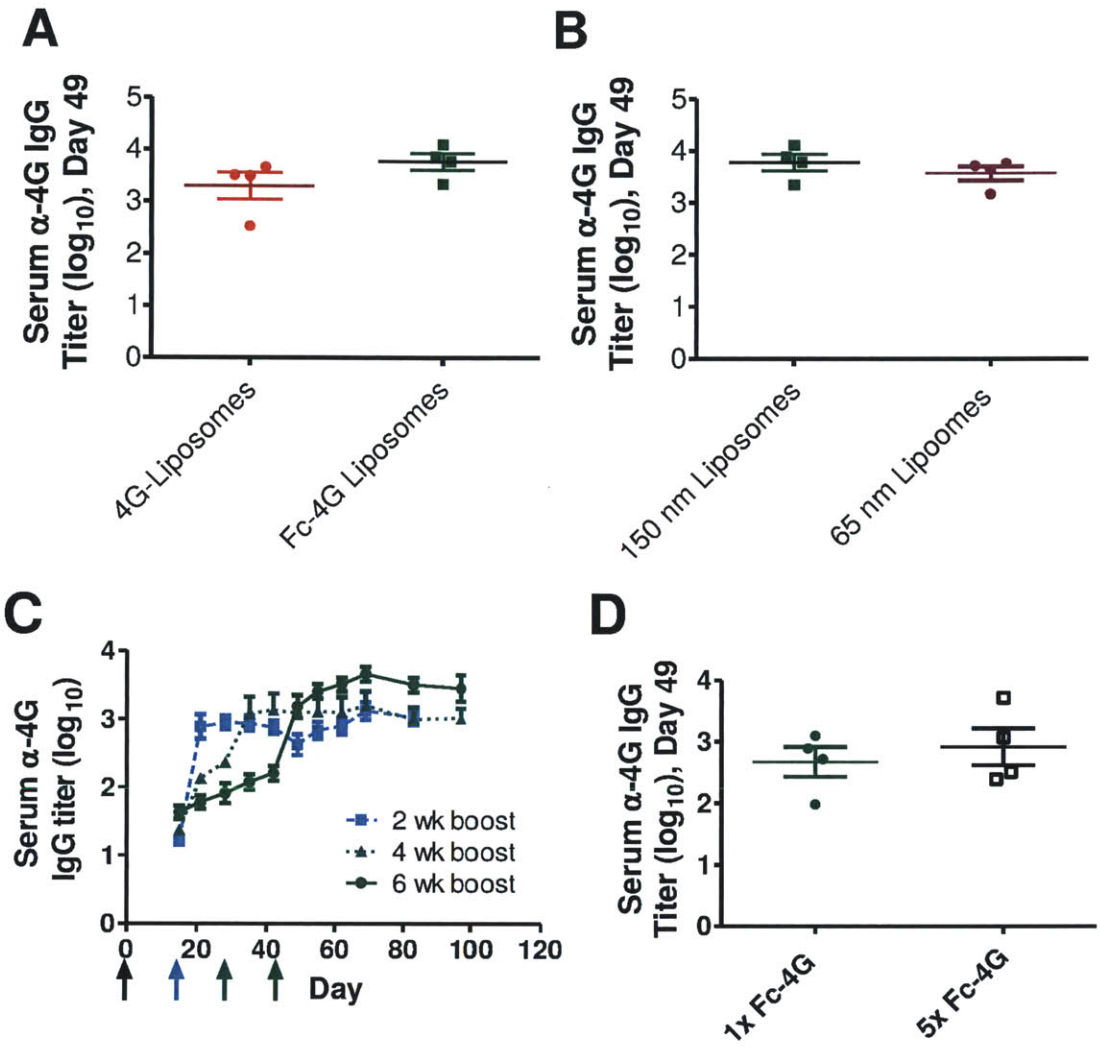

Figure 3-2. Optimization of formulation and vaccination parameters to enhance antibody responses.

(A) Balb/c mice (n=*4/group) were immunized on days 0 and 42 with Fc-4G or 4G delivered on liposomes with 1.3 μg MPLA per injection. Anti-4G serum IgG titers at day 49. (B) Balb/c mice* (n=*4/group) were immunized on days 0 and 42 with Fc-4G delivered on 150 or 65 nm diameter liposomes with 1.3 μg MPLA per injection. Anti-4G serum IgG titers at day 49. (C) Balb/c mice* (n=*5/group) were primed on day 0 and boosted at day 14, 28, or 42 with Fc-4G on liposomes with 1.3 μg MPLA per injection. Anti-4G serum IgG titers over time. (D) Balb/c mice* n=*4/group) were immunized on days 0 and 28 with Fc-4G at 1x dose (3.75 pmol) or 5x dose (18.75 pmol) on liposomes. Anti-4G serum IgG titers at day 49.*

3.3.3. VRC01-competing and class-switching capabilities of liposome-induced anti-gp120 sera.

With the optimized formulation of 150 nm liposomes displaying Fc-4G delivered at days 0 and 42 with 3.75 pmol of protein per mouse, we sought to characterize the quality of the immune responses against the immunogen, Fc-4G. VRC01 is a potent broadly neutralizing antibody against the CD4 epitope of gp120[20,21,116]. Eliciting VRC01-like antibodies is a major goal in the HIV vaccine field because broadly neutralizing antibodies will offer the greatest protection against infection in a vaccine model[7]. In order to determine if liposomal Fc-4G elicits "VRC01-like" antibodies, an ELISA-based VRC01 competition assay was developed (See Appendix B). Briefly, 4G-coated plates were incubated with serum from immunized or naïve animals, washed, then incubated with VRC01. The extent of VRC01 binding was assessed by detection with anti-human IgG-HRP. As shown in Figure 3-3, the percent uncompeted signal is representative of the amount of VRC01 capable of binding in the presence of serum from immunized mice normalized to the signal from VRC01 in the presence of serum from naïve mice. All formulations of antigen (Fc-4G or 4G) displayed on liposomes or in montanide were capable of blocking ~40% of VRC01 binding. In contrast, Fc-4G in alum induced no VRC01-blocking antibodies.

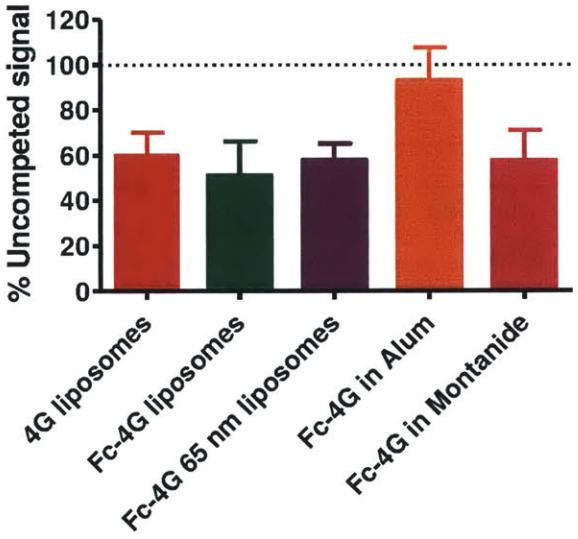

Figure 3-3. Liposomal Fc-4G elicits VRC01-competing antibodies.

Balb/c mice (n=4/group) were immunized on days 0 and 42 with 150 nm liposomes displaying 4G or Fc-4G, with 70 nm Fc-4G liposomes, with Fc-4G in alum, or with Fc-4G in montanide. All formulations contained 1.3 μg MPLA. Serum collected at 14 days post-boost (Day 56) was analyzed for ability to compete with VRC01 to bind gp120. Percent uncompleted VRC01 signal is shown.

3.4. Conclusions

4G is a "stripped core" variant of gp120, designed by Jordi Mata-Fink in the lab of K. Dane Wittrup. Fc-4G consists of a mouse IgG_{2A} Fc fragment with two 4G proteins attached. In the work shown here, we found that Fc-4G displayed on the surface of liposomes is capable of inducing anti-4G IgG titers equivalent to the potent adjuvant montanide, which, unlike liposomes [39], is too immunogenic for human use. The antibody responses induced by Fc-4G liposomes were IgM to IgG class-switched; this indicates that these humoral responses are $CD4^+$ T cell-dependent which is essential for the production of high affinity antibodies. In order to assess the potential of liposomes to serve vaccine delivery vehicles for gp120-based antigens, we optimized liposome size, dose and type of gp120, and prime-boost time interval. Anti-4G antibody responses were independent of liposome size, antigen dose, and type of gp120 used (Fc-4G or 4G only). The only factor to play a strong role in determining immunogenicity was timing of the boost; a 6 week interval was better than 2 week or 4 week intervals. The trend of strong anti-4G antibody induction regardless of antigen dose suggests that liposomal delivery is the driving force of anti-4G immunogenicity in these formulations. This optimization of vaccine delivery suggests that other adjuvant mechanisms (such as the inclusion of additional immunomodulators) will need to be explored in order to further enhance humoral responses to Fc-4G. Chapter 5 of this thesis explores the ability of co-delivered liposomes containing STING agonists to adjuvant liposomal vaccine formulations; future studies utilizing STING agonist liposomes with gp120 liposomes could be quite informative.

4. Optimization of liposomes with surface-displayed HIV peptides as vaccines

4.1. Introduction

As discussed in Chapter 1, the only proteins expressed on the surface of the HIV virion are the Env subunits gp120 and gp41, which form heterotrimeric spikes. The high mutation rate, low density of Env protein trimers on each viral particle, and the masking of highly conserved epitopes of the Env protein via glycosylation have all hindered efforts to develop an effective humoral immunogen against HIV[11,22]. While Chapter 3 detailed the development of lipid nanoparticles for a vaccine utilizing gp120 as an antigen, this chapter discusses the development of nanoparticulate-based vaccines displaying an antigen derived from gp41.

The membrane proximal external region (MPER) of gp41 is a particularly attractive vaccine target because it is a highly conserved linear peptide to which a number of BNAbs (e.g., 2F5, 4E10, 10E8 and Z13e1) bind[16,117–120]. One critical factor in MPER-targeting vaccine design is that this sequence comes just before the transmembrane region of gp41, and the conformation of the peptide is directly modulated by interaction with lipids. When associated with the surface of lipid micelles or membranes, MPER peptides form two hydrophobic helices connected by a flexible hinge region, and this unique conformation of membrane-displayed MPER substantially influences its binding to 2F5 and 4E10[74,121,122]. These findings have motivated strategies aiming to present MPER sequences in a defined helical structure[123,124]. For example, gp41 peptides have been incorporated as constrained epitopes within protein scaffolds[125–128] or displayed on virus-like particles (VLPs)[129] and although some formulations have been weakly immunogenic[130], other constructs have been able to produce 2F5-like antibodies with some neutralizing and ADCC activity after multiple booster immunizations [131].

Scaffolded epitopes can present a defined configuration but lack the surrounding lipid environment of the native MPER which may impact elicitation of BNAbs with 2F5 or 4E10-like characteristics. Thus, a second approach to promote a native conformation of gp41 epitopes has been to display MPER peptides on lipid vesicles, as shown in Schematic 4-1. Although MPER peptides are weakly immunogenic, liposomal vaccine formulations have generated antibody responses[132] which can be enhanced via multiple booster immunizations[133,134], administration with complete Freund's adjuvant[135], or through optimizing anchorage of lipid-conjugated MPER molecules in the lipid membrane[136,137].

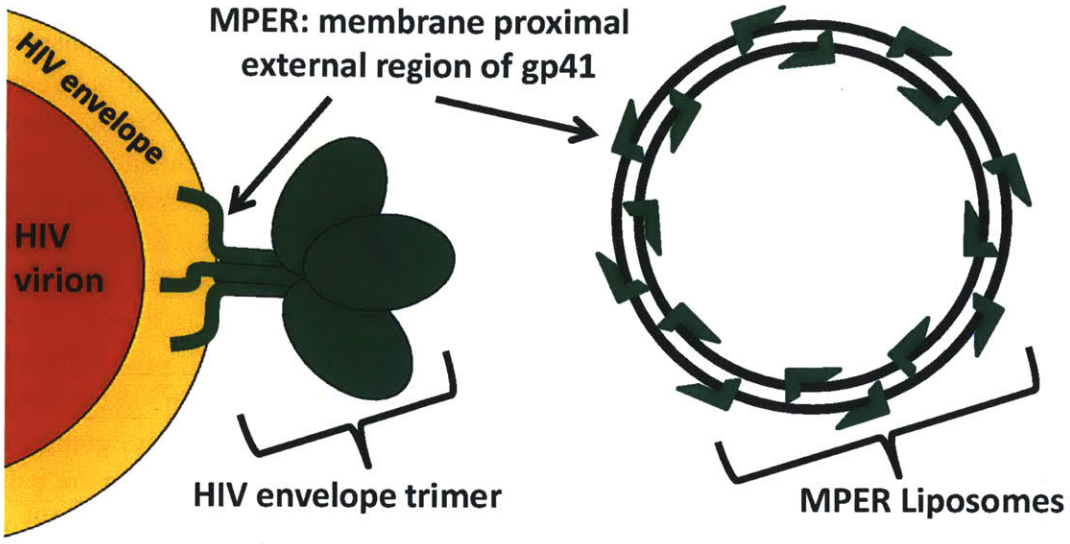

Schematic 4-1. Display of gp41-derived MPER peptide on unilamellar liposomes

Considering the requirements of presenting MPER in a conformation-mimicking display on the virus and the need to enhance MPER immunogenicity, liposomal delivery of structure-guided peptide antigens is a particularly attractive vaccination strategy. We recently reported that MPER anchored into a lipid membrane via a palmitoyl tail binds 2F5 and 4E10 and is more immunogenic than unmodified MPER absorbed onto lipid membrane surfaces[136], consistent with the findings of Watson et al. [137]. Here we evaluated the role of 3 key properties modulating the immunogenicity of MPER liposomal vaccines: liposome composition and size, inclusion of molecular adjuvants, and incorporation of intrastructural (within the same liposome) T-cell help. The majority of this work is in press at *Vaccine*. Citation: Hanson MC, et al. Liposomal vaccines incorporating molecular adjuvants and intrastructural T-cell help promote the immunogenicity of HIV membrane-proximal external region peptides. *Vaccine* (2014), http://dx.doi.org/10.1016/j.vaccine.2014.12.045.

4.2. Materials and Methods

4.2.1. Materials

Lipids 1,2-dioleoyl-*sn*-glycero-3-phosphocholine (DOPC), 1,2-dioleoyl-*sn*-glycero-3-phoshpo-(1'-rac-gylcerol) (DOPG), 1,2-dimyristoyl-*sn*-glycero-3-phosphocholine (DMPC), 1,2-distearoyl-*sn*-glycero-3-phosphoethanolamine-N-[methoxy(polyethylene glycol)-2000]

(DSPE-PEG), and 1,2-distearoyl-*sn*-glycero-3-phosphoethanolamine-N-[PDP(polyethylene glycol)-2000] (DSPE-PEG-PDP) were purchased from Avanti Polar Lipids (Alabaster, AL). Solvents, bovine serum albumin (BSA) and monophosphoryl lipid A (MPLA,from *Salmonella enterica* serotype minnesota Re 595 cat. no. L6895) were purchased from Sigma Aldrich (St. Louis, MO). Ovalbumin (OVA) was purchased from Worthington Biochemical (Lakewood, NJ) and purified via detoxi-gel endotoxin removal columns (Pierce Biotechnology, Rockford, IL). Montanide ISA 51 VG was purchased from Seppic (Puteaux, France). AddaVax and cylic-di-GMP were purchased from Invivogen (San Diego, CA). Lipo-S-S-$(PEG)_4$-CpG (Lipid-PEG-CpG) was synthesized as previously described [138]. Briefly, CpG 1826 was synthesized using an ABI 394 DNA synthesizer (Applied Biosystems, Carlsbad, CA) on a 1.0 micromole scale, 5' coupled to 4 repeats of DMT-hexaethyloxy-glycol phosphoramidite (Chemgenes, Wilmington, MA), thiol modifier C6 S-S (Glenres, Sterling, VA), and finally conjugated with lipid phosphoramidite (diacyl lipid phosphoramidite, synthesized according to published procedure [138]). After synthesis, lipid-PEG-CpG was purified by reverse phase HPLC. The $CD4^+$ T helper peptides LACK1 (ICFSPSLEHPIVVSGSWD) and HIV30 (RRNIIGDIRQAHCNISRAKW) and MPER peptide (ELDKWASLWNWFNITNWLWYIK) were synthesized at the Tufts University Core Facility (Boston, MA). MPER was purchased with either an N-terminal biotin (for ELISAs) or palmitoyl tail (for immunizations). For membrane-anchored DSPE-HIV30 conjugates, HIV30 was linked to DSPE-PEG-PDP via the cysteine residue of HIV30, by dissolving the peptide in DMF with 1.5 equivalents of DSPE-PEG-PDP and agitating at 25°C for 18 hours. The conjugate was then diluted in 10x deionized water, lyophilized into powder, and redissolved in deionized water. Peptide concentrations were determined by Direct Detect infrared spectroscopy analysis (EMD Millipore, Billerica, MA).

4.2.2. Synthesis and characterization of liposomes

A 4:1 molar ratio of DOPC:DOPG (for DOPC liposomes) or a 2:2:1 molar ratio of DMPC:DOPC:DOPG (for DMPC liposomes) in chloroform with or without 10 mol% of DSPE-PEG and palm-MPER added at a 1:200 MPER:lipid mole ratio was dried under nitrogen followed by incubation under vacuum at 25°C for 18 hr. Liposomes incorporating lipid-PEG-CpG, MPLA, or DSPE-HIV30 were prepared by including these components in the organic solution prior to drying lipid films. Lipids were hydrated with pH 7.4 PBS (containing 1 mg/mL LACK1 or 0.2 mg/mL HIV30 for soluble delivery of T-helper peptide) to a final concentration of 26.5 mM lipid and vortexed 30 seconds every 10 minutes for an hour. For 150 and 200 nm diameter liposomes, the resulting vesicles were passed through six freeze-thaw cycles between liquid nitrogen and a 37°C water bath followed by extrusion 21 times through 0.2 μm or 0.4 μm pore polycarbonate membranes (Whatman Inc, Sanford, ME), respectively. For 65 nm diameter liposomes, the lipid resuspension was subjected to 5 minutes of sonication alternating for 30 second periods between 10 watts and 3 watts output power on a Misonix XL-2000 probe sonicator. For c-di-GMP liposomes, a 38:38:19:5:0.95 molar ratio of

DMPC:DOPC:DOPG:DSPE-PEG:c-di-GMP in chloroform was dried under nitrogen followed by incubation under vacuum at 25°C for 18 hr and following drying, the resulting lipid/c-di-GMP films were resuspended at 240 μg/mL of c-di-GMP in PBS and then freeze/thawed and extruded to form 150 nm liposomes. Unencapsulated c-di-GMP was removed by centrifugation of the liposomes via Airfuge (Beckman-Coulter) and quantification of c-di-GMP encapsulation efficiency was determined by UV absorption at 254 nm. Cryoelectron microscopy (Jeol 2100F TEM) and dynamic light scattering (Wyatt Dyna Pro Plate Reader II) were performed by the Swanson Biotechnology Center at the Koch Institute.

4.2.3. In vivo immunization studies

Female BALB/c mice 6-7 weeks of age were purchased from Jackson Laboratories for all immunizations, and handled under federal, state, and local guidelines. Mice were immunized by injection of 100 μL MPER liposome solutions (40 μg MPER peptide) s.c. at the tail base, 50 μL on each flank, and boosted on days 21 and 42 with the same formulations. Where indicated, MPER liposomes included 17.5 μg MPLA or lipid-PEG-CpG as adjuvant. Alternatively, 100 uL cdGMP liposomes (5 μg cdGMP) were administered s.c. at the tail base, 50 uL per side, directly following MPER liposome injection. T-cell help was incorporated as 100 μg LACK1 peptide or 20 μg HIV30 peptide as indicated. Serum was collected weekly via retro-orbital bleeding for subsequent ELISA-based titer analyses.

4.2.4. Immune response analyses

For T-cell responses, mice were euthanized and 300,000 splenocytes in single cell suspensions were seeded into 96-well plates with or without 5 μM HIV30 peptide. Cells were incubated for 48 hours, and supernatants were collected for cytokine analysis using a Milliplex MAP mouse Th17 Magnetic Bead Kit from EMD Millipore (Billerica, MA) and the Bio-Plex 3D suspension array system from Bio-Rad (Hercules, CA). MPER-specific antibody levels were detected by ELISA: 96-well Nunc Polysorp plates (ThermoFisher) were coated with 25 μg/mL streptavidin (Jackson ImmunoResearch, West Grove, PA), blocked with 1% w/v BSA in PBS (BSA-PBS), washed with 0.05 Tween 20 in PBS, and incubated for 2 hours with 2 μg/mL biotin-MPER in BSA-PBS, washed, and then incubated for 2 hours with serially diluted serum samples. Following another washing step, the plates were incubated for 90 minutes with HRP-conjugated goat anti-mouse IgG (Bio-Rad) in BSA-PBS, washed, developed with TMB substrate, and read on a Tecan Infinite M200 Pro (Männedorf, Switzerland) absorbance plate reader. HIV30-specific antibody levels were detected via ELISA in a similar manner; plates were directly coated with 100 μg/mL of HIV30, blocked, washed, and incubated with serum and IgG-HRP as described above. Titers were defined as the inverse serum dilution giving an absorbance of 0.3. Frequencies of germinal center (GC) cells in inguinal and axillary lymph nodes were determined by flow cytometry analysis using a FACS Canto II (BD Biosciences) following staining with markers for GC cells (anti-B220, anti-GL-7, anti-IgD, peanut

agglutinin (PNA) as well as 4',6-diamidino-2-phenylindole (DAPI, for live-dead analysis). Data were analyzed using FlowJo software (TreeStar, Oregon, USA).

4.2.5. Histology

Inguinal lymph nodes were isolated from immunized mice and frozen in Tissue-Tek O.C.T. Compound (Sakura Finetek, Torrance, CA). 10 μm tissue sections were prepared by the Swanson Biotechnology Center at the Koch Institute, and imaged on a Zeiss LSM 510 confocal laser scanning microscope.

4.2.6. Statistical analysis

Statistical analyses were performed using GraphPad Prism software. Comparisons of formulations over time employed two-way ANOVA tests and comparisons of multiple formulations at a single time point were performed using one-way ANOVA and Tukey's tests. Two-tailed unpaired t-tests were used to determine statistical significance between two experimental groups for all other data unless otherwise noted.

4.3. Results and Discussion

4.3.1. Immunogenicity of liposomes in comparison to traditional adjuvants

We first compared several candidate lipophilic formulations as potential adjuvants for MPER peptides. Liposomes incorporating palmitoylated MPER (pMPER) were prepared by lipid rehydration and extrusion; the hydrophobic pMPER was incorporated into PEGylated and non-PEGylated liposomes with efficiencies of 95±2.3% and 94±4.8%, respectively. Cryoelectron microscopy imaging of 150 nm diam. liposomes revealed the presence of unilamellar and multilamellar vesicles and incorporation of pMPER had no impact on liposome structure (Fig. 4-1A). In addition to liposomes, water/oil emulsions are classical adjuvants [36], which could potentially adsorb the hydrophobic pMPER to promote uptake by immune cells. We thus compared the immunogenicity of pMPER carried by liposomes, an oil-in-water emulsion (AddaVax), or a water-in-oil emulsion (Montanide), and also compared to the traditional adjuvant alum. The TLR-4 agonist monophosphoryl lipid A (MPLA) was included in all formulations as a molecular adjuvant[139]. Strikingly, even in the presence of MPLA, only liposomes primed anti-MPER IgG responses in all animals (Fig. 4-1B). Immunization with liposomes carrying lipid-anchored MPER and helper peptide without additional molecular adjuvants elicited a detectable but very weak immune response, but MPER liposomes adjuvanted with several different molecular danger signals– MPLA, lipid-PEG-CpG, or liposomal STING agonist cyclic-di-GMP (cdGMP) [140–142]– all primed 600-4600-fold higher anti-MPER titers (Fig. 4-1C). Note that to separately control the MPER and cdGMP

doses it was necessary to co-deliver cdGMP in separate liposomes. We focused on liposomes adjuvanted with MPLA or cdGMP for further studies.

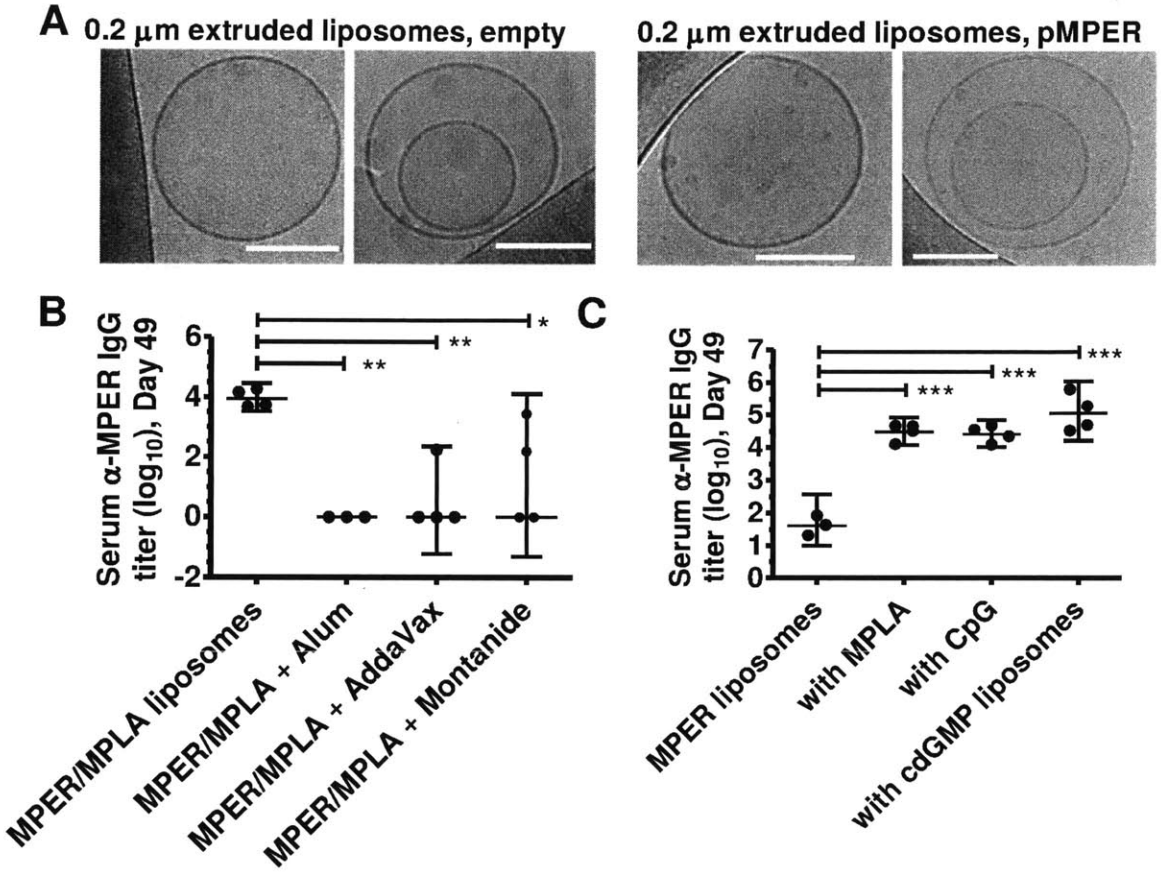

Figure 4-1. Humoral responses against MPER peptides are promoted by liposomal delivery and molecular adjuvants.

(A) Representative cryoelectron microscopy images of 150 nm mean diameter DOPC/DOPG liposomes with or without incorporated pMPER, scale bars 100 nm. (B-C) Groups of balb/c mice (n=3-4/group) were immunized on days 0, 21, and 42 with 40 μg pMPER peptide. (B) Anti-MPER serum IgG titers following immunization with pMPER delivered by liposomes, alum, or oil-based emulsions together with 100 μg soluble LACK1 helper peptide and 17.5 μg MPLA per injection. (C) Serum anti-MPER IgG titers following immunization with pMPER on 150 nm diameter liposomes adjuvanted with MPLA, lipid-PEG-CpG, or cyclic-di-GMP (cdGMP) liposomes. To provide $CD4^+$ T-cell help, formulations

*contained 20 μg of encapsulated HIV30. *, $p < 0.05$; **, $p < 0.01$; ***, $p < 0.001$ as determined by ANOVA followed by Tukey's multiple comparison test.*

4.3.2. Role of liposome physical properties in vaccine immunogenicity

Poly(ethylene glycol) (PEG) coatings are routinely used in drug delivery to limit liposome aggregation/fusion and enhance their penetration through tissue[143], and thus might promote trafficking of MPER liposomes to draining lymph nodes. However, because the MPER sequence embeds into the lipid membrane, PEGylation of MPER liposomes would also be expected to hinder antigen-specific B-cell engagement with the peptide. PEGylation has variously been reported to facilitate draining to lymph nodes [144] as well as to have no impact on lymph node draining[145]. We found that four hours after immunization with liposomes co-labeled with the lipid dye DiD and encapsulated AlexaFluor-conjugated ovalbumin (AF-OVA), both PEGylated and non-PEGylated liposomes were readily detected in both the primary (inguinal) and secondary (axillary) draining lymph nodes via IVIS-based fluorescent imaging of whole lymph nodes and confocal microscopy of histological lymph node sections (Fig. 4-2A-B). DiD (green) and AF-OVA (red) signals were co-localized in the subcapsular sinus of inguinal lymph nodes, suggesting that liposomes were still intact four hours post-immunization (Fig. 4-2A). Quantification of AF-OVA signal detected from whole lymph nodes via IVIS indicated that PEGylated liposomes trended toward increased accumulation in lymph nodes relative to non-PEGylated vesicles, but this did not reach statistical significance (Fig. 4-2B). However, this slight enhancement of vesicle trafficking achieved by PEGylation had no impact on immunogenicity (Fig. 4-2C).

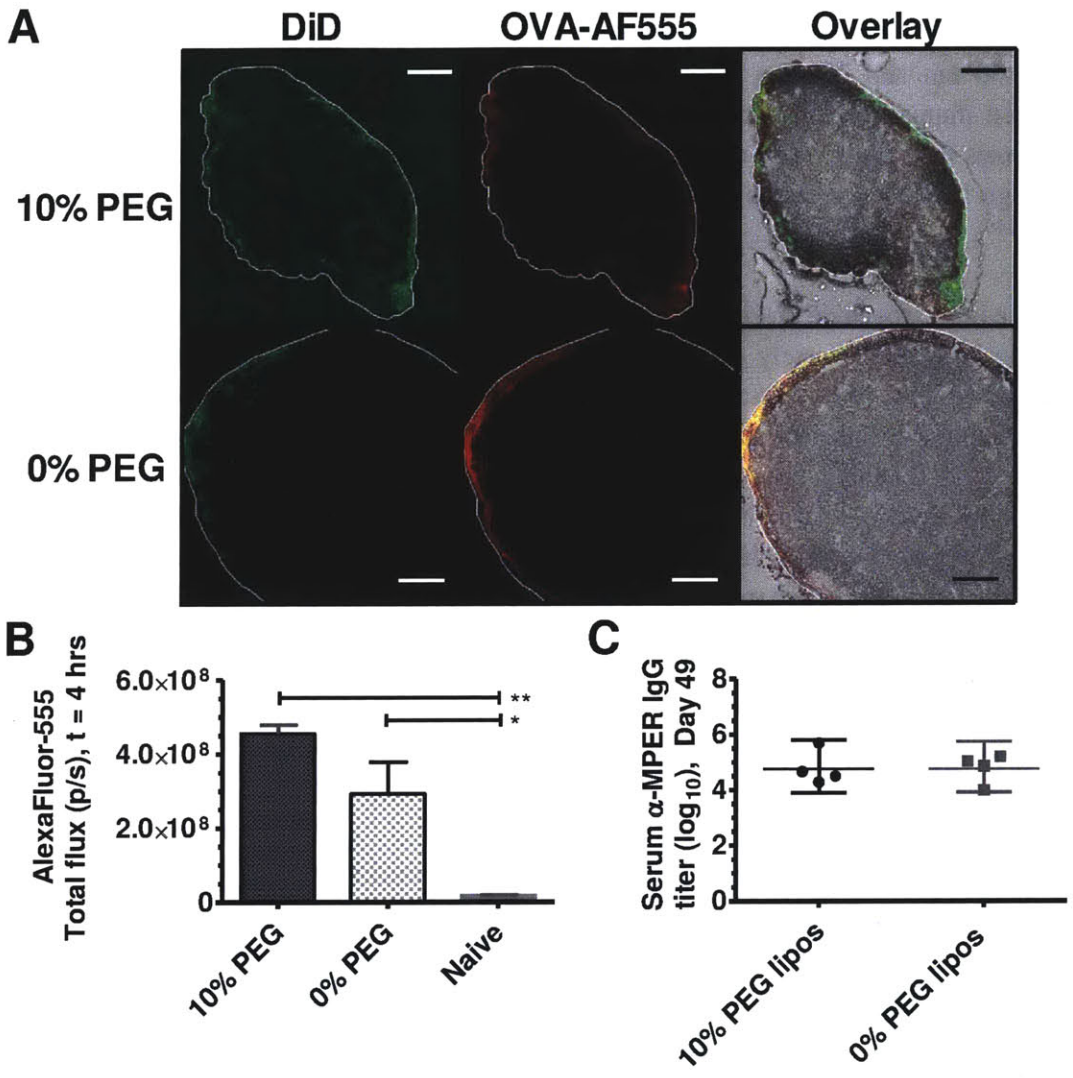

Figure 4-2. Anti-MPER humoral responses are independent of PEGylation.

*(A-B) Balb/c mice (n=3/group) were injected with 150 nm diameter pMPER liposomes with or without 10 mol% PEG-DSPE containing DiD lipid and OVA-AlexaFlour-555, followed by histological sectioning (red = OVA-AF555, green = DiD, 10x magnification, scale bar = 200 μm) of inguinal nodes (A) and IVIS-based fluorescence quantification of axillary and inguinal nodes at 4 hours post-immunization (B). *, $p < 0.05$; **, $p < 0.01$ as determined by Dunnett's test. (C) Anti-MPER titers at day 49 for balb/c mice (n=3/group) immunized as in (A) with pMPER/MPLA liposomes and LACK1 helper peptide on days 0, 21, and 42.*

Particle size plays a key role in vaccine responses, though optimal dimensions are likely dependent on particle composition and the type of immune responses desired[113]. In parallel to the liposome draining analyses, vesicles with mean diameters of 203±27 nm, 150±12 nm, or

64.5±5 nm were tested as MPER/MPLA delivery vehicles. Interestingly, immunization with the smallest 65 nm liposomes induced 20-fold and 15-fold lower MPER-specific IgG titers than 150 nm and 200 nm liposomes, respectively (Fig. 4-3A). This inverse relationship between immunogenicity and liposome size is in agreement with prior studies of flexible liposomes in the size range of 40 – 400 nm, where vesicle size was inversely correlated with drainage from the injection site but positively correlated with retention in draining lymph nodes[146].

The immunogenicity of protein or hapten antigens delivered by liposomes has been shown previously to be inversely proportional to membrane fluidity[104,147,148], and we expected a similar trend due to more stable anchoring of pMPER to vesicles with more rigid bilayers. In agreement with these predictions, immunization of mice with low-fluidity 2:2:1 DMPC:DOPC:DOPG liposomes (Average T_m = 6.7°C) or fully-fluid 4:1 DOPC:DOPG liposomes (Average T_m = -8.1C) showed that DMPC-containing vesicles elicited an average 6.2-fold higher titer than DOPC-only liposomes (Fig. 4-3B). We sought to test liposome compositions with higher mean melting temperatures, but found that pMPER peptides were unstable in lipid membranes with melting temperatures above 37°C (data not shown).

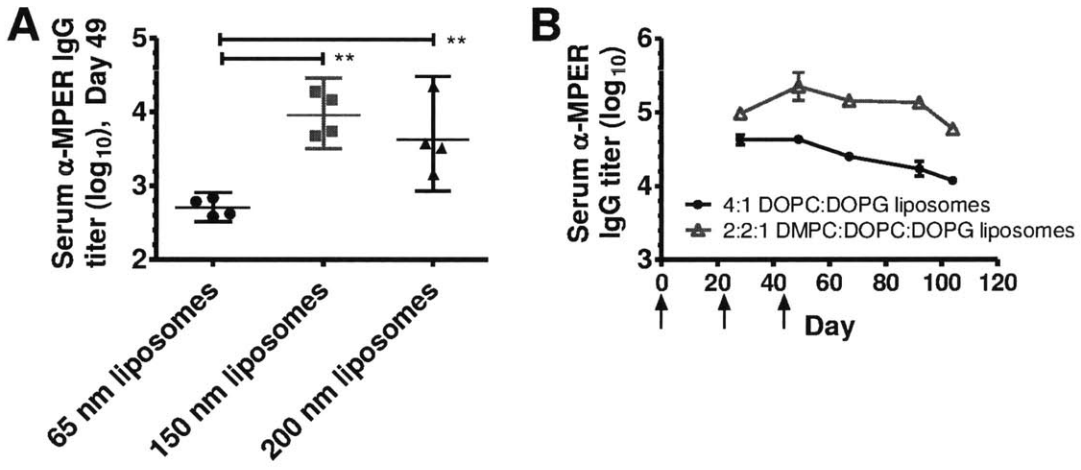

Figure 4-3. Anti-MPER humoral responses are shaped by particle size and liposome composition.

*(A) Serum anti-MPER IgG titers at one week after the third immunization in mice immunized with 65, 150 or 200 nm diameter PEGylated pMPER /MPLA liposomes and LACK1 helper peptide (** = p value < .01). (B) Mice were immunized as in (A) with 150 nm diameter PEGylated liposomes with a bilayer composition comprised of 4:1 DOPC:DOPG lipids or 2:2:1 DMPC:DOPC:DOPG lipids and serum MPER titers were followed over time; p < 0.0001 by two-way ANOVA.*

4.3.3. Relationship between antigen density and immunogenicity

Multivalent surface-display of antigen on particulates is known to enhance antibody responses, presumably by promoting BCR aggregation[55,149]. To understand how the surface density of antigen impacts pMPER immunogenicity, we immunized mice with a fixed total dose of antigen delivered on liposomes carrying varying quantities of pMPER per liposome. Serum antibody titers post-boosting indicated that 200 pMPER per liposome initially generated the highest MPER-specific IgG levels, but densities ranging from 40 to 1000 pMPER per liposome were all capable of generating high titers by day 50 (Fig. 4-4A). Interestingly, the highest antigen density tested, 2000 MPER/liposome, elicited substantially lower titers, suggesting that the optimal mean distance between peptides on the liposome surface is approximately 7 – 17 nm (Fig. 4-4B).

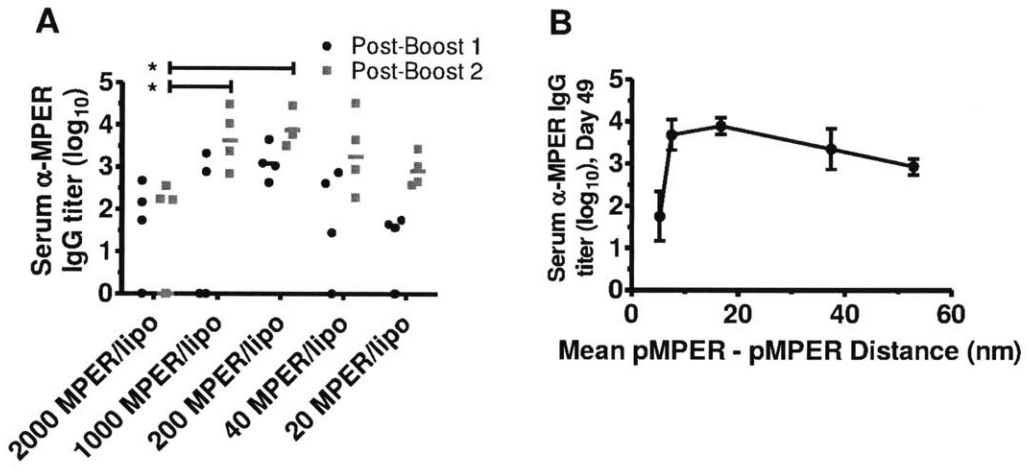

Figure 4-4. Anti-MPER humoral responses are maximized by liposomes carrying peptide with a mean spacing near 10 nm.

*Groups of balb/c mice (n=4/group) were immunized with PEGylated MPER/MPLA liposomes bearing 20-2000 peptides per vesicle on average, mixed with LACK1 helper peptide. (A) Dependence of serum anti-MPER IgG titers on the density of antigen per liposome. (B) Correlation of serum anti-MPER IgG titer and the mean distance between pMPER antigens on the liposome surfaces. *, $p < 0.05$ as determined by ANOVA followed by Tukey's multiple comparison test.*

4.3.4. Optimization of T-helper peptide delivery

Preliminary studies suggested that exogenous helper epitopes enhanced the humoral response against MPER peptides in balb/c mice[136], and thus our immunizations included either the model H-2^d-restricted LACK1 helper peptide (derived from Leishmania[150]) or HIV30, a

gp120-derived peptide known to be presented by both H-2^d in balb/c mice and HLAs of humans[151]. In order to maximize $CD4^+$ T-cell help through co-delivery of MPER and helper epitopes to B-cells while avoiding off-target antibody responses against the helper peptide, we tested three different methods for incorporating helper peptides into liposomes (Fig. 4-5A): Palmitoylated HIV30 anchored to the lipid bilayer ("palm HIV30"); HIV30 anchored through a disulfide linkage to a PEG tether on the bilayer ("uncleaved HIV30"); or disulfide/PEG-linked HIV30 cleaved from the external surfaces of the vesicles, leaving it incorporated only on the interior of the liposomes ("cleaved HIV30"). The latter formulations were obtained by exposing uncleaved HIV30 liposomes to the membrane-impermeable reducing agent TCEP, followed by removal of free peptide. We first compared the T-cell priming capacity of these 3 modes of intrastructural HIV30 co-delivery, vs. soluble HIV30 mixed with liposomes. Splenocytes from animals immunized with all 3 forms of MPER/HIV30 liposomes and restimulated *ex vivo* with HIV30 peptide secreted IL-4 (Fig. 4-5B) and IL-5 (Fig. 4-5C), but liposomes containing PEG-anchored HIV30 (cleaved or uncleaved) generated stronger TNF-α responses (Fig. 4-5D).

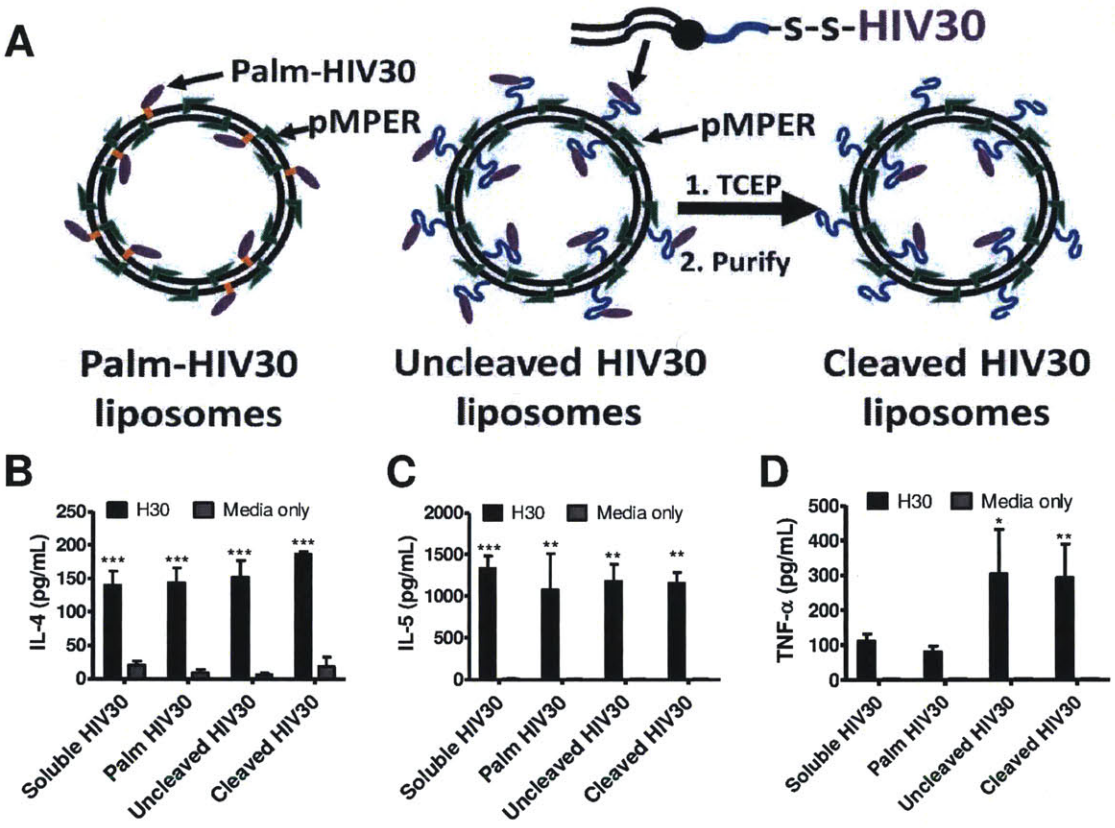

Figure 4-5. Liposomes carrying encapsulated bilayer-anchored helper peptide stimulate both Th1 and Th2 cytokine production from antigen-specific T-cells.

*(A) Schematic of 3 forms of T-helper epitope incorporation in MPER liposomes. (B-D) Groups of balb/c mice (n=3/group) were immunized as in Fig. 1 with 150 nm diameter pMPER liposomes containing the T-helper peptide HIV30 either in soluble form or incorporated into the MPER liposomes via a palmitoyl anchor or DSPE-PEG-S-S-HIV30 (cleaved or uncleaved) and all groups were adjuvanted by mixing with cdGMP liposomes. On day 28, splenocytes were isolated and restimulated ex vivo for 48 hours in the presence of 5 μM HIV30 peptide and concentrations of (B) IL-4, (C) IL-5, and (D) TNF-□, were determined via bead-based ELISA. *, $p < 0.05$; **, $p < 0.01$; ***, $p < 0.001$ for HIV30 vs. media only restimulation conditions as determined by two-way ANOVA and Bonferonni post-test.*

We next confirmed that HIV30 could enhance antibody responses to MPER, using the cleaved HIV30 form to co-incorporate the helper peptide into MPER liposomes. As shown in Fig. 4-6A, induction of anti-MPER IgG following immunization with MPER liposomes adjuvanted by cdGMP liposomes was dependent on the presence of HIV30, confirming

importance of the T-helper epitope. To compare the relative effectiveness of the 3 modes of helper epitope incorporation, mice were immunized with pMPER liposomes containing palm HIV30, uncleaved HIV30, cleaved HIV30, or pMPER liposomes co-administered with unencapsulated soluble HIV30; each vaccine was adjuvanted with cdGMP liposomes. While all 4 formulations elicited strong anti-MPER titers at 7 days post-boost, soluble HIV30 and cleaved HIV30 minimized off-target anti-HIV30 IgG titers (Fig. 4-6B). Flow cytometry-based assessment of germinal center B cell populations at 7 days post-boost indicated that all 4 formulations primed substantial germinal center B-cell populations (Fig. 4-6C). These results suggest that cleaved HIV30 offers the optimal balance between strong humoral MPER-specific responses, weak off-target antibody generation and strong induction of Th_1- and Th_2-associated cytokines.

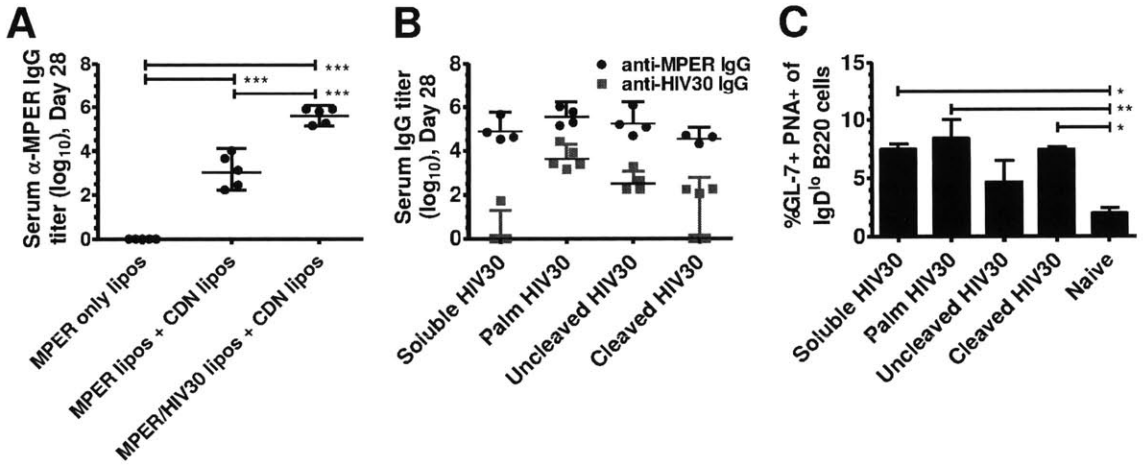

Figure 4-6. Liposomes with surface-displayed pMPER and encapsulated HIV30 promote strong B-cell responses against MPER while minimizing off-target responses against the helper epitope.

*(A) Balb/c mice (n=5/group) were immunized with cdGMP liposomes mixed with 150 nm diam. pMPER liposomes with or without cleaved DSPE-PEG-S-S-HIV30 helper epitope on days 0 and 21, and serum IgG titers were measured on day 28. ***, p value < 0.001 (B-C) Balb/c mice (n=3-4/group) were immunized as in Fig. 1 with 150nm MPER liposomes containing the T-helper peptide HIV30 either in soluble form or incorporated into the MPER liposomes via a palmitoyl anchor or DSPE-PEG-S-S-HIV30 (cleaved or uncleaved); all groups were adjuvanted with cdGMP liposomes. Shown are serum anti-MPER and anti-HIV30 IgG titers at seven days post-boost 1 (B) and frequencies of germinal center B-cells in draining lymph nodes at 7 days post-boost 2 (C). *, $p < 0.05$; **, $p < 0.01$ as determined by Dunnett's comparison to control test.*

4.4. Conclusions

MPER is a highly hydrophobic sequence near the transmembrane domain of gp41, which exhibits substantially enhanced immunogenicity when displayed on the surface of liposomes. In order to design a potent MPER vaccine, we systematically optimized three critical elements of a liposomal MPER vaccine: liposome properties, adjuvant incorporation, and T-cell help. The present studies demonstrate that humoral responses to liposomal MPER vaccines are impacted by all three of these components. Importantly, anti-MPER antibody responses are potently adjuvanted by the inclusion of TLR-4, TLR-9, or STING agonists, and are maximized by incorporation of high surface densities of MPER and the inclusion of high melting temperature lipids. The data suggest that 150 nm diameter, 2:2:1 DMPC:DOPC:DOPG liposomes adjuvanted with MPLA or cdGMP and incorporating encapsulated T-cell helper epitopes achieve strong and durable antibody responses against gp41 MPER peptides, while limiting competing humoral responses against the helper sequence itself. Further structural studies are necessary to optimize the orientation of MPER peptides for broadly neutralizing responses to HIV[136], but these results provide a clear guide to enhancing the immunogenicity of novel MPER constructs.

5. Development of cyclic-di-nucleotides as potent humoral adjuvants

5.1. Introduction

Adjuvant have become essential components of vaccine formulations in order to promote durable and effective immune responses to subunit vaccines[152–154]. Advances in our understanding of innate immunity have enabled the identification of new danger-sensing receptors relevant for design of molecular adjuvants acting on defined innate immune signaling pathways. In particular, pattern recognition receptors (PRRs) are key receptors of the innate immune system whose role is to identify pathogenic microorganisms and promote appropriate immune responses. The most-studied PRRs so far are the Toll-like receptors (TLRs), and monophosphoryl lipid A (MPLA), a derivative of lipopolysaccharide that binds Toll-like receptor-4 (TLR4), is the first example of a molecular adjuvant targeting a defined PRR approved for use in human vaccines[39]. The development of immunomodulators capable of stimulating additional PRR pathways offers the possibility of tuning immune responses to achieve appropriate protective immune responses to poorly immunogenic subunit antigens.

Recently, much attention has focused on cytosolic danger sensors, and particularly the cytosolic nucleotide sensor STING (stimulator of interferon genes). STING, which localizes to the endoplasmic reticulum, is a potent inductor of type I interferons in response to sensing cyclic dinucleotides (CDNs)[42]. The cyclic dinucleotides recognized by STING are small molecule second messengers used by all phyla of bacteria[44], and are also produced as endogenous products of the cytosolic DNA sensor cyclic GMP-AMP synthase (cGAS)[45–47]. The canonical bacterial CDN, cyclic-di-guanosine monosphophate (cdGMP), has been shown to directly bind STING and subsequently initiate IRF3- and NF-κB-dependent immune responses[48–50].

In parallel to these structural and molecular biology studies defining the pathways by which CDNs stimulate innate immunity, chemically synthesized cyclic dinucleotides including cyclic di-GMP, cyclic di-IMP, and cyclic di-AMP have begun to be explored as possible adjuvants for subunit vaccines, with particular success in promoting mucosal immunity to intranasal (i.n.) vaccines[42,155–157]. While these early studies point to the potential of CDNs as adjuvants promoting both T-cell and humoral responses to subunit vaccines, the potency of STING agonists as parenteral adjuvants for systemic immunity remains unclear. For example, while vaccines administered with modest doses of cdGMP (5 μg) have been reported to elicit substantial antibody titers to highly immunogenic model antigens such as ovalbumin or beta-galatosidase[156,158,159], this same dose of cdGMP administered with haemagluttinin protein as a clinically-relevant influenza antigen was completely ineffective as a parenteral vaccine[142]. Similarly, cdGMP administered s.c. with HIV pseudovirions was

also ineffective at adjuvanting humoral responses against the HIV *env* protein[160]. Karaolis et al. reported that parenteral (i.m.) vaccination with cdGMP adjuvanted humoral responses to the *Staphylococcus aureus* clumping factor A antigen, but much higher doses of CDN (145 μg) were used[161]. Parenteral immunization with 70-290 μg cdGMP and heptatitis B surface antigen similarly elicited robust humoral responses, but this response was also accompanied by substantial inflammatory cytokine and chemokine production in the systemic circulation 24 hr post immunization[162]. Such systemic inflammatory signatures are problematic for prophylactic vaccines, and are likely due to systemic dissemination of these low molecular weight adjuvants, as has been seen with other small-molecule adjuvants such as resiquimod[163]. Altogether, these reports suggest that cyclic dinucleotides may be effective adjuvants for weakly immunogenic antigens, but that finding an acceptable balance between potency and toxicity may be challenging for unformulated CDNs[164].

An effective strategy to simultaneously enhance the potency and safety of molecular adjuvants is to formulate these compounds in carriers such as nanoparticles. Nanoparticle vehicles such as polymer particles or liposomes can promote adjuvant transport through lymphatics to draining lymph nodes while blocking dissemination into the systemic circulation[165,166]. Concentration of molecular adjuvants in lymph nodes using nanoparticle carriers can also enable profound dose sparing of molecular adjuvants and this approach has been demonstrated for a number of TLR agonists including monophosphoryl lipid A, CpG DNA, polyI:C and small-molecule TLR7/8 compounds[40,58,62,86,167–169]. Importantly, a number of TLR agonist-carrying particle formulations have been demonstrated to effectively adjuvant the immune response when simply admixed with particulate or soluble antigen, i.e. without requiring co-incorporation of antigen and adjuvant together in particles[62,170–172]. Liposomal and oil-based nanoparticle emulsions carrying TLR agonists have also been shown to be effective in early stage clinical trials[39,72,173].

Motivated by these findings, here we tested the hypothesis that concentration of CDNs within lymphoid tissues through the use of a nanoparticle delivery vehicle could both enhance their relative potency and decrease systemic inflammatory side effects, providing a means to exploit STING signaling for enhanced cellular and humoral immunity without toxicity. Using a liposomal nanoparticle formulation of cdGMP, we found that efficient lymphatic delivery of CDNs has a broad impact on both innate and adaptive immune responses including potent activation of antigen-presenting cells, expansion of vaccine-specific helper T-cells, and robust induction of germinal center B-cell differentiation. These cellular responses to nanoparticle-CDN vaccination correlated with strong and durable vaccine-specific antibody induction equivalent to ~30-fold higher doses of soluble cyclic dinucleotides, without the systemic inflammatory toxicity of the latter. These enhancements in humoral immunity achieved by nanoparticle-delivered CDN adjuvants were dependent on TNF-α signaling but

not type I interferons. The majority of this work has been submitted as a first author publication in the *Journal of Clinical Investigation.*

5.2. Materials and Methods

5.2.1. Materials

Lipids 1,2-dioleoyl-*sn*-glycero-3-phosphocholine (DOPC), 1,2-dioleoyl-*sn*-glycero-3-phoshpo-(1'-rac-gylcerol) (DOPG), 1,2-dimyristoyl-*sn*-glycero-3-phosphocholine (DMPC), 1,2-distearoyl-*sn*-glycero-3-phosphoethanolamine-N-[methoxy(polyethylene glycol)-2000] (DSPE-PEG), and 1,2-distearoyl-*sn*-glycero-3-phosphoethanolamine-N-[PDP(polyethylene glycol)-2000] (DSPE-PEG-PDP) were purchased from Avanti Polar Lipids. Solvents, bovine serum albumin (BSA) and monophosphoryl lipid A (MPLA,from *Salmonella enterica* serotype minnesota Re 595 cat. no. L6895) were purchased from Sigma Aldrich. Cyclic di-GMP was purchased from Invivogen and $cdGMP_{DY547}$ from BIOLOG Life Science Institute and dissolved in ddH_2O. The $CD4^+$ T-cell helper peptides OT-II (CKISQAVHAAHAEINEAGREV) and HIV30 (RRNIIGDIRQAHCNISRAKW) and the MPER peptide (ELDKWASLWNWFNITNWLWYIK) were synthesized at the Tufts University Core Facility. MPER was purchased with either an N-terminal biotin (for ELISAs) or palmitoyl tail (for immunizations). For membrane-anchored DSPE-HIV30 and DSPE-OT-II conjugates, HIV30 or OT-II were linked to DSPE-PEG-PDP via the cysteine residue of each peptide, by dissolving HIV30 or OT-II in DMF with 1.5 equivalents of DSPE-PEG-PDP and agitating at 25°C for 18 hours. The conjugates were then diluted in 10x deionized water, lyophilized into powder, and redissolved in deionized water. Peptide concentrations were determined by Direct Detect infrared spectroscopy analysis (EMD Millipore).

5.2.2. NP-MPER and NP-cdGMP synthesis

A 2:2:1 molar ratio of DMPC:DOPC:DOPG in chloroform with palm-MPER added at a 1:200 MPER:lipid mole ratio was dried under nitrogen followed by incubation under vacuum at 25°C for 18 hr. Liposomes incorporating MPLA, DSPE-HIV30 or DSPE-OTII were prepared by including these components in the organic solution prior to drying lipid films. Lipids were hydrated with pH 7.4 PBS to a final concentration of 26.5 mM lipid and vortexed 30 seconds every 10 minutes for an hour. The resulting NP-MPER vesicles were passed through six freeze-thaw cycles between liquid nitrogen and a 37°C water bath followed by extrusion 21 times through 0.2 μm pore polycarbonate membranes (Whatman Inc), respectively. For NP-cdGMP, a 38:38:19:5:0.95 molar ratio of DMPC:DOPC:DOPG:DSPE-PEG:c-di-GMP in chloroform was dried under nitrogen followed by incubation under vacuum at 25°C for 18 hr and following drying, the resulting lipid/c-di-GMP films were resuspended

at 240 μg/mL of c-di-GMP in PBS and then freeze/thawed and extruded to form 150 nm liposomes. Unencapsulated c-di-GMP was removed by centrifugation of the liposomes via Airfuge (Beckman-Coulter) and quantification of c-di-GMP encapsulation efficiency was determined by UV absorption at 254 nm. To synthesize $cdGMP_{DY547}$ lipid nanoparticles, $cdGMP_{DY547}$ was used in lieu of cdGMP at the lipid dry down step. To synthesize fluorescently labeled 'mock' cdGMP lipid nanoparticles, a dried lipid film of DMPC:DOPC:DOPG:DSPE-PEG (at a 38:38:19:5:0.95 molar ratio) was rehydrated in 520 μg/mL OVA_{AF647} (Invitrogen) in PBS (lipid concentration = 35.6 mM) and synthesized as before.

5.2.3. In vivo immunization studies

Balb/c, C56BL/6 (B6), and CD90.1 OT-II B6 mice were purchased from The Jackson Laboratory. Experiments were conducted using female mice 6-8 weeks of age and handled under federal, state, and local guidelines under an IACUC protocol. Groups of mice were immunized with 100 μL MPER liposomes in PBS (40 μg MPER peptide) s.c. at the tail base, 50 μL per side. Where indicated, 100 μL soluble or liposomal cdGMP in PBS (5 ug cdGMP unless otherwise noted) was administered immediately following NP-MPER injection, s.c. at the tail base, 50 μL per side. Serum was collected via retro-orbital bleeding on a weekly basis for subsequent ELISA-based analyses. For TNF-α blockade experiments, mice received 0.5 mg of anti-TNF-α antibody (clone XT3.11, Bio X Cell) or IgG_1 isotype control antibody (clone HRPN, Bio X Cell) i.p. at 24 hrs and 0.5 hrs prior to immunization, as described previously [174]. For IFN-α/β receptor blockade experiments, mice received 1 mg of anti-IFNAR1 antibody (clone MAR1-5A3, Bio X cell) or IgG_1 isotype control antibody (clone MOPC-21, Bio X Cell) i.p. 24 hrs prior to immunization, as described previously [175]. For plasmacytoid dendritic cell depletion experiments, mice received 0.5 mg of anti-PDCA1 antibody (clone 120G8, Bio X Cell) or IgG_1 isotype control antibody (clone HRPN, Bio X Cell) i.p. at 48 hours prior to immunization [176].

5.2.4. CDN characterization studies

For *in vitro* CDN release from lipid nanoparticles studies, aliquots of $cdGMP_{DY547}$ liposomes in in PBS containing 10% BSA (dose of 1 μg $cdGMP_{DY547}$) were placed into 10,000 MWCO Slide-A-Lyzer MINI Dialysis units (ThermoFischer) and each aliquot was incubated in reservoirs of 10% BSA in PBS at 37°C. Presence of $cdGMP_{DY547}$ in reservoirs over time was measured (3 samples per timepoint) via fluorescence (ex. 545/em. 584) using a Tecan Infinite M200 Pro (Männedorf, Switzerland) absorbance/fluorescence plate reader. For *in vivo* studies of lymph node drainage of CDN, mice were injected s.c. with 100 μL PBS (50 μL on each side of the tail base) containing 2 μg $cdGMP_{DY547}$ either in soluble or NP form. For each mouse, inguinal and axillary lymph nodes were subsequently collected (3 mice per time point), pooled together, massed, and incubated for 18 hrs in 1:25 Liberase TM (Roche) in PBS. Lymph nodes were then sonicated for 30 seconds at 3 watts output power using a Misonix XL-2000

probe sonicator. Following addition of 10% trichloroacetic acid in methanol, samples were centrifuged at 18,000 rcf for 15 mins. Detection of $cdGMP_{DY547}$ in supernatants was measured via fluorescence (ex. 545/em. 584) using a Tecan Infinite M200 Pro absorbance/fluorescence plate reader.

5.2.5. OT-II T-cell adoptive transfer and ex vivo restimulation studies

For adoptive transfer studies, $OTII^+$ $CD4^+$ T-cells were isolated from CD90.1 OT-II B6 mouse splenocytes using an EasySep CD4 T-cell isolation kit (StemCell Technologies,) and transferred to C57Bl/6 recipients by i.v. retro-orbital injection at 1 x 10^5 cells/mouse. 24 hours later, mice were immunized with NP-MPER vaccines containing the DSPE-OTII helper peptide. Seven days after immunization, inguinal and axillary lymph nodes were collected for subsequent analysis via flow cytometry. For *ex vivo* OT-II restimulation studies, B6 mice were immunized on days 1, 28 and 42 with OT-II-containing vaccines. On day 49, $3x10^5$ splenocytes in single cell suspensions were seeded onto 96-well plates with or without 5 μM OT-II peptide, incubated for 48 hours, and cytokine levels in supernatants were assessed using a Milliplex MAP mouse Th17 Magnetic Bead Kit from EMD Millipore and the Bio-Plex 3D suspension array system from Bio-Rad.

5.2.6. Antibodies and Flow cytometry

For analyses of antigen presenting cells, inguinal and axillary lymph nodes were subjected to enzymatic digestion (Collagenase/Dispase and DNAse I, Roche) in order to obtain single cell suspensions as previously described [177]. For all other flow cytometric-based analyses, single cell suspensions were obtained by passage of tissues through a 70 μm filter (BD Biosciences). Cells were incubated for 15 mins at 25°C with anti-CD16/32 and then for 30 mins at 25°C with the following antibodies, all purchased from eBioscience unless otherwise specified. For the activation of antigen presenting cells: CD4, CD69, CD11c, B220, CD11b, Ly6G, NK1.1, CD8α, PDCA1 (927), CD86, and MHCII. For germinal center staining: B220, CD138, CD3, GL-7, IgD, and PNA. For $OT\text{-}II^+$ $CD4^+$ T-cell staining: CD90.1, CXCR5, CD8α, CD4, B220, and CD44. Flow cytometric analysis was carried out using a BD Canto or BD Fortessa (BD Biosciences), and analysis of cells was performed using FlowJo software (Tree star Inc.).

5.2.7. Quantitative PCR analysis

Lymph nodes were isolated from immunized mice, snap frozen in liquid nitrogen and stored at -80°C for future use. Frozen lymph nodes were homogenized and RNA was isolated using the RNeasy Pluse Universal Mini Kit (Quiagen) according to the manufacturer's protocol. Total RNA was extracted using RNeasy Plus Universal Kit (Qiagen) and quantified using a NanoDrop spectrophotometer (Thermo Fischer). Multiplex primers were designed

using the PrimeTime qPCR assay (Integrated DNA Technologies). Primer sequences are as follows: *mouse IFNB1,* (forward) *5'*-CGAGCAGAGATCTTCAGGAAC-3' and reverse 5'-TCACTACCAGTCCCAGAGTC-3'; *mouseRSAD2,* (forward) 5'-ACACAGCCAAGACATCCTTC-3' and (reverse) 5'-CAAGTATTCACCCCTGTCCTG-3'; and *mouseGAPDH,* (forward) 5'-CTTTGTCAAGCTCATTTCCTGG-3' and (reverse) 5'-TCTTGCTCAGTGTCCTTGC-3'. One-step cDNA synthesis and RT-PCR reactions were set up with 200 ng total RNA using LightCycler 480 RNA Master Hydrolysis Probes kit (Roche) according to manufacturer instructions, and analysis was performed on a Roche Light Cycler 480 II real-time system.

5.2.8. Plate and bead-based ELISAs

MPER-specific antibody levels were detected by ELISA: 96-well Nunc Polysorp plates (ThermoFisher) were coated with 25 μg/mL streptavidin (Jackson ImmunoResearch, West Grove, PA), blocked with 1% w/v BSA in PBS (BSA-PBS), washed with 0.05% Tween 20 in PBS, and incubated for 2 hours with 2 μg/mL biotin-MPER in BSA-PBS, washed, and then incubated for 2 hours with serially diluted serum samples. Following another washing step, the plates were incubated for 90 minutes with HRP-conjugated goat anti-mouse IgG (Bio-Rad) in BSA-PBS, washed, developed with TMB substrate, and absorbance at 450 nm was read on a Tecan Infinite M200 Pro plate reader. HIV30-specific antibody levels were detected via ELISA in a similar manner; plates were directly coated with 100 μg/mL of HIV30, blocked, washed, and incubated with serum and IgG-HRP as described above. Titers were defined as the inverse serum dilution giving an absorbance of 0.3. To determine post-immunization serum cytokine responses, serum was collected at 6 hours post-immunization and levels of IFN-β were detected by VeriKine-HS Mouse IFN-β serum ELISA kit (PBL Assay Science) and levels of IFN-γ, TNF-α, and IL-6 were determined by Milliplex MPA mouse Th17 Magnetic bead kit (EMD Millipore).

5.2.9. Statistical analysis

Statistical analyses were performed using GraphPad Prism software. Comparisons of formulations over time employed two-way ANOVA tests and comparisons of multiple formulations at a single time point were performed using one-way ANOVA and Tukey's tests. Two-tailed unpaired t-tests were used to determine statistical significance between two experimental groups for all other data unless otherwise noted.

5.3. Results and Discussion

5.3.1. Lipid nanoparticles concentrate cdGMP in lymph node APCs

In preliminary studies, we confirmed that as reported for other antigens[142,160], modest doses (5 μg) of cyclic di-GMP (cdGMP) administered with weakly immunogenic proteins (e.g. HIV gp120) or low doses of highly immunogenic antigens like ovalbumin were ineffective for adjuvanting humoral responses above protein alone following parenteral immunization (data not shown). To determine if this lack of efficacy reflected insufficient transport of CDNs to draining lymph nodes (dLNs), we assessed lymph node accumulation of cdGMP following s.c. injection, employing a fluorophore-conjugated derivative to enable detection of cdGMP in the tissue. As shown in Figure 5-1A, CDN levels in the dLN remained < 4 ng/mg tissue at all time-points post-injection of unformulated cdGMP. By flow cytometry, cdGMP fluorescence was undetectable above background in $B220^+$ B-cells, $CD11c^+CD8\alpha^+$ dendritic cells (DCs), or $CD11c^+CD8\alpha^-$ DCs, and only found in 2.1±2.6% of macrophages (identified as $NK1.1^-CD11c^-CD11b^+Ly6G^-SSC^{lo}$ cells[178], Appendix A, Supplemental Figure S5-1) from inguinal or axillary LNs (Figure 5-1B-C). Inefficient capture of cdGMP in the lymph nodes is consistent with the low molecular weight of cyclic dinucleotides, which will be capable of absorption directly into blood capillaries from the injection site. Indeed, measurement of cdGMP in the blood showed rapid systemic dissemination of the soluble CDN following injection (Figure 5-1A).

Both the potency and safety of CDNs as candidate adjuvant compounds should be enhanced by concentration in local lymphoid tissues. We thus developed a liposomal nanoparticle formulation of cdGMP to enhance the delivery of these compounds to lymphatics and promote their capture in draining lymph nodes by APCs. Cyclic di-GMP was encapsulated in phosphatidylcholine liposomes containing 5 mol% of a PEGylated lipid; PEG reduces nonspecific interactions of the vesicles with serum proteins/matrix, enabling better retention of encapsulated drugs [179] and modestly enhances lymphatic uptake of liposomes [180,181]. PEGylated lipid nanoparticles loaded with fluorescently-labeled cdGMP were relatively stable in serum, releasing only 4% of the encapsulated CDN when incubated in the presence of 10% serum at 37°C for 3 days (Figure 5-1D). *In vitro*, DCs internalized cdGMP in soluble or nanoparticle forms to equivalently high levels (Figure 5-1E). However, in contrast to the results with free CDN, subcutaneous injection of nanoparticle-cdGMP (NP-cdGMP) led to substantial accumulation of the STING agonist in the dLNs, peaking at ~60 ng/mg tissue at 24 hr (15-fold greater than unformulated CDN) and slowly decaying over the subsequent 2 days (Figure 5-5-1A). At 24 hr post injection, particle-delivered cdGMP was detected in ~8% of LN macrophages and 3-4% of $CD8\alpha^-$ and $CD8\alpha^+$ DCs, but with little uptake observed in B-cells (Figure 5-1B-C). To track the kinetics of lipid nanoparticle uptake by dendritic cells over time, we encapsulated fluorescent ovalbumin (OVA_{AF647}) in the particles as a bright tracer, co-injected a 50/50 mixture of NP-cdGMP and NP-OVA_{AF647}, and analyzed the frequency of NP-OVA_{AF647}^+ cells in dLNs over time. As shown in Figure 5-1F, the frequency of $NP^+CD8\alpha^+$

DCs remained relatively constant over 2 days, but $NP^{+}CD8\alpha^{-}$ DCs continued to increase in frequency to a peak of ~8% at 48 hr before decaying. Coincident with increased delivery to lymph nodes, nanoparticle delivery of cdGMP blocked dissemination of cdGMP into the systemic circulation (Figure 5-1A).

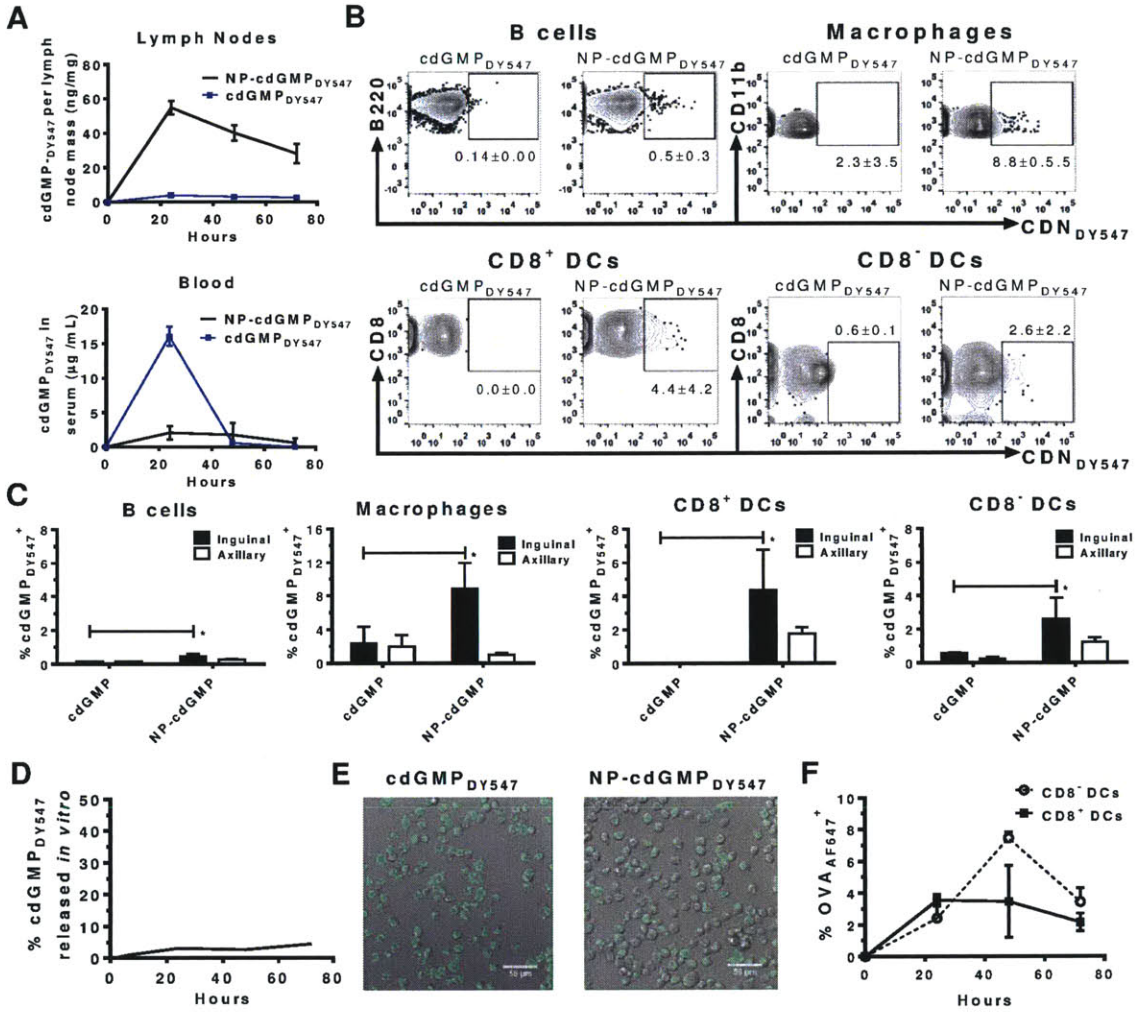

Figure 5-1. NP-cdGMP enhances lymph node uptake of cyclic dinucleotides.

*(**A**) Groups of balb/c mice were injected with $dGMP_{DY547}$ and CDN in draining lymph nodes (top panel, 2 μg $cdGMP_{DY547}$/mouse, n=3/group) or serum (lower panel, 5 μg $cdGMP_{DY547}$/mouse, n=5/group) were traced by fluorescence spectroscopy. (**B**) Representative flow cytometry plots of CDN fluorescence in APCs 24 hrs following s.c. injection of 2 μg $cdGMP_{DY547}$ or NP- $cdGMP_{DY547}$. (**C**) Mean percentages of $cdGMP_{DY547}^+$ of APCs in inguinal or axillary lymph nodes at 24 hrs after immunization of NP- or soluble $cdGMP_{DY547}$ (n=3/group). *, $p < 0.05$; as determined by ANOVA followed by Tukey's multiple comparison test. (**D**) Kinetics of $cdGMP_{DY547}$ release from NPs incubated in PBS containing 10% serum at 37°C. (**E**) Representative images of DC2.4 cells after 2 hour incubations with NP- or soluble $cdGMP_{DY547}$. (**F**) Percent OVA_{AF647}^+ of dendritic cells over time following injection of NP-cdGMP and NP-OVA_{AF647} (n=4/group).*

5.3.2. *NP-cdGMP induces type I IFN directly in lymph nodes and elicits greater APC activation than soluble CDN*

To determine the impact of enhanced lymph node delivery on the adjuvant activity of cyclic dinucleotides, we evaluated CDNs as adjuvants for a poorly immunogenic vaccine antigen, the membrane proximal external region (MPER) from HIV gp41. The MPER antigen, which as part of the HIV envelope trimer is thought to reside in juxtaposition to the viral membrane [123,124], was formulated as a palmitoyl-anchored peptide displayed on the surface of liposomes that also contained a helper epitope derived from gp120 (denoted HIV30[151]) tethered by PEG to the inner leaflet of the vesicles (Figure 5-2A). We have previously shown that this nanoparticle MPER formulation (NP-MPER) elicits extremely weak anti-MPER humoral responses in the absence of co-administered molecular adjuvants[136]. Thus, we compared NP-MPER vaccines adjuvanted with soluble cdGMP or NP-cdGMP (Figure 5-2A).

We first assessed the activation of antigen presenting cells (APCs) in dLNs following cdGMP/NP-MPER immunizations. Twenty hours after NP-MPER + NP-cdGMP vaccination, both CD86 and MHC-II were strongly upregulated on $CD8\alpha^+$ and $CD8\alpha^-$ dendritic cells (Figure 5-2B-C), while NP-MPER + soluble cdGMP elicited much weaker CD86 and MHC-II expression. CD86 and CD69 were also upregulated on a large proportion of B-cells following NP-cdGMP immunization, while soluble cdGMP induced these activation markers on a minority of these cells (Figure 5-2D). Tracking the frequencies of $CD86^+$ APCs over time revealed distinct dynamics for APC activation induced by soluble vs. nanoparticle cdGMP: DC activation was low and peaked at 48 hr following NP-MPER vaccination with soluble cdGMP as adjuvant. By contrast, vaccination with NP-cdGMP as adjuvant elicited ~4-fold higher frequencies of activated DCs, which remained elevated for 48 hr before decaying toward baseline (Figure 5-2E). In addition, the peak frequency of macrophage activation was 3-fold higher in NP-cdGMP-adjuvanted vaccination than in soluble cdGMP-adjuvanted vaccination. As expected, non-adjuvanted NP-MPER vaccines elicited lower frequencies of activated APCs than either of the cdGMP-adjuvanted groups.

The induction of activation markers on a majority of lymph node APCs following NP-cdGMP immunization indicated that many more APCs were activated than directly acquired cdGMP, indicating strong *in trans* activation of B-cells and DCs by $cdGMP^+$ cells. To distinguish between direct action of CDNs locally in dLNs vs. stimulation of lymph nodes remotely via cytokines produced at the vaccine injection site, we evaluated the expression of IFN-β, a signature product of STING activation by cdGMP[182,183]. RT-PCR analysis of dLNs showed that NP-MPER + NP-cdGMP immunization induced robust expression of both *IFNB1* and its downstream gene target *RSAD2* that peaked 20 hr post-injection, reaching 35-fold higher levels relative to soluble cdGMP vaccination (Figure 5-2F). Non-adjuvanted vaccines showed minimal IFN-β expression at any time point. Thus, concentration of CDNs in LNs by

nanoparticle delivery induced by a much greater frequency of activated APCs and higher expression of activation markers on a per-cell basis compared to vaccination with unformulated CDNs, which correlated with evidence for direct activation of type I IFN expression in lymph nodes by the nanoparticle formulation.

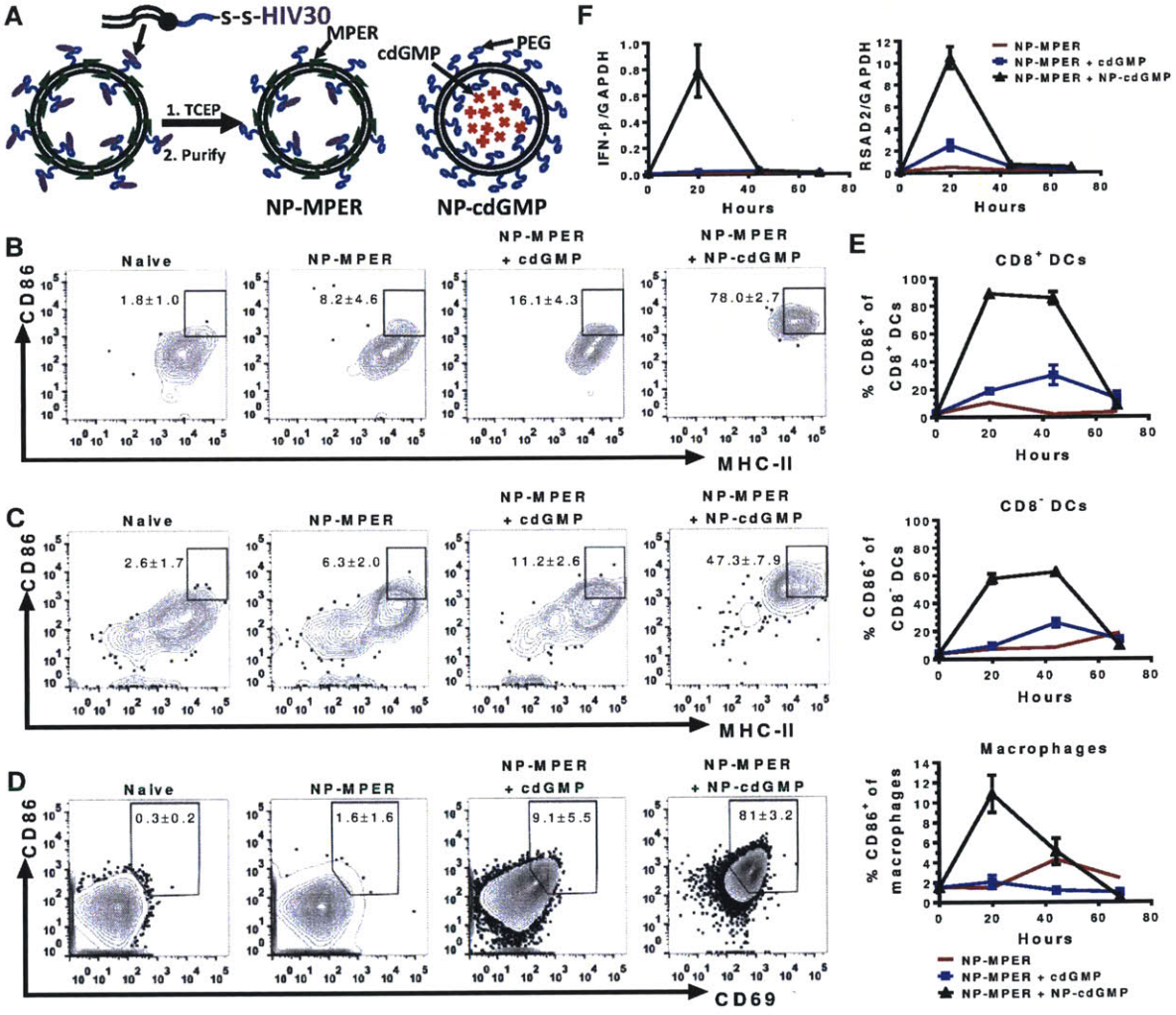

Figure 5-2. NP-cdGMP potently activates antigen presenting cells.

*(**A**) Schematic of NP-MPER + NP-cdGMP vaccine. (**B-F**) Balb/c mice (n=4/group) were immunized with NP-MPER alone, NP-MPER + 5 μg cdGMP, or NP-MPER + 5 μg NP-cdGMP, and draining lymph nodes were collected 20, 42, or 68 hours later for analysis. Shown are representative flow cytometry data for CD86 and MHCII expression on $CD8\alpha^+CD11c^+$ cells (**B**), $CD8\alpha^-CD11c^+$ cells (**C**), and $B220^+$ B-cells (**D**). Gates are annotated with mean frequency±SD for each group. (**E**) Expression levels of IFN-β and RSAD2 over time in dLNs as determined by RT-PCR. (**F**) Percent $CD86^+$ APC populations as a function of time. Shown are representative data from one of two independent experiments.*

5.3.3. Nanoparticle delivery of cdGMP enhances expansion of helper T-cells and promotes germinal center induction

Follicular helper T-cells (T_{FH} cells) provide critical signals to germinal center B-cells in support of humoral immunity[184]. To test the impact of cdGMP adjuvants on the expansion of vaccine-specific helper T-cells and T_{FH} cell differentiation, we used an adoptive transfer model employing OVA-specific OT-II TCR-transgenic $CD4^+$ T-cells and liposomal MPER vaccines incorporating the OT-II cognate peptide antigen instead of HIV30 as a helper epitope. $CD90.1^+$ OT-II $CD4^+$ T-cells were adoptively transferred into C57Bl/6 recipients, which were immunized 24 hrs later with MPER vaccines carrying the OT-II epitope with or without addition of cdGMP or NP-cdGMP. One week post-immunization animals were sacrificed for flow cytometry analysis. As shown in Figure 5-3A, immunization with liposomes lacking T-helper peptide or using soluble cdGMP adjuvant failed to significantly expand $OT\text{-}II^+$ cells compared to unadjuvanted liposomes. By contrast, vaccination with MPER/OT-II + NP-cdGMP induced a substantial expansion of the transferred OVA-specific T-cells, with 5.1-fold more $OT\text{-}II^+$ cells recovered on day 7 compared to soluble cdGMP-adjuvanted vaccines (Figure 5-3A-B). The greater increase in T-cell expansion for NP-cdGMP seen in total cell counts compared to cell frequencies was a result of substantially greater lymph node swelling and total LN cell numbers in NP-cdGMP-vaccinated mice (data not shown). The frequency of antigen-specific T-cells differentiating to a $CXCR5^+PD\text{-}1^+$ follicular helper phenotype was only slightly greater for NP-cdGMP- vs. soluble- cdGMP adjuvanted vaccines (Figure 5-3C), but the much greater overall expansion of the antigen-specific T-cell population in the former vaccines led to 5.3-fold more OT-II T_{FH} cells (Figure 5-3D). In parallel, we assessed endogenous T-cell responses to NP-MPER/OT-II + CDN vaccines in C57Bl/6 mice (with no adoptive transfers). Splenocytes from all of the vaccine groups that received helper peptide produced IL-4 and IL-5 when restimulated with OT-II peptide ex vivo, but only animals vaccinated with NP-cdGMP as adjuvant also produced IFN-γ and TNF-α (Figure 5-3E).

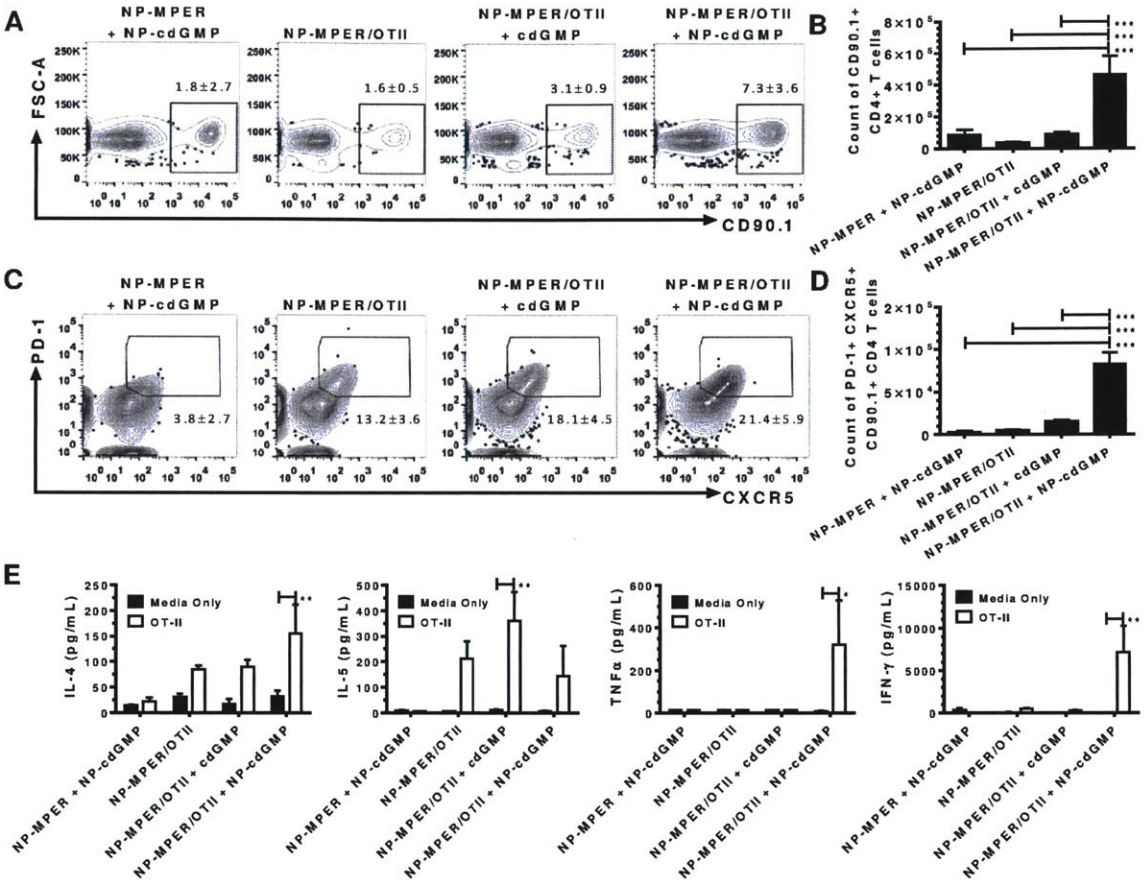

Figure 5-3. NP-cdGMP promotes antigen-specific CD4⁺ T-cell expansion.

(A-D) *C57Bl/6 mice (n=4/group) received adoptive transfer of 10^5 CD90.1⁺ OT-II CD4 T-cells, and were immunized 24 hrs later with NP-MPER with or without the OT-II helper epitope and with or without addition of cdGMP or NP-cdGMP. One week later, OT-II T-cell responses were characterized via flow cytometry. Shown are representative flow cytometry plots* ***(A, C)*** *and total cell counts* ***(B, D)*** *of total CD90.1⁺ OT-II T-cells and CXCR5⁺PD-1⁺ OT-II cells, respectivley. Data are combined from two independent experiments (in total n=8 mice/group).* ***(E)*** *C57Bl/6 mice (n=3/group) without OT-II adoptive transfer were immunized were immunized as in (A) on days 0, 21, and 42 and on day 49 splenocytes were restimulated for 48 hrs with OT-II peptide or media only and supernatants for assessed for cytokines by bead-based ELISA. *, $p < 0.05$; **, $p < 0.01$; ***, $p < 0.001$; as determined by ANOVA followed by Tukey's multiple comparison test for* ***(B, D)*** *and Bonferroni's multiple comparison test for* ***(E)****.*

Given the enhanced expansion of follicular helper cells stimulated by NP-cdGMP, we next examined B-cell differentiation and germinal center (GC) induction following CDN-adjuvanted immunizations. Groups of mice were immunized with NP-MPER with or without

cdGMP adjuvants, and 8 days post-immunization, B-cell differentiation in draining lymph nodes was analyzed via flow cytometry. None of these primary NP-MPER immunizations induced substantial plasmablast differentiation (Figure 5-4A-B). However, germinal center induction was strongly impacted by NP-cdGMP adjuvants; mice which received NP-MPER + NP-cdGMP showed greatly increased numbers of PNA^+ $GL\text{-}7^+$ GC B-cells (Figure 5-4C-D).

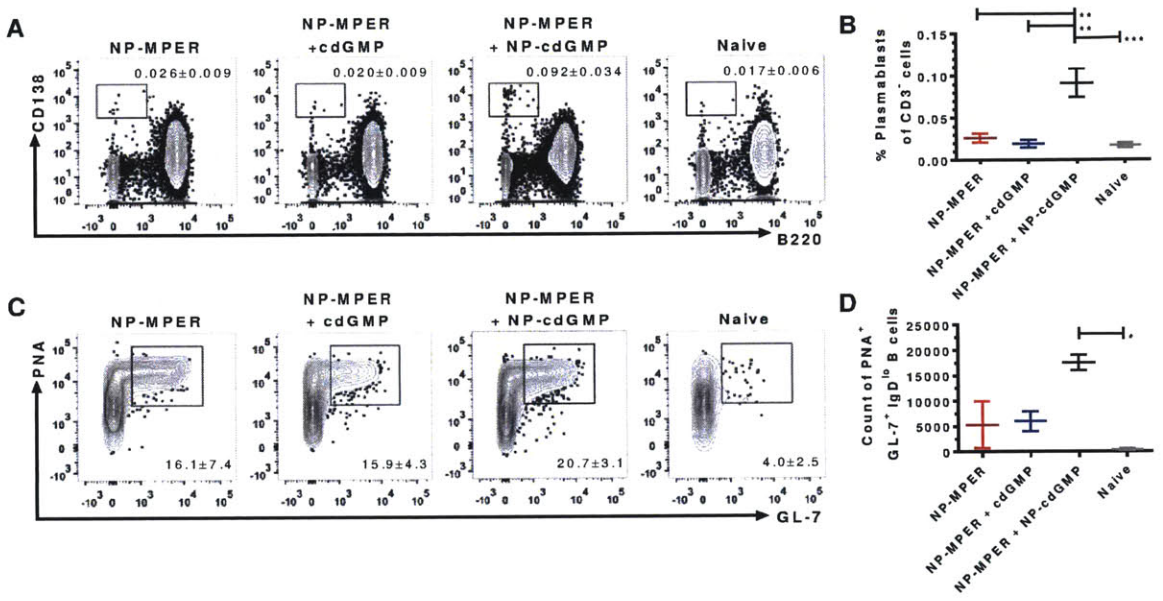

Figure 5-4: Primary plasmablast and germinal center formation is enhanced with NP-cdGMP.

*(**A-D**) Balb/c mice (n=4/group) were immunized with NP-MPER/HIV30 alone or adjuvanted with 5 μg cdGMP or NP-cdGMP. Draining lymph nodes were collected 8 days post-immunization for analysis via flow cytometry. (**A, B**) Representative flow cytometry plots (**A**) and frequencies (**B**) of $CD138^+B220^-CD3\varepsilon^-$ plasmablasts. (**C, D**) Representative flow cytometry plots (**C**) and cell counts (**D**) of $GL\text{-}7^+PNA^+IgD^{lo}B220^+$ germinal center B-cells. (**D**) Cell counts of GC B cells. *, $p < 0.05$; **, $p < 0.01$; ***, $p < 0.001$; as determined by ANOVA followed by Tukey's multiple comparison test.*

5.3.4. cdGMP nanoparticles promote strong humoral responses while avoiding systemic cytokine induction

To determine the impact of enhanced helper T-cell expansion and germinal center induction by NP-cdGMP on the humoral immune response, we next assessed antibody titers elicited by CDN-adjuvanted vaccines. To address relative potency of the soluble vs. formulated cyclic dinucleotides, NP-MPER vaccines were administered as a prime and boost with 5 μg of NP-cdGMP, and compared to vaccines adjuvanted by soluble cdGMP in doses ranging from 5

to 150 μg. NP-cdGMP-adjuvanted vaccines elicited 8.2-fold higher levels of total anti-MPER serum IgG than the equivalent soluble cdGMP dosage, and 2 of 4 mice immunized with soluble cdGMP failed to mount any detectable IgG response at this dose of cdGMP (Figure 5-5A). NP-cdGMP similarly elicited enhanced MPER-specific IgG1 and IgG3 responses. Increasing the dose of unformulated cdGMP led to increasing MPER-specific IgG resonses, but only the highest dose of soluble cdGMP (150 μg) elicited antibody titers comparable to the nanoparticle CDN formulation (Figure 5-5A). However, measurement of serum inflammatory cytokines 6 hr post-immunization revealed that this roughly equi-potent dose of soluble cdGMP elicited much higher levels of systemic IL-6, TNF-α, and IFN-β than NP-cdGMP immunization (Figure 5-5B), with the latter suggesting systemic triggering of STING. Thus, NP-mediated concentration of cdGMP in lymph nodes enabled robust humoral immune responses to a poorly immunogenic vaccine to be achieved without concomitant induction of systemic inflammatory toxicity.

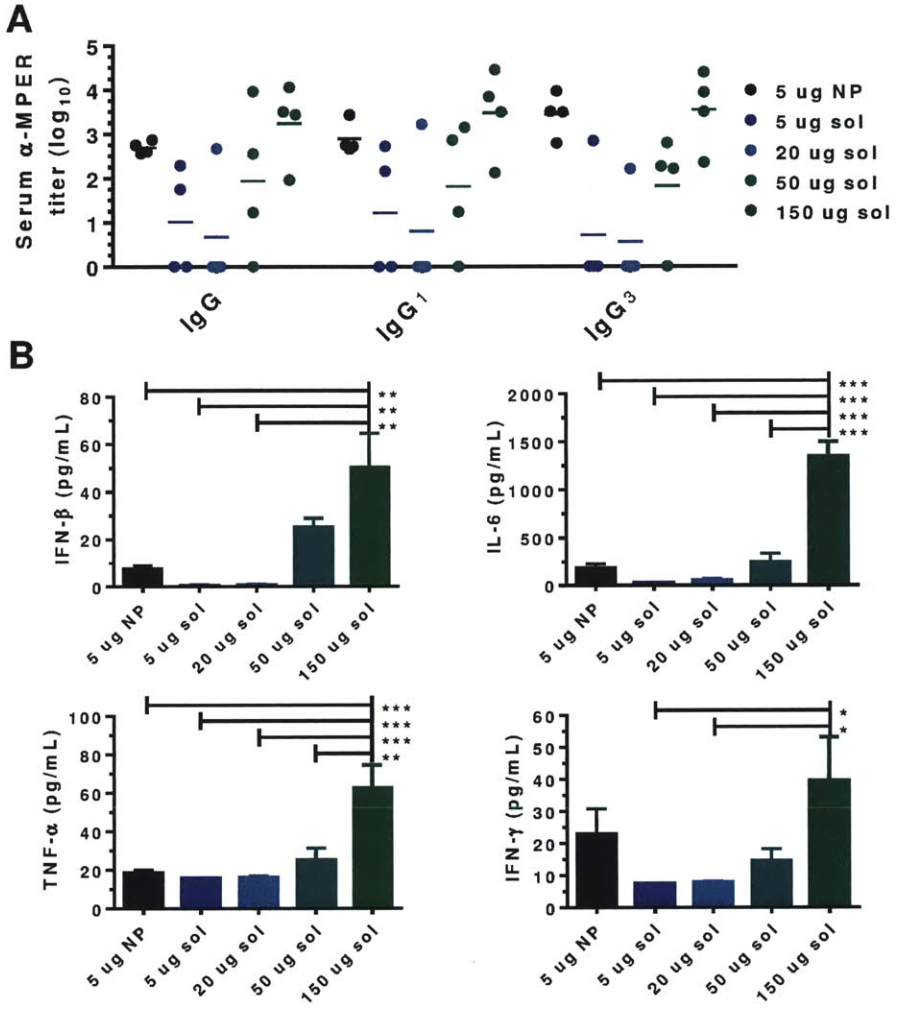

Figure 5-5. NP-cdGMP promotes robust humoral immunity while minimizing systemic cytokine induction.

Balb/c mice (n=4/group) were immunized on days 0 and 21 with NP-MPER/HIV30 combined with 5 μg NP-cdGMP or graded doses of soluble cdGMP. ***(A)*** *ELISA analysis of serum anti-MPER IgG, IgG_1 and IgG_3 titers at day 28.* ***(B)*** *Serum cytokine levels assessed at 6 hrs post-immunization via ELISA. *, $p < 0.05$; **, $p < 0.01$; ***, $p < 0.001$ as determined by ANOVA followed by Turkey's multiple comparison test.*

We next assessed the durability of humoral responses elicited by cyclic dinucleotide adjuvants and compared their potency to monophosphoryl lipid A (MPLA), a well-studied and effective adjuvant for humoral immunity representative of the Toll-like receptor 4 agonist adjuvants in several licensed vaccines[39,185]. Mice were immunized on days 0, 21, and 42 with NP-MPER alone, NP-MPER with co-incorporated MPLA, or NP-MPER adjuvanted by cdGMP or NP-cdGMP. Peak antibody titers 7 days after the second boost were 11-fold greater

for vaccines adjuvanted by NP-cdGMP compared to either soluble cdGMP or MPLA as adjuvant (Figure 5-6A). Antibody isotype analysis demonstrated that NP-cdGMP-adjuvanted vaccines consistently induced 20-100-fold higher MPER-specific IgG_1, IgG_{2A}, and IgG_3 responses compared to soluble cdGMP- or MPLA-adjuvanted vaccines (Figure 5-6B). Further, at 4.5 months after priming, MPER titers elicited by the MPLA-adjuvanted vaccine had waned by 40%, while vaccines administered with NP-cdGMP showed no decay in total serum MPER-specific IgG (Figure 5-6A). Even following two booster immunizations, vaccines adjuvanted by NP-cdMGP trended toward higher frequencies of germinal center cells in lymph nodes compared to NP-MPER/MPLA or NP-MPER + cdGMP vaccines (Figure 5-6C). Because distinct danger signal pathways can act in synergy [186,187] we also evaluated the relative effectiveness of MPER-NP vaccines adjuvanted with both MPLA and cdGMP. Addition of soluble cdGMP to MPLA/MPER-NP vaccines increased their post boost peak titer by 5.3-fold, while the addition of NP-cdGMP to the MPLA/MPER-NP vaccine increased peak anti-MPER IgG responses 67-fold, a response which remained approximately 10-fold above titers elicited by MPLA-only-adjuvanted vaccines for at least 150 days (Figure 5-6D). This same trend of enhancement was also observed in IgG_1, IgG_{2A}, and IgG_3 titers at day 49 (Figure 5-6E). Thus, cyclic dinucleotides promoted durable antibody responses, and even when compared to another nanoparticle-formulated molecular adjuvant (liposomal MPLA), NP-cdGMP elicited 11-fold greater steady-state antibody titers, which could be further modestly boosted by combining MPLA and CDNs as tandem adjuvants.

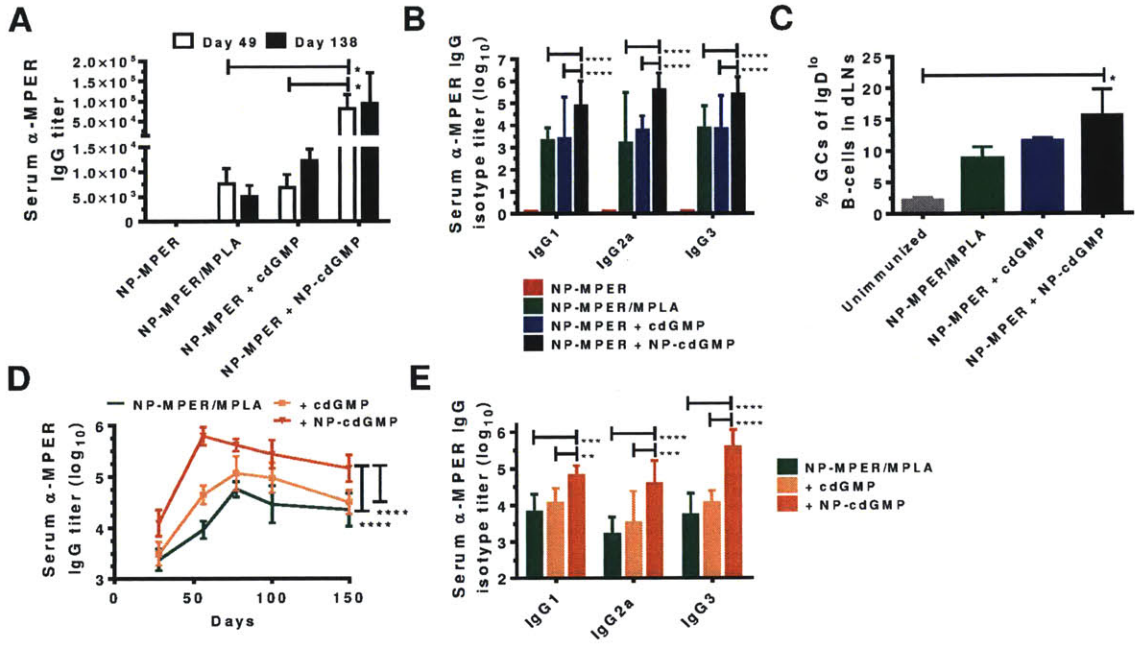

Figure 5-6. NP-cdGMP elicits durable class-switched humoral responses and synergizes with MPLA to adjuvant MPER vaccines.

*(**A-C**) Balb/c mice were immunized on days 0, 21, and 42 with NP-MPER/HIV30 alone, NP-MPER/HIV30/MPLA, or NP-MPER/HIV30 + cdGMP or NP-cdGMP. (**A**) Serum anti-MPER total IgG titers assessed via ELISA on days 49 138 (n=3/group). *, $p < 0.05$; as determined by ANOVA followed by Tukey's multiple comparison test. (**B**) ELISA analysis of specific isotypes of serum anti-MPER Ig at day 49 (n=3/group). (**C**) Percentages of $PNA^{+}GL\text{-}7^{+}IgD^{lo}B220^{+}$ germinal center B-cells in dLNs at day 49 (n= 3/group). *, $p < 0.05$ as determined by ANOVA followed by Tukey's multiple comparison test. Shown are data from one representative of two independent experiments. (**D-E**) Balb/c mice (n=4/group) were immunized on days 0, 21, and 42 with NP-MPER/HIV30/MPLA alone or additionally adjuvanted with cdGMP or NP-cdGMP. Shown are serum anti-MPER IgG titers over time (**D**) and specific isotype responses at day 49 (**E**) assessed via ELISA. Comparison of NP-MPER/MPLA vs + NP-cdGMP groups over time = $p < 0.0001$. Comparison of + soluble cdGMP vs + NP-cdGMP over time = $p < 0.0001$ as determined ANOVA followed by Tukey's multiple comparison test. **, $p < 0.01$; ***, $p < 0.001$; ****, $p < 0.0001$ as determined ANOVA followed by Tukey's multiple comparison test.*

5.3.5. Vaccine responses are independent of plasmacytoid dendritic cells

Although plasmacytoid dendritic cells (pDCs) are both major producers of type I interferon and activated by IFNs[188,189], it is unknown how CDNs affect pDCs and whether they play a role in the adjuvant activity of CDNs *in vivo*. To investigate how lymph node targeting of

cdGMP affected pDCs, mice were immunized with NP-MPER alone or with cdGMP adjuvants. Draining lymph nodes were collected 1 day later and $B220^+CD11c^+PDCA1^+$ plasmacytoid DCs were analyzed by flow cytometry (Supplemental Figure S5-2A). As shown in Figs. 5-7A-B, all of the immunizations induced an early decrease in the number of pDCs in draining lymph nodes, but cdGMP vaccines induced a remarkable sustained loss of these cells; pDCs were almost completely eliminated from dLNs of NP-cdGMP-immunized animals for several days. Quantification of pDC numbers in draining lymph nodes revealed that soluble cdMP and NP-cdGMP rapidly induced 3-fold and 11-fold losses of pDCs compared to naïve animals, respectively (Figure 5-7B). It has previously been shown that pDCs are engaged in an autocrine negative feedback loop with type I IFN: during viral infections, pDCs produce large quantities of interferons, which in turn induces their apoptosis in an autocrine manner and transiently depletes these cells[190]. However, the rapid loss of pDC populations by 20 hr following CDN-adjuvanted immunization suggests that these cells are not the source of the elevated levels of type I IFN expression detected in dLNs at this time point (Figure 5-2F). To confirm that pDCs were not playing an important role in the humoral response elicited by CDNs, mice were treated with a pDC-depleting antibody (or isotype control, Supplemental Figure S5-2B) and then immunized with NP-MPER + NP-cdGMP. Analysis of APC activation in draining lymph nodes indicated no difference in APC activation in pDC-depleted or control groups (Figure 5-7C). IgG antibody responses to the weakly immunogenic MPER peptide are weak to undetectable in the first two weeks after a single priming immunization, but responses against the HIV30 helper epitope co-carried by the liposomal vaccine were detectable at day 14 post-prime. Using these responses against the helper epitope as an early readout of the impact of pDC depletion on antibody production, we found that depletion of pDCs also had no effect on vaccine-specific antibody titers on day 14 (Figure 5-7D). Thus, pDCs do not appear to play an important role in the adjuvant activity of cyclic dinucleotides in the setting of parenteral immunization.

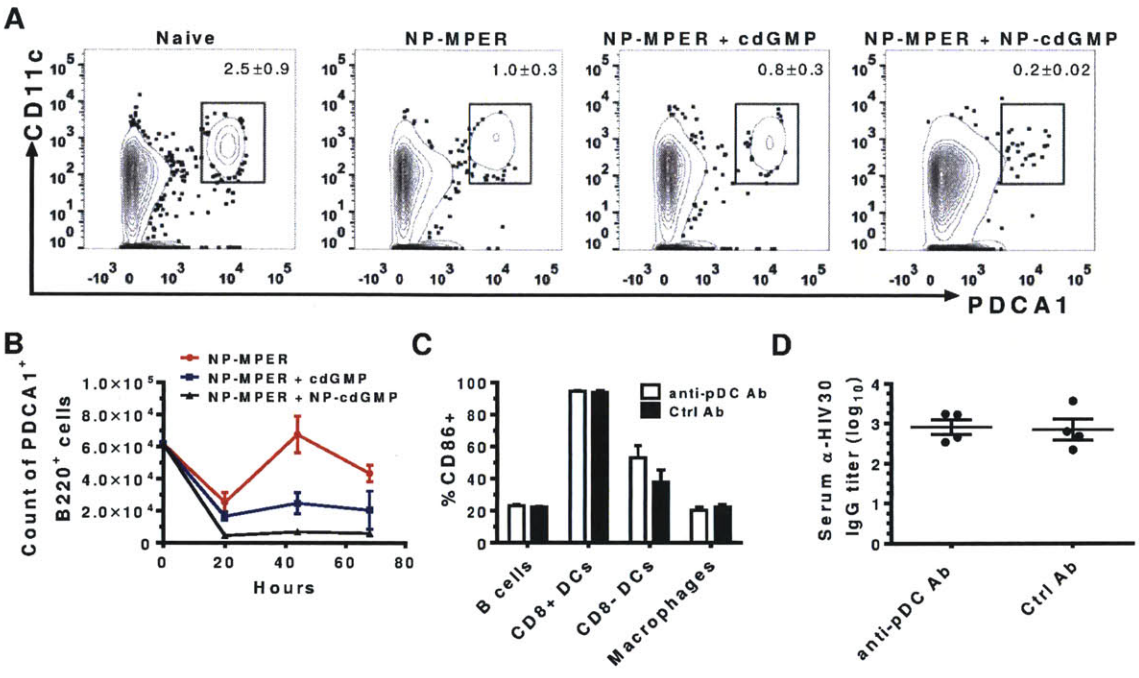

Figure 5-7. NP-cdGMP-adjuvanted vaccine responses are independent of plasmacytoid dendritic cells. (A-B)

*Balb/c mice (n=4/group) were immunized with NP-MPER alone or combined with cdGMP adjuvants. Shown are representative flow cyotmetry plots (**A**) and total cell counts (**B**) of PDCA1$^+$ CD11c$^+$ B220$^+$ plasmacytoid dendritic cells (pDCs) at 24 hours post-immunization. Gates in (A) shown mean±SD percentages of pDCs. Shown are data from one representative of two independent experiments. **(C-D)** Balb/c mice (n=4/group) were treated with pDC-depleting or isotype control antibodies and then immunized with NP-MPER/HIV30 + NP-cdGMP. **(C)** Mean percent CD86$^+$ APCs at 20 hours post-immunization. **(D)** Vaccine-specific anti-HIV30 antibody responses at 14 days post-immunization.*

5.3.6. Type I IFN and TNF-α play complementary roles following NP-cdGMP vaccination

The discordance between the frequency of APCs directly taking up NP-cdGMP and the extent of APC activation elicited by this adjuvant suggests that cytokine signaling in trans plays a critical role in the adjuvant activity of CDN nanoparticles. Type I interferons and TNF-α are major downstream products following cdGMP-induced activation of STING[155,191] and given the strong upregulation of IFN-β expression in lymph nodes 20 hr after NP-cdGMP immunization, we first examined the role of type I IFN in the response to NP-cdGMP immunization. To test the role of type I IFN signaling, mice were administered a blocking anti-

IFN-α/β receptor antibody (anti-IFNAR1) or its isotype control and then immunized with NP-MPER + NP-cdGMP. 24 hr post-immunization, animals treated with anti-IFNαR1 showed greatly reduced frequencies of CD86+ B-cells, macrophages, CD8α+ DCs, and CD8α- DCs relative to the isotype control group (Figure 5-8A). However, this reduction in early APC activation had no influence on early antibody titers against the HIV30 helper peptide at day 14 (Figure 5-8B). Blaauboer et al. previously observed that antibody responses to mucosal vaccines adjuvanted with soluble cdGMP were independent of type I IFN but dependent on TNF-α[191]. Although Blaauboer et al. used TNFR1-/- mice to demonstrate the role of this cytokine on the adjuvant action of cdGMP, we chose to investigate this question by administration of an anti-TNF-α blocking antibody, due to the absence of follicular dendritic cell networks observed in TNFR1-/- mice[192]. Twenty-four hours post-immunization with NP-MPER and NP-cdGMP, TNF-α-blocked mice exhibited marginal impairment in APC activation (Figure 5-8C), but at two weeks post-prime, TNF-α-blockade reduced vaccine-specific antibody titers 115-fold (Figure 5-8D). Thus, cdGMP targeted to lymph nodes via nanoparticle delivery acts through type I IFN and TNF-α to promote early APC activation and class-switched IgG production, respectively.

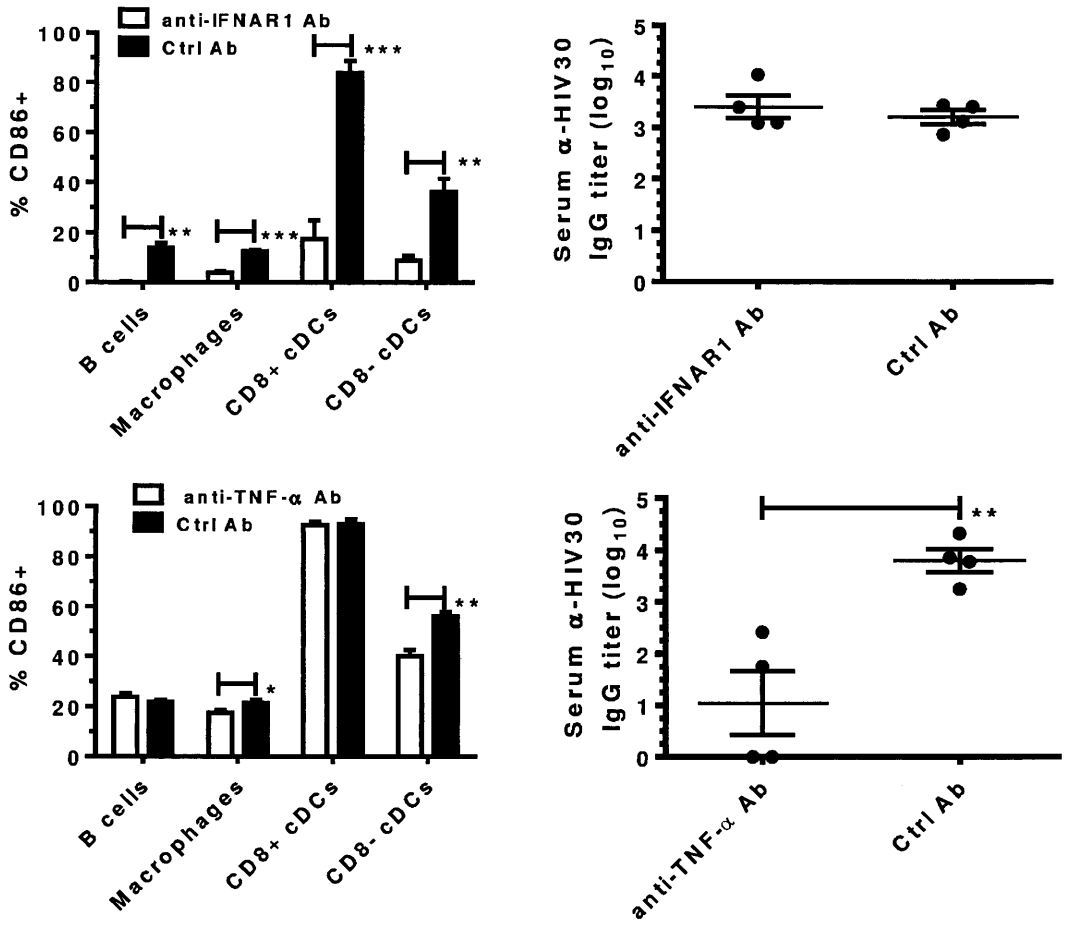

Figure 5-8. Type I IFN shapes early activation of antigen-presenting cells (APCS) while TNF-α is critical for IgG production following cdGMP-adjuvanted immunization.

*Balb/c mice (n=4/group) were treated with anti-IFN-α/β receptor 1 (IFNAR1), anti-TNF-α, or respective isotype control antibodies, then immunized with NP-MPER/HIV30 + NP-cdGMP. (A) Percentages of CD86⁺ APCs in the presence of anti-IFNAR1 or isotype control antibody at 24 hrs post-immunization. Data shown from one representative of two independent experiments. (B) Antigen-specific IgG titers at 14 days post-immunization in the presence or absence of IFNαR1 blockade. (C) Percentages of CD86⁺ APCs in the presence of anti-TNF-α or isotype control antibody at 24 hrs post-immunization. (D) Antigen-specific IgG titers in the presence or absence of TNF-α blockade at 14 days post-immunization. Data shown from one representative of two independent experiments. *, $p < 0.05$; **, $p < 0.01$; ***, $p < 0.001$ as determined by individual t-tests.*

5.3.7. Discussion

Cyclic dinucleotides are a relatively new class of immunomodulatory compounds with the potential to promote protective immunity through a unique pathway employing the cytosolic danger sensor STING and its downstream transcription factors NF-κB and IRF-3[42,140]. The publication of crystal structures demonstrating the structural basis for CDN sensing through STING[141,193] and the identification of endogenous CDNs as signaling products produced by cyclic GMP-AMP synthase sensing of double-stranded DNA[46,47,194] have provided both a rationale and mechanistic guidance for the development of cyclic dinucleotides as adjuvants acting through type I interferons and NF-kB activation in host cells. Indeed, several laboratories have recently demonstrated innate immune stimulatory[155,162,191] and adjuvant activities[140] with CDNs, particularly when applied as mucosal adjuvants. For example, Ebensen et al. first demonstrated that intranasal administration of soluble antigen and cdGMP induced higher antigen-specific serum IgG and mucosal IgA when using the model antigen β-galactosidase[156]. When administered intranasally with the *S. pneumonia* antigen pneumococcal surface protein A, cdGMP protected against *S. pneumonia* colonization[195]. The ability of structurally-related CDNs such as c-di-IMP and c-di-AMP to adjuvant mucosal immunizations has also been reported[158,196].

In contrast to the robust response to cyclic dinucleotides in mucosal immunization, the efficacy of CDNs as adjuvants in the setting of traditional parenteral immunization has been less clear, with much of the early published data focused on the use of CDNs to boost immunity against highly immunogenic model antigens and/or employing large doses of cyclic dinucleotides. As shown here, the limited potency of parenterally-administered CDNs reflects poor lymphatic uptake of these small molecule immunomodulators; they are instead cleared from tissues via the blood. This biodistribution issue is a property of molecular size: because the blood absorbs ~10-fold more fluid from tissues than lymph, molecules small enough to permeate blood vessels (< ~1 KDa) tend to show predominant clearance to the blood[197]. Therefore, increasing CDN-mediated vaccine responses through increased dosing of unformulated CDNs is accompanied by parallel increases in systemic inflammatory toxicity. This pharmacokinetic behavior is shared by other small-molecule adjuvant compounds such as resiquimod (R848) and related imidazoquinoline TLR7/8 agonist compounds, muramyl dipeptides that trigger NLRs, and RNA oligonucleotide ligands of RIG-I[163,198,199]. For example, parenteral injection of R848 is known to rapidly trigger systemic inflammatory cytokines similar to the systemic signature observed here for CDNs, and induces transient systemic lymphopenia within hours of injection[172,200]. To overcome these issues, a number of strategies have been explored to limit systemic exposure and/or re-focus molecular adjuvant delivery to lymph nodes, including conjugation of adjuvant compounds with lipid tails [200–202], directly coupling to large molecular weight antigens[203,204], or encapsulating in nano/micro-particles[62,86,168,172].

Here we demonstrate that nanoparticle delivery using PEGylated liposomal carriers substantially enhances the potency of the canonical CDN cyclic di-GMP, eliciting high titer, durable humoral responses to a model weakly immunogenic antigen at low doses of NP-cdGMP. These responses were only matched by ~30-fold higher doses of unformulated CDNs that may not be translatable to large animals or humans, and which induced substantial systemic cytokine induction. This increase in potency was achieved by increased lymph node accumulation of NP-cdGMP by 15-fold relative to soluble cdGMP injection. NP-cdGMP was avidly pinocytosed/endocytosed by dendritic cells *in vitro*, and despite the fact that these PEGylated nanoparticles were not designed to promote delivery of CDNs to the cytosol, we observed robust APC activation *in vivo*. However, it has recently been reported that STING is capable of sensing cyclic dinucleotides contained within impermeable vacuoles of host cells during *Chlamydia trachomatis* infection and it is hypothesized that the ER wraps around the vacuole, enabling ER-localized STING to detect vacuole-entrapped cdGMP[205]. Thus, APCs may harbor intrinsic mechanisms to sense endosomal CDNs.

Type I interferons are signature downstream products of STING activation by CDNs in host cells[182,183], and NP-cdGMP led to direct induction of type I IFN and downstream target gene expression in the draining lymph nodes. By contrast, soluble CDN administration induced no type I IFN in the dLNs, implying that its effects on APC activation are mediated by inflammatory cytokines produced at the injection site acting remotely on draining nodes. Such *in trans* activation of dendritic cells by inflammatory cytokines has been shown to elicit weaker priming of T-cell responses compared to *cis* activation of DCs directly through pathogen sensing receptors[206,207]. Direct type I IFN induction in LNs by NP-cdGMP correlated with more robust upregulation of costimulatory and activation markers on LN APCs, which occurred earlier and was more sustained (over ~48 hr) compared to soluble CDN vaccination. Coincident with enhanced APC activation, NP-cdGMP drove a 5-fold increase in vaccine-specific $CD4^+$ T-cell expansion compared to unformulated cyclic dinucleotides. Thus, nanoparticle delivery of CDNs enhanced both early antigen presenting cell activation and subsequent T-cell responses.

Our subsequent analyses focused on determining the impact of NP CDN delivery on humoral immunity, employing a liposomal gp41 peptide as a model poorly immunogenic vaccine antigen. First we examined the induction of antigen-specific follicular helper cells, because type I IFN induction in LNs by NP-cdGMP might be expected to drive T_{FH} differentiation[208]. Nanoparticle delivery of cdGMP only moderately affected the frequency of $CD4^+$ T-cells differentiating toward a follicular helper phenotype, but the much greater overall expansion of antigen-specific $CD4^+$ T-cells by NP-cdGMP compared to soluble CDN adjuvants in turn translated into 5.3-fold more vaccine-specific T_{FH} cells. In line with their expected importance in class switching and germinal center formation[184], increased numbers of specific T_{FH} were accompanied by enhanced germinal center B-cell differentiation, 11-fold

increased antigen-specific IgG titers, and humoral responses that were more durable than vaccines administered with the well-known TLR agonist MPLA. However, sera from these MPER-immunized animals did not neutralize HIV (data not shown), indicating that further structural refinements are required for this antigen to elicit antibodies capable of recognizing the functional stalk of the HIV envelope trimer[136].

The presence of interferon expression suggesting STING activation directly in dLNs led us to explore the source of type I IFNs following NP-cdGMP vaccination and to quantify the relative importance of the key downstream products of STING activation on the observed humoral responses. Plasmacytoid DCs are major producers of type I IFN, but paradoxically these cells appeared to be strongly ablated following immunization with cdGMP. pDC depletion was detected by 20 hr post immunization, contemporaneous with peak interferon expression, suggesting these cells are not the source of the type I IFN induced by NP-cdGMP. This finding is in agreement with a prior study reporting minimal human pDC activation by CDNs [155]. In further support of the idea that pDCs do not play an important role in the adjuvant function of CDNs, pDC depletion had no impact on either early APC activation or subsequent IgG production following NP-cdGMP immunization. While type I interferons are a characteristic product of STING activation, CDNs also trigger the production of TNF-α through NF-κB[183,191]. Both type I IFN and TNF-α have been shown to be important regulators of humoral immunity[174,209,210] but a recent study suggested that cdGMP applied intranasally adjuvants mucosal immunity in an type I IFN-independent, TNF-α-dependent manner[191]. Here we found that following NP-cdGMP vaccination, both pathways of STING signaling are involved, with early APC activation dependent on IFN-α signaling and early (day 14) class-switched antibody responses dependent on TNF-α.

In the interest of translational relevance, we employed a PEGylated liposome formulation with a composition similar in nature to clinically approved liposomal drugs[211]. A limitation of our bench-scale formulation approach was the relatively low CDN loading efficiency (~35%). However, more advanced polymer or lipid nanoparticle carriers[40,41] that achieve more efficient drug loading and/or lipophilic modifications to CDNs to promote liposome association (a strategy used successfully with imidazoquinoline adjuvants[200]) can readily be envisioned to circumvent this issue. Delivery of pattern recognition receptor agonists as adjuvants has variously been reported to require co-encapsulation in the same particle as the antigen (*in cis*)[212] or simply simultaneous delivery on separate particles (*in trans*)[62,172]. The ability of NP-cdGMP to adjuvant immune responses *in trans* to particulate antigen provides flexibility for vaccine production and facilitates inclusion of NP-cdGMP into existing vaccine platforms. Although many danger signals are effective in promoting immune responses in mice, type I IFN-inducing adjuvants have shown particular promise in non-human primate models[213,214] and humans[215,216] for promoting superior cellular and humoral immunity. The nanoparticle delivery strategy demonstrated here provides a simple means to promote both the

safety and efficacy of cyclic dinucleotides as a novel type I IFN-promoting adjuvant with potential relevance to human vaccine development. Altogether, these results suggest that lymph node-targeted CDNs can promote both strong antigen-specific T-cell priming and high-titer, durable antibody responses that outperform the strong benchmark adjuvant MPLA, suggesting these compounds are of interest for further development as candidate adjuvants.

5.4. Conclusions

Cyclic dinucleotides (CDNs) are agonists of the innate immune receptor stimulator of interferon genes (STING) and are of interest as potential molecular vaccine adjuvants. However, cyclic di-GMP (cdGMP) injected subcutaneously showed minimal uptake into lymphatics/draining lymph nodes (dLNs) and instead distributed rapidly to the bloodstream, leading to systemic inflammation. To redirect cdGMP to dLNs, we encapsulated the CDN in PEGylated lipid nanoparticles, which blocked systemic dissemination of the compound and enhanced its accumulation in dLNs 15-fold compared to unformulated cyclic dinucleotide. Combining CDNs with a liposomal HIV gp41 peptide as a model poorly immunogenic vaccine antigen, nanoparticle-cdGMP (NP-cdGMP) robustly induced type I interferon in dLNs, induced 5-fold greater expansion of vaccine-specific $CD4^+$ T-cells, and greatly increased the number of germinal center B-cells in dLNs compared to soluble CDN. Further, NP-cdGMP promoted durable antibody titers >10-fold higher than the well-studied TLR agonist monophosphoryl lipid A, and comparable to a 30-fold larger dose of unformulated cdGMP without the systemic toxicity of the latter. Thus, lymph node targeting of cyclic dinucleotides via nanoparticulate delivery simultaneously promoted enhanced safety and efficacy of CDNs, an approach broadly applicable to small molecule immunomodulators of interest for vaccines and immunotherapy.

6. Conclusions and future work

6.1. Lipid nanoparticles as vaccine adjuvants

We have designed and characterized a system for vaccine delivery that utilizes several advantages of lipid nanoparticles: surface display of antigen, efficient lymphatic drainage, and versatile packaging of immunomodulating adjuvants and T-helper peptides. While liposomes have a long history of use as adjuvants, this thesis is uniquely comprehensive in its exploration of liposomes for both peptide and protein antigens, its characterization of how liposome properties impact humoral immunogenicity, and its use of liposome-loaded immunomodulators as adjuvants. While the results described here are directly applicable to HIV vaccine development, they also broadly applicable to vaccine and cancer immunotherapy development in general.

Small, unilamellar liposomes were the focus of the bulk of this work after the investigation into the potency of lipid-coated microparticles (LCMPs) in Chapter 2. Here, we found that the lipid bilayer of LCMPs delaminated off of the PLGA core, and formed 180 nm diameter liposomes. We demonstrated that the *in situ* formation of these delaminated liposomes was responsible for the enhanced immunogenicity of LCMPs compared to synthetic liposomes or stabilized-bilayer LCMPs (whose bilayer does not delaminate). The decision to pursue synthetic liposomes rather than LCMPs was made due to the significantly better conjugation efficiency of antigen to liposomes and furthermore, in previous studies performed by Anna Bershteyn, MPER-loaded LCMPs elicited significantly weaker anti-MPER titers than MPER-loaded liposomes (data not shown).

In studies utilizing liposomes with surface-displayed gp120 monomer, humoral antibody responses were independent of the size of liposomes, the dose of gp120, and presentation of gp120 (Fc-4G or 4G). Conjugation of gp120 to liposomes was essential for humoral responses; soluble gp120 and plain liposomes alone elicited no response. Interestingly, anti-MPER titers proved to be more sensitive to liposome parameters. Density of MPER peptides per liposome, the presence of higher-T_M lipid (DMPC), and the size of liposome all affected MPER humoral responses. Due to the ease of MPER liposome synthesis (MPER peptide is produced synthetically in large quantities and MPER liposomes do not require purification), MPER-liposomes developed into our primary tool for studying the adjuvant abilities of liposomes. As it became clear that we had optimized liposome parameters (size, composition, etc) and yet still had only moderate immune responses, we shifted focus to providing $CD4^+$ T-cell help and PAMP-based help.

Although no particular form of T helper peptide construct resulted in significantly stronger anti-MPER titers, the cleaved form of DSPE-S-S-HIV30 (present only on the inner bilayer of

liposomes) was an ideal construct because it generated strong Th1/Th2 cytokine responses and minimal off-target anti-HIV30 titers. With respect to PAMP-based help, we developed liposome-encapsulated cyclic dinucleotides (CDNs) as a potent co-adjuvant formulation. Soluble CDN is rapidly disseminated systemically while liposomal CDN efficiently traffics to draining lymph nodes, where is induces the activation of APCs, the secretion of type I interferon, expansion of germinal centers B cells and vaccine-specific $CD4^+$ T-cells, and ultimately robust and long-lived anti-vaccine IgG responses. This TLR-independent adjuvant system is particularly attractive in its ability to synergize with TLR-based agonists (such as MPLA) and because CDN liposomes can co-delivered with any antigen formulation, which allows for rapid prototyping building off of existing vaccine systems.

6.2.Potential future work

Although 4G is an exciting potential HIV immunogen due to its ability to elicit VRC01-competing antibodies, we found that overall, the magnitude of antibody response elicited was too long to enable the purification of enough anti-gp120 antibodies to test for broadly-neutralizing antibodies when MPLA was the adjuvant. In future work, the potential of CDN liposomes to adjuvant gp120 liposome vaccines should be explored. In general, since CDN liposomes worked very well with the weakly immunogenic MPER peptide, it would be interesting to explore the application of CDN liposomes with other peptide-based cancer or infectious disease vaccines[217].

While we optimized the adjuvant and delivery parameters of the MPER vaccine system, there remains a fair amount of work to be done in antigen design. The palm-MPER induces antibodies focused primarily at the C-terminus (away from the palmitoyl anchor). As the bnAb 4E10 binds residues in the middle of the MPER peptide, the Ellis Reinherz group isactively working to find an MPER construct which elicits antibodies more 4E10-like. Furthermore, the stability of palm-MPER when exposed to serum is also an issue. Development of an improved anchor for MPER is in progress with a synthetic lipid strategy (Tyson Moyer of the Irvine Lab) and by utilizing the transmembrane region of gp41 (the Ellis Reinherz group).

Lastly, although the CDN liposome formulation is a potent adjuvant, to our knowledge, this is the first report of CDN nanoparticles as an infectious disease adjuvant. This means that there is a lot of exciting, unexplored scientific space within the field of nanoparticulate CDN. For example, the ability of CDN nanoparticles to elicit $CD8^+$ T-cell responses is unknown and the use of CDN (soluble or nanoparticulate) as a cancer vaccine adjuvant has thus far been limited to only a few studies[218,219]. In our studies, dendritic cells were major consumers of liposomal CDN; actively targeting DCs could enhance vaccine efficacy. Furthermore, we observed liposomal CDN uptake to be primarily in an endocytic manner; designing endosomal escape-capable CDN delivery vehicles could enable CDN dose-sparing

7. Appendix

7.1. Appendix A: Supplementary Figures

7.1.1. Gating strategy for macrophage identification via flow cytometry

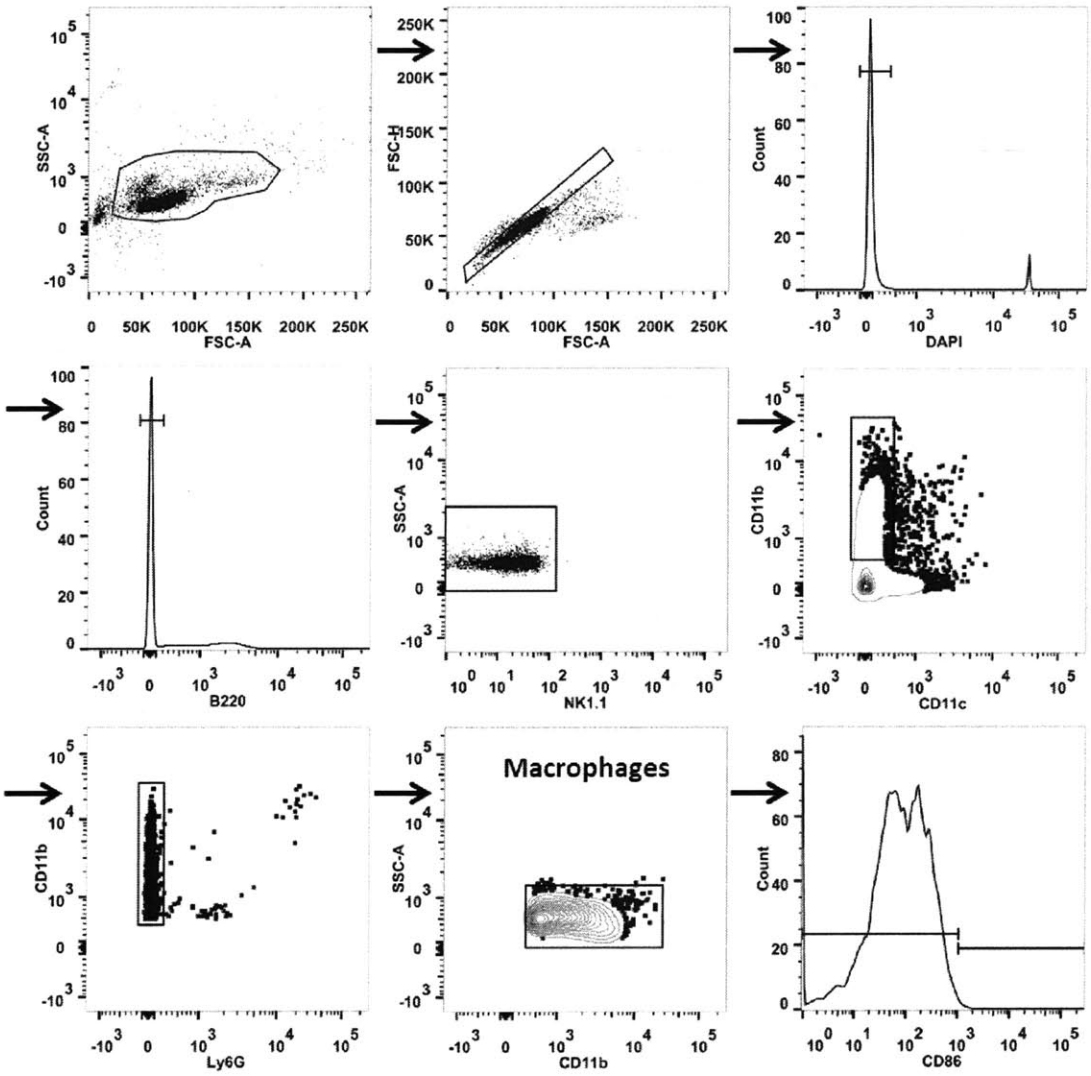

Supplemental Figure S5-1: Gating to identify lymph node macrophages.

Representative staining of naïve balb/c mice for lymph node macrophages,which were defined as B220$^-$NK1.1$^-$CD11c$^-$CD11b$^+$Ly6G$^-$SSC^{lo} of single live cells. For activation studies, CD86$^+$ macrophages were defined by histogram gating.

7.1.2. Identification of plasmacytoid dendritic cells and confirmation of plasmacytoid dendritic cell depletion *in vivo*

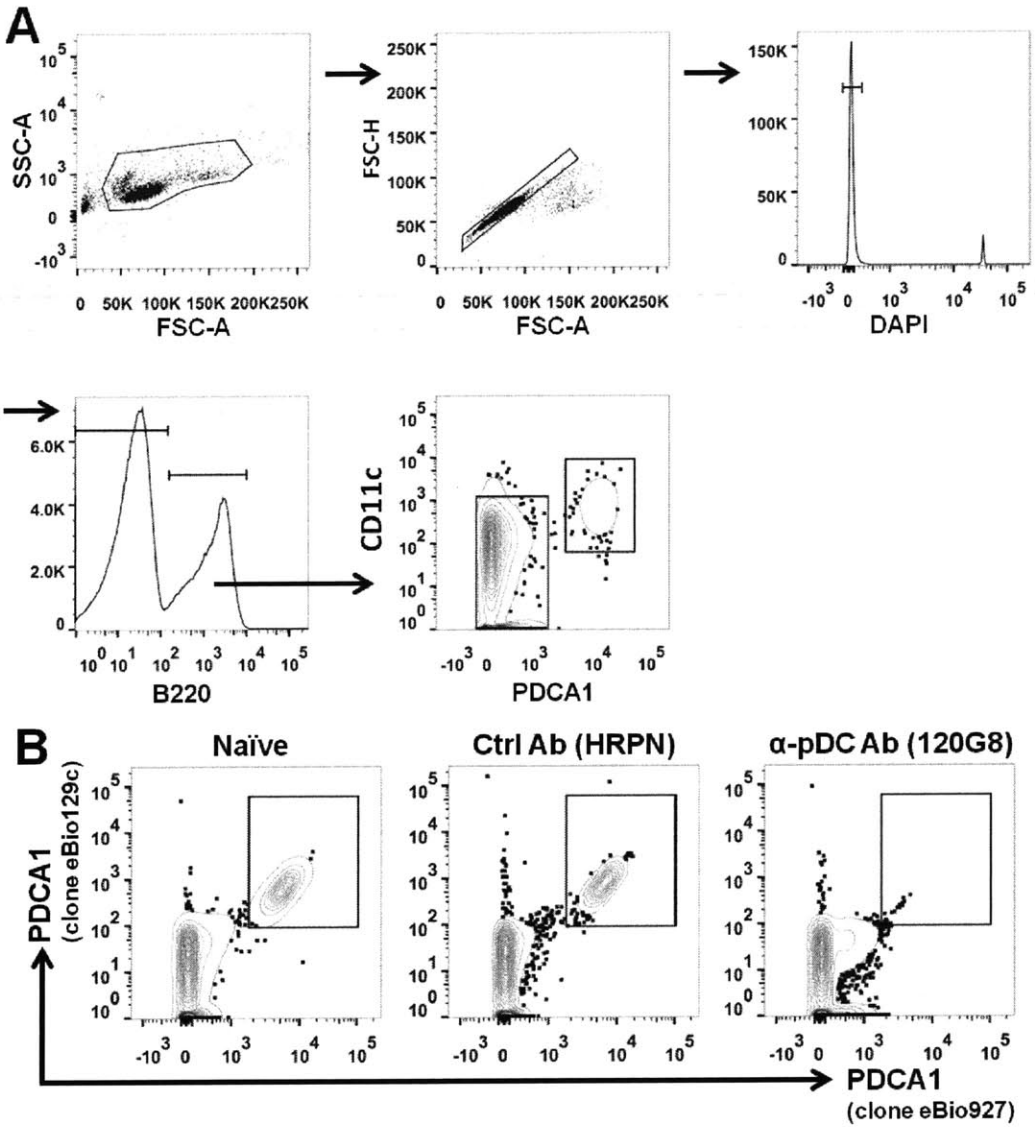

Supplemental Figure S5-2: Flow cytometry gating and depletion of plasmacytoid dendritic cells.

(A) *Representative gating of naïve balb/c mice for identification of plasmacytoid dendritic cells, which were defined as PDCA1$^+$ CD11c$^+$ of B220$^+$ of live cells of single cells of total cells. (B) Representative dual PDCA1 staining of pDCs to confirm depletion of pDCs in mice treated with 500 μg 120G8 i.p. at 24 hours prior to necropsy and staining. pDCs were defined as PDCA1(clone eBio927)$^+$ PDCA1(clone eBio129C)$^+$ of CD11c$^+$ B220$^+$ live cells.*

7.1.3. Stability of palm-MPER on liposomes

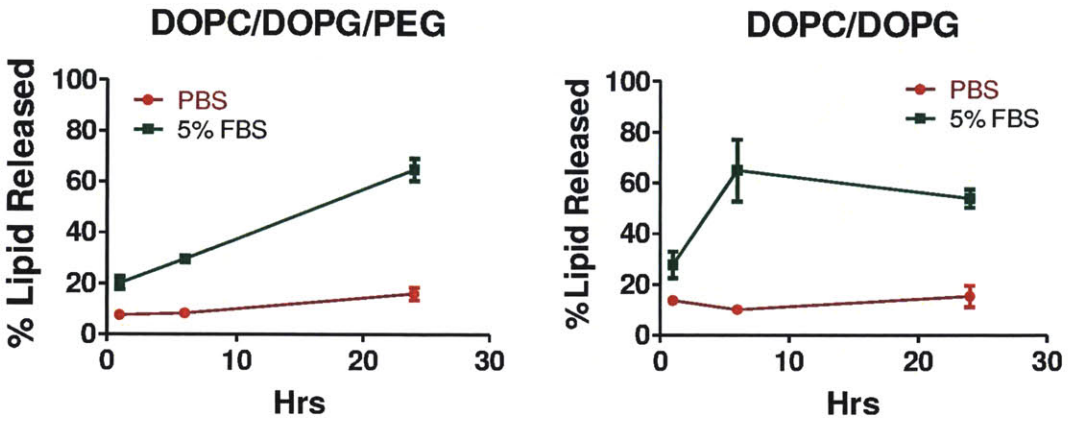

Supplemental Figure S6-1: Kinetics of palm-MPER loss from liposomes.

4:1 DOPC/DOPG liposomes with or without 10% DSPE-PEG loaded with a FITC-labeled palm-MPER were incubated at 37°C in PBS or PBS containing 5% fetal bovine serum (FBS). Although initially stable, by 24 hours most of the palm-MPER is lost from either liposome formulation, although the presence of PEG delays this loss.

7.2. Appendix B: Protocols

Although not comprehensive, the protocols included here are techniques developed in this thesis work that are not currently used by other members in the Irvine lab, but could foreseeably be useful in the future. Please don't hesitate to contact me with any questions or clarifications about these procedures.

7.2.1. ELISA to quantify the loading of ovalbumin on liposomes

1. Coat wells of MAXIsorp NUNC plates with 100 uL/well of 10ug/mL α-chick egg albumin Ab (Sigma A6075, Clone OVA-14). Incubate O/N at RT.
2. Empty plates, add 300 uL/well of PBS 1% BSA. Incubate for at least 2 hrs at RT.
3. Now these plates can be sealed and stored until use.
4. Set up sample dilutions in a V-bottom plate. (Typically 1:100 initial diluation and 4x serial dilution.)
5. Prep 2 sets of serially diluted OVA at 1000 ng/mL as initial dilution for standard.

6. Wash α-OVA-coated plates 4x. Transfer 100 uL/well of sample dilutions to each plate. Incubate 1 hour @ RT. Don't rotate.
7. Wash 4x. Add 100 uL/well of 1:5000 α-ovalbumin-HRP (from Abcam) in PBS 1% BSA. Incubate 45 mins.
8. Wash 4x. Add 100 uL/well of TMB. Incubate 20 min.
    1. Stop TMB development with 50 uL H_2SO_4. Read absorbance on plate reader at 450 nm, with background at 540 nm.
9. For surface-displayed ova on liposomes, it's unnecessary to use a surfactant (eg Tween 20 or Trition-100) to disrupt the liposomes prior to this ELISA. However, if quantifying an encapsulated protein, use of a surfactant is essential. Be sure to also include the surfactant in the serial dilution buffer and ova-standard buffer to account for possible signal alteration due to surfactant presence.

7.2.2. ELISA for the detection of anti-gp120 (4G) antibodies

1. Coat wells of MAXIsorp NUNC plates with 100 uL/well of poly-L-Lysine (Sigma, cat. no. P0879) at 0.5 mg/mL in PBS. Rotate for 4 hrs @ RT (or O/N)
2. Empty plates, add 200 uL/well of PBS 1% BSA. Incubate O/N @ 4°C.
3. Now these plates can be stored wrapped until use.
4. Wash 4x, add 100 uL of 50 nM 4G gp120 (no Fc group). Rotate 2 hours at RT.
5. Meanwhile, set up serum dilutions.
6. Wash peptide-coated plates 4x. Transfer 100 uL/well of serum dilutions to each plate. Incubate 1.5 hours @ RT.
7. Wash 4x. Add 100 uL/well of 1:5000 α-mouse IgG-HRP in PBS 1% BSA. Incubate 1 hour.
8. Wash 4x. Add 100 uL/well of TMB. (Common stock in the door of MCH fridge.) Incubate 20 min. If you have more than 4 plates, stagger the addition of TMB by 2 mins each. Keep the plates in wash buffer till right before the TMB addition.
9. Stop TMB development with 50 uL H_2SO_4. Read absorbance on plate reader at 450 nm, with background at 540 nm.

7.2.3. ELISA to quantify the loading of gp120 on liposomes

1. Coat wells of MAXIsorp NUNC plates with 2.5 ug/mL mouse B12 (anti-gp120) antibody in PBS for four hours. (Mouse-B12 was produced by Jordi Mata-Fink, Wittrup Lab.)
2. Block overnight with PBS 1% BSA.

3. Prep serial dilutions of gp120-liposome samples as well as standard gp120 protein (starting at 20 nM).
4. Wash mB12 plates 4x, add 100 uL/well of serial dilutions. Incubate 1 hr at RT.
5. Wash 4x, incubate 45 mins with 1:2000 anti-his HRP at RT, 100 ul/well.
6. Wash 4x. Add 100 uL/well of TMB. Incubate 20 min.
7. Stop TMB development with 50 uL H_2SO_4. Read absorbance on plate reader at 450 nm, with background at 540 nm.

7.2.4. ELISA to determine VCR01-competition ability of anti-gp120 sera

8. Coat wells of MAXIsorp NUNC plates with 100 uL/well of poly-L-Lysine (Sigma Aldrich, cat. no. P8954) at 0.5 mg/mL in PBS. Block, 4G @ 50nm, rotate for 2 hrs @ 4°C (or O/N)
9. Empty plates, add 200 uL/well of PBS 1% BSA. Incubate O/N @ 4°C.
10. Now these plates can be stored wrapped until use.
11. Wash 4x, add 100 uL of 50 nM 4G gp120 (no Fc group). Rotate 2 hours at RT.
12. Set up 1:100 serum dilutions for each sample. Best to do in duplicate if possible. Include serum from naïve mice as well.
13. Wash 4G-coated plates 4x. Transfer 100 uL/well of serum dilutions to 4G-coated plates. Incubate 1.5 hours @ RT. Do not rotate.
14. Empty plates (don't wash), and add 100 uL/well of 50 nM VRC01 in PBS 1% BSA
15. Incubate for 1 hour at room temp, do not rotate.
16. Wash 4x. Add 100 uL/well of 1:5000 α-human-Fc-IgG-HRP in PBS 1% BSA (which detects VRC01 binding). Incubate 1 hr.
17. Wash 4x. Add 100 uL/well of TMB. Incubate 20 min.
18. Stop TMB development with 50 uL H_2SO_4. Read absorbance on plate reader at 450 nm, with background at 540 nm.
19. Divide absorbance signal per each sample by the average naïve serum signal (represents 100% binding) to determine the fraction of competed VCR01 binding.

7.2.5. UV-based quantification of CDN encapsulation efficiency into liposomes

Background: Although it's possible to detect cyclic dinucleotides via HPLC, we were unable to entirely remove trace lipids from the supernatant of Airfuge-pelleted liposomes, and found that these trace lipids over time built up in C18 columns, resulting in unreliable CDN peaks and were extremely difficult to remove from the columns. Therefore, we developed this method to quantify the encapsulation of CDN in liposomes via basic UV spectroscopy. The peak absorbance for c-di-GMP is 254 nm, and we found there is a

slight shift in signal due to lipid presence. Thus, this method first determines the amount of lipid present in the CDN liposome supernatant and then adds this amount of lipid to the CDN standard curve, thus standardizing the signal due to lipid presence. Due to variance in centrifugation efficacy via Airfuge, it is important to measure the lipid presence each time CDN liposomes are prepped.

Preparation of Standard Lipids

1. Prepare plain liposome batch (10 mg total lipid) – 2:2:1 DOPC:DMPC:DOPG with 5% DSPE-PEG. Resuspend in 1200 uL PBS and synthesize as normally.
2. Airfuge liposomes for 30 mins and collect and store supernatant.
3. Prepare and store lipid standard curve (dilutions of supernatant) in PBS: 100%, 75%, 50%, 20%, 10%, and 0% lipid supernatant in PBS.

Sample processing

1. Airfuge CDN liposomes for 1 hr. Measure initial volume (V1), supernatant volume (V2) and final CDN liposome volume (V3).
2. Add 80ul of CDN sup to cuvette, as well as 80ul of each standard from lipid standard curve.
3. Measure UV at 350nm.
4. Open UV template on excel and plot lipid standard curve. This template can be found on the DUMAS server: IRVINELAB – PROTOCOLS – Melissa.
5. Fill CDN UV and copy linear equation from fit on corresponding cell.
6. Under "vol" a number will appear, corresponding to the amount of plain liposome supernatant necessary to add to each standard to have the same lipid concentration as CDN supernatant.
7. Prepare 60, 40, 30, 20 and 10 ug/ml CDN standards. Take "volume of standard to add" from Excel sheet and add it to "vol" of plain liposome supernatant.
8. Prepare two 10x dilutions of CDN supernatant in PBS.
9. Transfer 80ul of samples and standards to cuvettes.
10. Read UV 254nm.
11. Add standard curve values on excel sheet, fill in CDN sup values and copy equation from linear fit of plot.
12. Make sure to fill in V1, V2, V3, and update original ug of CDN added, as well as mice needed to immunize to get final volumes needed.

8. References

1. UNAIDS. *GLOBAL REPORT: UNAIDS report on the global AIDS epidemic 2013. UNAIDS* 198 (2013). doi:JC2502/1/E

2. UNAIDS. *AIDS by the numbers*. 12 (2013).

3. UNAIDS. *Access to antiretroviral therapy in Africa: status report on progress towards the 2015 targets*. (2013).

4. 10 greatest public health achievements of the 20th century. *U.S. Cent. Dis. Control Prev.* (2008). at <http://www.cdc.gov/about/history/tengpha.htm>

5. Zhou, F. *et al.* Economic evaluation of the 7-vaccine routine childhood immunization schedule in the United States, 2001. *Arch. Pediatr. Adolesc. Med.* **159,** 1136–44 (2005).

6. White, C. C., Koplan, J. P. & Orenstein, W. a. Benefits, risks and costs of immunization for measles, mumps and rubella. *Am. J. Public Health* **75,** 739–44 (1985).

7. Zolla-Pazner, S. A critical question for HIV vaccine development: Which antibodies to induce? *Science (80-.).* **345,** 167–168 (2014).

8. Virgin, H. W. & Walker, B. D. Immunology and the elusive AIDS vaccine. *Nature* **464,** 224–31 (2010).

9. McCoy, L. E. & Weiss, R. A. Neutralizing antibodies to HIV-1 induced by immunization. *J. Exp. Med.* **210,** 209–23 (2013).

10. Walker, B. D. & Burton, D. R. Toward an AIDS vaccine. *Science* **320,** 760–4 (2008).

11. Haynes, B. & Shattock, R. Critical issues in mucosal immunity for HIV-1 vaccine development. *J. Allergy Clin. Immunol.* **122,** 3–11 (2008).

12. Balazs, A. B. *et al.* Antibody-based protection against HIV infection by vectored immunoprophylaxis. *Nature* **481,** 1–6 (2011).

13. McElrath, M. J. & Haynes, B. F. Induction of immunity to human immunodeficiency virus type-1 by vaccination. *Immunity* **33,** 542–54 (2010).

14. Trkola, a *et al.* Human monoclonal antibody 2G12 defines a distinctive neutralization epitope on the gp120 glycoprotein of human immunodeficiency virus type 1. *J. Virol.* **70,** 1100–8 (1996).

15. Ofek, G. *et al.* Structure and Mechanistic Analysis of the Anti-Human Immunodeficiency Virus Type 1 Antibody 2F5 in Complex with Its gp41 Epitope. *Test* **78,** 10724–10737 (2004).

16. Nelson, J. D. *et al.* An affinity-enhanced neutralizing antibody against the membrane-proximal external region of human immunodeficiency virus type 1 gp41 recognizes an epitope between those of 2F5 and 4E10. *J. Virol.* **81,** 4033–43 (2007).

17. Cardoso, R. *et al.* Broadly neutralizing anti-HIV antibody 4E10 recognizes a helical conformation of a highly conserved fusion-associated motif in gp41. *Immunity* **22,** 163–173 (2005).

18. Burton, D. R. *et al.* Efficient neutralization of primary isolates of HIV-1 by a recombinant human monoclonal antibody. *Science* **266,** 1024–7 (1994).

19. Burton, D. R. *et al.* A large array of human monoclonal antibodies to type 1 human immunodeficiency virus from combinatorial libraries of asymptomatic seropositive individuals. *Proc. Natl. Acad. Sci. U. S. A.* **88,** 10134–7 (1991).

20. Li, Y. *et al.* Mechanism of neutralization by the broadly neutralizing HIV-1 monoclonal antibody VRC01. *J. Virol.* (2011). doi:10.1128/JVI.00754-11

21. Zhou, T. *et al.* Structural Basis for Broad and Potent Neutralization of HIV-1 by Antibody VRC01. *Science (80-.).* **329,** 811–817 (2010).

22. Kwong, P. D. *et al.* HIV-1 evades antibody-mediated neutralization through conformational masking of receptor-binding sites. *Nature* **420,** 678–682 (2002).

23. Mascola, J. R. & Montefiori, D. C. The role of antibodies in HIV vaccines. *Annu. Rev. Immunol.* **28,** 413–44 (2010).

24. Scheid, J. F. *et al.* Broad diversity of neutralizing antibodies isolated from memory B cells in HIV-infected individuals. *Nature* **458,** 636–40 (2009).

25. Huang, C. *et al.* Structural basis of tyrosine sulfation and VH-gene usage in antibodies that recognize the HIV type 1 coreceptor-binding site on gp120. *Proc. Natl. Acad. Sci. U. S. A.* **101,** 2706–11 (2004).

26. Van Kaer, L., Parekh, V. V & Wu, L. Invariant natural killer T cells: bridging innate and adaptive immunity. *Cell Tissue Res.* 43–55 (2010). doi:10.1007/s00441-010-1023-3

27. Gavin, A. L. *et al.* Adjuvant-enhanced antibody responses in the absence of toll-like receptor signaling. *Science* **314,** 1936–8 (2006).

28. Meyer-Bahlburg, A., Khim, S. & Rawlings, D. J. B cell intrinsic TLR signals amplify but are not required for humoral immunity. *J. Exp. Med.* **204,** 3095–101 (2007).

29. Reed, S. G., Bertholet, S., Coler, R. N. & Friede, M. New horizons in adjuvants for vaccine development. *Trends Immunol.* **30,** 23–32 (2009).

30. Walker, L. M. *et al.* Broad and potent neutralizing antibodies from an African donor reveal a new HIV-1 vaccine target. *Science* **326,** 285–9 (2009).

31. Wack, A. & Rappuoli, R. Vaccinology at the beginning of the 21st century. *Curr. Opin. Immunol.* **17,** 411–8 (2005).

32. Guy, B. The perfect mix: recent progress in adjuvant research. *Nat. Rev. Microbiol.* **5,** 505–17 (2007).

33. Reed, S. G., Orr, M. T. & Fox, C. B. Key roles of adjuvants in modern vaccines. *Nat. Med.* **19,** 1597–608 (2013).

34. Pitisuttithum, P. *et al.* Efficacy Trial of a Bivalent Recombinant Glycoprotein 120 HIV-1 Vaccine among Injection Drug Users in Bangkok , Thailand. *Vaccine* (2006).

35. Petrovsky, N. & Aguilar, J. C. Vaccine adjuvants: current state and future trends. *Immunol. Cell Biol.* **82,** 488–96 (2004).

36. Fox, C. B. & Haensler, J. An update on safety and immunogenicity of vaccines containing emulsion-based adjuvants. *Expert Rev. Vaccines* **12,** 747–58 (2013).

37. Kawai, T. & Akira, S. Toll-like Receptors and Their Crosstalk with Other Innate Receptors in Infection and Immunity. *Immunity* **34,** 637–50 (2011).

38. Rhee, E. G. & Barouch, D. H. Translational Mini-Review Series on Vaccines for HIV: Harnessing innate immunity for HIV vaccine development. *Clin. Exp. Immunol.* **157,** 174–80 (2009).

39. Garçon, N. & Van Mechelen, M. Recent clinical experience with vaccines using MPL- and QS-21-containing adjuvant systems. *Expert Rev. Vaccines* **10,** 471–86 (2011).

40. Bershteyn, A. *et al.* Robust IgG responses to nanograms of antigen using a biomimetic lipid-coated particle vaccine. *J. Control. Release* **157,** 354–65 (2012).

41. Moon, J. J. *et al.* Interbilayer-crosslinked multilamellar vesicles as synthetic vaccines for potent humoral and cellular immune responses. *Nat. Mater.* **10,** 243–251 (2011).

42. Dubensky, T. W., Kanne, D. B. & Leong, M. L. Rationale, progress and development of vaccines utilizing STING-activating cyclic dinucleotide adjuvants. *Ther. Adv. vaccines* **1,** 131–143 (2013).

43. Higgins, S. C. & Mills, K. H. G. TLR, NLR Agonists, and Other Immune Modulators as Infectious Disease Vaccine Adjuvants. *Curr. Infect. Dis. Rep.* **12,** 4–12 (2010).

44. Römling, U., Galperin, M. Y. & Gomelsky, M. Cyclic di-GMP: the first 25 years of a universal bacterial second messenger. *Microbiol. Mol. Biol. Rev.* **77,** 1–52 (2013).

45. Ablasser, A. *et al.* cGAS produces a 2'-5'-linked cyclic dinucleotide second messenger that activates STING. *Nature* **498,** 380–4 (2013).

46. Wu, J. *et al.* Cyclic GMP-AMP is an endogenous second messenger in innate immune signaling by cytosolic DNA. *Science* **339,** 826–30 (2013).

47. Sun, L., Wu, J., Du, F., Chen, X. & Chen, Z. J. Cyclic GMP-AMP synthase is a cytosolic DNA sensor that activates the type I interferon pathway. *Science* **339,** 786–91 (2013).

48. Ishikawa, H. & Barber, G. N. STING is an endoplasmic reticulum adaptor that facilitates innate immune signalling. *Nature* **455,** 674–8 (2008).

49. Woodward, J. J., Iavarone, A. T. & Portnoy, D. A. c-di-AMP secreted by intracellular Listeria monocytogenes activates a host type I interferon response. *Science* **328,** 1703–5 (2010).

50. Burdette, D. L. *et al.* STING is a direct innate immune sensor of cyclic di-GMP. *Nature* **478,** 515–8 (2011).

51. Bachmann, M. F. & Jennings, G. T. Vaccine delivery: a matter of size, geometry, kinetics and molecular patterns. *Nat. Rev. Immunol.* **10,** 787–796 (2010).

52. Kovacsovics-Bankowski, M., Clark, K., Benacerraf, B. & Rock, K. L. Efficient major histocompatibility complex class I presentation of exogenous antigen upon phagocytosis by macrophages. *Proc. Natl. Acad. Sci. U. S. A.* **90,** 4942–6 (1993).

53. Harding, C. V & Song, R. Phagocytic processing of exogenous particulate antigens by macrophages for presentation by class I MHC molecules. *J. Immunol.* **153,** 4925–33 (1994).

54. Manolova, V. *et al.* Nanoparticles target distinct dendritic cell populations according to their size. *Eur. J. Immunol.* **38,** 1404–13 (2008).

55. Ghasparian, A. *et al.* Engineered synthetic virus-like particles and their use in vaccine delivery. *Chembiochem* **12,** 100–9 (2011).

56. Watson, D. S., Platt, V. M., Cao, L., Venditto, V. J. & Szoka, F. C. Antibody response to polyhistidine-tagged peptide and protein antigens attached to liposomes via lipid-linked nitrilotriacetic acid in mice. *Clin. Vaccine Immunol.* **18,** 289–97 (2011).

57. Hoffmann, P. R. *et al.* Interaction between phosphatidylserine and the phosphatidylserine receptor inhibits immune responses in vivo. *J. Immunol.* **174,** 1393–404 (2005).

58. Pihlgren, M. *et al.* TLR4- and TRIF-dependent stimulation of B lymphocytes by peptide liposomes enables T cell-independent isotype switch in mice. *Blood* **121,** 85–94 (2013).

59. Taneichi, M. *et al.* Antigen chemically coupled to the surface of liposomes are cross-presented to CD8+ T cells and induce potent antitumor immunity. *J. Immunol.* **177,** 2324–30 (2006).

60. Fifis, T. *et al.* Size-dependent immunogenicity: therapeutic and protective properties of nano-vaccines against tumors. *J. Immunol.* **173,** 3148–54 (2004).

61. Titta, A. De *et al.* Nanoparticle conjugation of CpG enhances adjuvancy for cellular immunity and memory recall at low dose. *Proc. Natl. Acad. Sci.* **110,** 19902–19907 (2013).

62. Kasturi, S. P. *et al.* Programming the magnitude and persistence of antibody responses with innate immunity. *Nature* **470,** 543–547 (2011).

63. Krishnamachari, Y., Geary, S. M., Lemke, C. D. & Salem, A. K. Nanoparticle Delivery Systems in Cancer Vaccines. *Pharm. Res.* 215–236 (2010). doi:10.1007/s11095-010-0241-4

64. Peek, L. J., Middaugh, C. R. & Berkland, C. Nanotechnology in vaccine delivery. *Adv. Drug Deliv. Rev.* **60,** 915–28 (2008).

65. Felnerova, D., Viret, J.-F., Glück, R. & Moser, C. Liposomes and virosomes as delivery systems for antigens, nucleic acids and drugs. *Curr. Opin. Biotechnol.* **15,** 518–29 (2004).

66. Wang, B.-Z. *et al.* Incorporation of high levels of chimeric human immunodeficiency virus envelope glycoproteins into virus-like particles. *J. Virol.* **81,** 10869–78 (2007).

67. Poon, B., Hsu, J. F., Gudeman, V. & Chen, I. S. Y. Formaldehyde-Treated , Heat-Inactivated Virions with Increased Human Immunodeficiency Virus Type 1 Env Can Be Used To Induce High-Titer Neutralizing Antibody Responses. *Society* **79,** 10210–10217 (2005).

68. Allison, A. & Gregoriadis, G. Liposomes as immunological adjuvants. *Nature1* **252,** (974).

69. Dos, N. *et al.* Influence of poly (ethylene glycol) grafting density and polymer length on liposomes : Relating plasma circulation lifetimes to protein binding. *Lipids* **1768,** 1367 – 1377 (2007).

70. Henriksen-Lacey, M., Korsholm, K. S., Andersen, P., Perrie, Y. & Christensen, D. Liposomal vaccine delivery systems. *Expert Opin. Drug Deliv.* **8,** 505–519 (2011).

71. J.F, C. *et al.* Recombinant Liver Stage Antigen-1 (LSA-1) formulated with AS01 or AS02 is safe, elicits high titer antibody, and induces IFN-γ/IL-2 CD4+ T cells but does not protect against experimental Plasmodium falciparum infection. *Vaccine* **28,** 5135–5144 (2010).

72. Partnership, S. C. T. Efficacy and Safety of the RTS,S/AS01 Malaria Vaccine during 18 Months after Vaccination: A Phase 3 Randomized, Controlled Trial in Children and Young Infants at 11 African Sites. *PLoS Med.* **11,** e1001685 (2014).

73. Leroux-Roels, I., Lerouz-Roels, G. & Voss, G. Strong and persisten CD4+ T-cell response in healthy adults immunized with a candidate HIV-1 vaccine containing gp120, Nef and Tat antigens formulated in three adjuvant systems. *Vaccine* **28,** 7016–7024 (2010).

74. Song, L. *et al.* Broadly neutralizing anti-HIV-1 antibodies disrupt a hinge-related function of gp41 at the membrane interface. *Proc. Natl. Acad. Sci. U. S. A.* **106,** 9057–62 (2009).

75. Adamina, M. *et al.* Encapsulation into sterically stabilised liposomes enhances the immunogenicity of melanoma-associated Melan-A/MART-1 epitopes. *Br. J. Cancer* **90,** 263–9 (2004).

76. Li, W. M., Dragowska, W. H., Bally, M. & Schutze-Redelmeier, M.-P. Effective induction of CD8+ T-cell response using CpG oligodeoxynucleotides and HER-2/neu-derived peptide co-encapsulated in liposomes. *Vaccine* **21,** 3319–3329 (2003).

77. Ignatius, R. *et al.* Presentation of proteins encapsulated in sterically stabilized liposomes by dendritic cells initiates CD8(+) T-cell responses in vivo. *Blood* **96,** 3505–13 (2000).

78. Singh, S. K. & Bisen, P. S. Adjuvanticity of stealth liposomes on the immunogenicity of synthetic gp41 epitope of HIV-1. *Vaccine* **24,** 4161–4166 (2006).

79. Kanzler, H., Barrat, F. J., Hessel, E. M. & Coffman, R. L. Therapeutic targeting of innate immunity with Toll-like receptor agonists and antagonists. *Nat. Med.* **13,** 552–9 (2007).

80. Fredenberg, S., Wahlgren, M., Reslow, M. & Axelsson, A. The mechanisms of drug release in poly(lactic-co-glycolic acid)-based drug delivery systems--a review. *Int. J. Pharm.* **415,** 34–52 (2011).

81. Jiang, W., Gupta, R. K., Deshpande, M. C. & Schwendeman, S. P. Biodegradable poly(lactic-co-glycolic acid) microparticles for injectable delivery of vaccine antigens. *Adv. Drug Deliv. Rev.* **57,** 391–410 (2005).

82. Gupta, R., Singh, M. & O'Hagan, D. Poly(lactide-co-glycolide) microparticles for the development of single-dose controlled-release vaccines. *Adv. Drug Deliv. Rev.* **32,** 225–246 (1998).

83. Fu, K., Pack, D. W., Klibanov, a M. & Langer, R. Visual evidence of acidic environment within degrading poly(lactic-co-glycolic acid) (PLGA) microspheres. *Pharm. Res.* **17,** 100–6 (2000).

84. Richards, R. L. *et al.* Liposomes containing lipid A serve as an adjuvant for induction of antibody and cytotoxic T-cell responses against RTS,S malaria antigen. *Infect. Immun.* **66,** 2859–65 (1998).

85. Tamauchi, H., Tadakuma, T., Yasuda, T., Tsumita, T. & Saito, K. Enhancement of immunogenicity by incorporation of lipid A into liposomal model membranes and its application to membrane-associated antigens. *Immunology* **50,** 605–12 (1983).

86. Jewell, C. M., López, S. C. B. & Irvine, D. J. In situ engineering of the lymph node microenvironment via intranodal injection of adjuvant-releasing polymer particles. *Proc. Natl. Acad. Sci. U. S. A.* **108,** 15745–50 (2011).

87. Westwood, A., Elvin, S. J., Healey, G. D., Williamson, E. D. & Eyles, J. E. Immunological responses after immunisation of mice with microparticles containing antigen and single stranded RNA (polyuridylic acid). *Vaccine* **24,** 1736–43 (2006).

88. Schlosser, E. *et al.* TLR ligands and antigen need to be coencapsulated into the same biodegradable microsphere for the generation of potent cytotoxic T lymphocyte responses. *Vaccine* **26,** 1626–37 (2008).

89. Jain, S., O'Hagan, D. T. & Singh, M. The long-term potential of biodegradable poly(lactide-co-glycolide) microparticles as the next-generation vaccine adjuvant. *Expert Rev. Vaccines* **10,** 1731–42 (2011).

90. Bershteyn, A. *et al.* Polymer-supported lipid shells, onions, and flowers. *Soft Matter* **4,** 1787–1791 (2008).

91. Moon, J. *et al.* Antigen-displaying lipid-enveloped PLGA nanoparticles as delivery agents for a Plasmodium vivax malaria vaccine. *PloS oneP* **7,** e31472 (2012).

92. Bershteyn, A. Lipid-coated micro- and nanoparticles as a biomimetic vaccine delivery platform. 1–164 (2010).

93. Hanson, M. C., Bershteyn, A., Crespo, M. P. & Irvine, D. J. Antigen delivery by lipid-enveloped PLGA microparticle vaccines mediated by in situ vesicle shedding. *Biomacromolecules* **15,** 2475–81 (2014).

94. Iden, D. L. & Allen, T. M. In vitro and in vivo comparison of immunoliposomes made by conventional coupling techniques with those made by a new post-insertion approach. *Biochim. Biophys. Acta - Biomembr.* **1513,** 207–216 (2001).

95. Damen, J. A. N., Regts, J. & Scherphof, G. Transfer and Exchange of Phospholipid between Small Unilamellar Liposomes and Rat Plasma High Density Lipoproteins. *Biochim. Biophys. Acta* **665,** 538–545 (1981).

96. Allen, T. M. A study of phospholipid interactions between high-density lipoproteins and small unilamellar vesicles. *Biochim. Biophys. Acta* **640,** 385–97 (1981).

97. Zborowski, J., Roerdink, F. & Scherphof, G. Leakage of sucrose from phosphatidylcholine liposomes induced by interaction with serum albumin. *Biochim. Biophys. Acta* **497,** 183–191 (1977).

98. Phillips, M. C., Johnson, W. J. & Rothblat, G. H. Mechanisms and consequences of cellular cholesterol exchange and transfer. *Biochemistry* **906,** 223–276 (1987).

99. Kirby, C., Clarke, J. & Gregoriadis, G. CHOLESTEROL CONTENT OF SMALL UNILAMELLAR LIPOSOMES CONTROLS PHOSPHOLIPID LOSS TO HIGH DENSITY LIPOPROTEINS IN THE PRESENCE OF SERUM. *FEBS Lett.* **111,** (1980).

100. Massey, J. B., Gotto, A. M. & Pownall, H. J. Kinetics and Mechanism of the Spontaneous Transfer of Fluorescent Phosphatidylcholines between Apoplipoprotein-Phospholipid Recombinants. *Biochemistry* **21,** 3630–3636 (1982).

101. Kirby, C., Clarke, J. & Gregoriadis, G. Effect of the cholesterol content of small unilamellar liposomes on their stability in vivo and in vitro. *Biochem. J.* **186,** 591–8 (1980).

102. Silvius, J. Role of cholesterol in lipid raft formation: lessons from lipid model systems. *Biochim. Biophys. Acta - Biomembr.* **1610,** 174–183 (2003).

103. Karmakar, S., Sarangi, B. R. & Raghunathan, V. a. Phase behaviour of lipid–cholesterol membranes. *Solid State Commun.* **139,** 630–634 (2006).

104. Watson, D. S., Endsley, A. N. & Huang, L. Design considerations for liposomal vaccines: influence of formulation parameters on antibody and cell-mediated immune responses to liposome associated antigens. *Vaccine* **30,** 2256–72 (2012).

105. Nkolola, J. P. *et al.* Breadth of neutralizing antibodies elicited by stable, homogeneous clade A and clade C HIV-1 gp140 envelope trimers in guinea pigs. *J. Virol.* **84,** 3270–9 (2010).

106. Kovacs, J. M. *et al.* HIV-1 envelope trimer elicits more potent neutralizing antibody responses than monomeric gp120. *Proc. Natl. Acad. Sci. U. S. A.* **109,** 12111–6 (2012).

107. Sattentau, Q. Envelope Glycoprotein Trimers as HIV-1 Vaccine Immunogens. *Vaccines* **1,** 497–512 (2013).

108. Mata-Fink, J. Engineering of HIV gp120 by yeast surface display for neutralizing antibody characterization and immunogen design. 1–147 (2013).

109. Mata-Fink, J. *et al.* Rapid conformational epitope mapping of anti-gp120 antibodies with a designed mutant panel displayed on yeast. *J. Mol. Biol.* **425,** 444–56 (2013).

110. Marrack, P., McKee, A. S. & Munks, M. W. Towards an understanding of the adjuvant action of aluminium. *Nat. Rev. Immunol.* **9,** 287–93 (2009).

111. Janda, K. D. & Treweek, J. B. Vaccines targeting drugs of abuse: is the glass half-empty or half-full? *Nat. Rev. Immunol.* **12,** 67–72 (2012).

112. Elgueta, R. *et al.* Molecular mechanism and function of CD40/CD40L engagement in the immune system. *Immunol. Rev.* **229,** 152–72 (2009).

113. Oyewumi, M. O., Kumar, A. & Cui, Z. Nano-microparticles as immune adjuvants: correlating particle sizes and the resultant immune responses. *Expert Rev. Vaccines* **9,** 1095–107 (2010).

114. Anderson, K. P. *et al.* Effect of dose and immunization schedule on immune response of baboons to recombinant glycoprotein 120 of HIV-1. *J. Infect. Dis.* **160,** 960–9 (1989).

115. Ledgerwood, J. E. *et al.* Prime-boost interval matters: a randomized phase 1 study to identify the minimum interval necessary to observe the H5 DNA influenza vaccine priming effect. *J. Infect. Dis.* **208,** 418–22 (2013).

116. Wu, X. *et al.* Rational design of envelope identifies broadly neutralizing human monoclonal antibodies to HIV-1. *Science* **329,** 856–61 (2010).

117. Muster, T. *et al.* A conserved neutralizing epitope on gp41 of human immunodeficiency virus type 1. *J. Virol.* **67,** 6642–6647 (1993).

118. Zwick, M. B. *et al.* Broadly neutralizing antibodies targeted to the membrane-proximal external region of human immunodeficiency virus type 1 glycoprotein gp41. *J. Virol.* **75,** 10892–905 (2001).

119. Stiegler, G. *et al.* A potent cross-clade neutralizing human monoclonal antibody against a novel epitope on gp41 of human immunodeficiency virus type 1. *AIDS Res. Hum. Retroviruses* **17,** 1757–65 (2001).

120. Huang, J. *et al.* Broad and potent neutralization of HIV-1 by a gp41-specific human antibody. *Nature* **491,** 406–12 (2012).

121. Sun, Z.-Y. J. *et al.* HIV-1 broadly neutralizing antibody extracts its epitope from a kinked gp41 ectodomain region on the viral membrane. *Immunity* **28,** 52–63 (2008).

122. Kim, M. *et al.* Antibody mechanics on a membrane-bound HIV segment essential for GP41-targeted viral neutralization. *Nat. Struct. Mol. Biol.* **18,** 1235–43 (2011).

123. Montero, M., van Houten, N. E., Wang, X. & Scott, J. K. The membrane-proximal external region of the human immunodeficiency virus type 1 envelope: dominant site of antibody neutralization and target for vaccine design. *Microbiol. Mol. Biol. Rev.* **72,** 54–84 (2008).

124. Gach, J. S., Leaman, D. P. & Zwick, M. B. Targeting HIV-1 gp41 in close proximity to the membrane using antibody and other molecules. *Curr. Top. Med. Chem.* **11,** 2997–3021 (2011).

125. Coëffier, E. *et al.* Antigenicity and immunogenicity of the HIV-1 gp41 epitope ELDKWA inserted into permissive sites of the MalE protein. *Vaccine* **19,** 684–93 (2000).

126. Correia, B. E. *et al.* Computational design of epitope-scaffolds allows induction of antibodies specific for a poorly immunogenic HIV vaccine epitope. *Structure* **18,** 1116–26 (2010).

127. Law, M., Cardoso, R. M. F., Wilson, I. a & Burton, D. R. Antigenic and immunogenic study of membrane-proximal external region-grafted gp120 antigens by a DNA prime-protein boost immunization strategy. *J. Virol.* **81,** 4272–85 (2007).

128. Ofek, G. *et al.* Elicitation of structure-specific antibodies by epitope scaffolds. *Proc. Natl. Acad. Sci. U. S. A.* **107,** 17880–7 (2010).

129. Kim, M., Qiao, Z., Yu, J., Montefiori, D. & Reinherz, E. L. Immunogenicity of recombinant human immunodeficiency virus type 1-like particles expressing gp41 derivatives in a pre-fusion state. *Vaccine* **25,** 5102–14 (2007).

130. Kamdem Toukam, D. *et al.* Targeting antibody responses to the membrane proximal external region of the envelope glycoprotein of human immunodeficiency virus. *PLoS One* **7,** e38068 (2012).

131. Pastori, C. *et al.* Virus like particle based strategy to elicit HIV-protective antibodies to the alpha-helic regions of gp41. *Virology* **431,** 1–11 (2012).

132. Matyas, G. R. *et al.* Neutralizing antibodies induced by liposomal HIV-1 glycoprotein 41 peptide simultaneously bind to both the 2F5 or 4E10 epitope and lipid epitopes. *AIDS* **23,** 2069–77 (2009).

133. Zhang, J. *et al.* Modulation of nonneutralizing HIV-1 gp41 responses by an MHC-restricted TH epitope overlapping those of membrane proximal external region broadly neutralizing antibodies. *J. Immunol.* **192,** 1693–706 (2014).

134. Dennison, S. M. *et al.* Induction of Antibodies in Rhesus Macaques That Recognize a Fusion-Intermediate Conformation of HIV-1 gp41. *PLoS One* **6,** e27824 (2011).

135. Venditto, V. J., Watson, D. S., Motion, M., Montefiori, D. & Szoka, F. C. Rational design of membrane proximal external region lipopeptides containing chemical modifications for HIV-1 vaccination. *Clin. Vaccine Immunol.* **20,** 39–45 (2013).

136. Kim, M. *et al.* Immunogenicity of membrane-bound HIV-1 gp41 membrane-proximal external region (MPER) segments is dominated by residue accessibility and modulated by stereochemistry. *J. Biol. Chem.* **288,** 31888–901 (2013).

137. Watson, D. S. & Szoka, F. C. Role of lipid structure in the humoral immune response in mice to covalent lipid-peptides from the membrane proximal region of HIV-1 gp41. *Vaccine* **27,** 4672–83 (2009).

138. Liu, H. *et al.* DNA-based micelles: synthesis, micellar properties and size-dependent cell permeability. *Chemistry* **16,** 3791–7 (2010).

139. Alving, C. R., Rao, M., Steers, N. J., Matyas, G. R. & Mayorov, A. V. Liposomes containing lipid A: an effective, safe, generic adjuvant system for synthetic vaccines. *Expert Rev. Vaccines* **11,** 733–44 (2012).

140. Libanova, R., Becker, P. D. & Guzmán, C. a. Cyclic di-nucleotides: new era for small molecules as adjuvants. *Microb. Biotechnol.* **5,** 168–76 (2012).

141. Shu, C., Yi, G., Watts, T., Kao, C. C. & Li, P. Structure of STING bound to cyclic di-GMP reveals the mechanism of cyclic dinucleotide recognition by the immune system. *Nat. Struct. Mol. Biol.* **19,** 722–4 (2012).

142. Madhun, A. S. *et al.* Intranasal c-di-GMP-adjuvanted plant-derived H5 influenza vaccine induces multifunctional Th1 CD4+ cells and strong mucosal and systemic antibody responses in mice. *Vaccine* **29,** 4973–82 (2011).

143. Dos Santos, N. *et al.* Influence of poly(ethylene glycol) grafting density and polymer length on liposomes: relating plasma circulation lifetimes to protein binding. *Biochim. Biophys. Acta* **1768,** 1367–77 (2007).

144. Bestman-Smith, J., Gourde, P., Désormeaux, A., Tremblay, M. J. & Bergeron, M. G. Sterically stabilized liposomes bearing anti-HLA-DR antibodies for targeting the primary cellular reservoirs of HIV-1. *Biochim. Biophys. Acta - Biomembr.* **1468,** 161–174 (2000).

145. Moghimi, S. M. The effect of methoxy-PEG chain length and molecular architecture on lymph node targeting of immuno-PEG liposomes. *Biomaterials* **27,** 136–44 (2006).

146. Oussoren, C., Zuidema, J., Crommelin, D. J. A. & Storm, G. Lymphatic uptake and biodistribution of liposomes after subcutaneous injection. II. Influence of liposomal size, lipid composition and lipid dose. *Biochim. Biophys. Acta - Biomembr.* **1328,** 261–272 (1997).

147. Dancey, G. F., Yasuda, T. & Kinsky, S. C. Effect of liposomal model membrane composition on immunogenicity. *J. Immunol.* **120,** 1109–13 (1978).

148. Bakouche, O. & Gerlier, D. Enhancement of immunogenicity of tumour virus antigen by liposomes: the effect of lipid composition. *Immunology* **58,** 507–13 (1986).

149. Puffer, E. B., Pontrello, J. K., Hollenbeck, J. J., Kink, J. A. & Kiessling, L. L. Activating B cell signaling with defined multivalent ligands. *ACS Chem. Biol.* **2,** 252–62 (2007).

150. Lazarski, C. A. *et al.* The kinetic stability of MHC class II:peptide complexes is a key parameter that dictates immunodominance. *Immunity* **23,** 29–40 (2005).

151. Dai, G., Steede, N. K. & Landry, S. J. Allocation of helper T-cell epitope immunodominance according to three-dimensional structure in the human immunodeficiency virus type I envelope glycoprotein gp120. *J. Biol. Chem.* **276,** 41913–20 (2001).

152. Koff, W. C. *et al.* Accelerating next-generation vaccine development for global disease prevention. *Science* **340,** 1232910 (2013).

153. Rappuoli, R., Mandl, C. W., Black, S. & De Gregorio, E. Vaccines for the twenty-first century society. *Nat. Rev. Immunol.* **11,** 865–72 (2011).

154. Coffman, R. L., Sher, A. & Seder, R. A. Vaccine adjuvants: putting innate immunity to work. *Immunity* **33,** 492–503 (2010).

155. Karaolis, D. K. R. *et al.* Bacterial c-di-GMP Is an Immunostimulatory Molecule. *J. Immunol.* **178,** 2171–2181 (2007).

156. Ebensen, T., Schulze, K., Riese, P., Morr, M. & Guzmán, C. a. The bacterial second messenger cdiGMP exhibits promising activity as a mucosal adjuvant. *Clin. Vaccine Immunol.* **14,** 952–8 (2007).

157. Yan, H. *et al.* 3',5'-Cyclic diguanylic acid elicits mucosal immunity against bacterial infection. *Biochem. Biophys. Res. Commun.* **387,** 581–4 (2009).

158. Libanova, R. *et al.* The member of the cyclic di-nucleotide family bis-(3', 5')-cyclic dimeric inosine monophosphate exerts potent activity as mucosal adjuvant. *Vaccine* **28,** 2249–58 (2010).

159. Ebensen, T. *et al.* The bacterial second messenger cyclic diGMP exhibits potent adjuvant properties. *Vaccine* **25,** 1464–9 (2007).

160. Bosch, V. *et al.* HIV pseudovirion vaccine exposing Env "fusion intermediates"-response to immunisation in human CD4/CCR5-transgenic rats. *Vaccine* **27,** 2202–12 (2009).

161. Hu, D.-L. *et al.* c-di-GMP as a vaccine adjuvant enhances protection against systemic methicillin-resistant Staphylococcus aureus (MRSA) infection. *Vaccine* **27,** 4867–73 (2009).

162. Gray, P. M. *et al.* Evidence for cyclic diguanylate as a vaccine adjuvant with novel immunostimulatory activities. *Cell. Immunol.* **278,** 113–9 (2012).

163. Harrison, L. I., Astry, C., Kumar, S. & Yunis, C. Pharmacokinetics of 852A, an imidazoquinoline Toll-like receptor 7-specific agonist, following intravenous, subcutaneous, and oral administrations in humans. *J. Clin. Pharmacol.* **47,** 962–9 (2007).

164. Chen, W., Kuolee, R. & Yan, H. The potential of 3',5'-cyclic diguanylic acid (c-di-GMP) as an effective vaccine adjuvant. *Vaccine* **28,** 3080–5 (2010).

165. Irvine, D. J., Swartz, M. A. & Szeto, G. L. Engineering synthetic vaccines using cues from natural immunity. *Nat. Mater.* **12,** 978–90 (2013).

166. Storni, T., Kündig, T. M., Senti, G. & Johansen, P. Immunity in response to particulate antigen-delivery systems. *Adv. Drug Deliv. Rev.* **57,** 333–55 (2005).

167. Demento, S. L. *et al.* Role of sustained antigen release from nanoparticle vaccines in shaping the T cell memory phenotype. *Biomaterials* **33,** 4957–64 (2012).

168. Moon, J. J. *et al.* Enhancing humoral responses to a malaria antigen with nanoparticle vaccines that expand Tfh cells and promote germinal center induction. *Proc. Natl. Acad. Sci. U. S. A.* **109,** 1080–5 (2012).

169. Diwan, M., Elamanchili, P., Cao, M. & Samuel, J. Dose sparing of CpG oligodeoxynucleotide vaccine adjuvants by nanoparticle delivery. *Curr. Drug Deliv.* **1,** 405–12 (2004).

170. Xie, H. *et al.* CpG oligodeoxynucleotides adsorbed onto polylactide-co-glycolide microparticles improve the immunogenicity and protective activity of the licensed anthrax vaccine. *Infect. Immun.* **73,** 828–33 (2005).

171. Coler, R. N. *et al.* A synthetic adjuvant to enhance and expand immune responses to influenza vaccines. *PLoS One* **5,** e13677 (2010).

172. Ilyinskii, P. O. *et al.* Adjuvant-carrying synthetic vaccine particles augment the immune response to encapsulated antigen and exhibit strong local immune activation without inducing systemic cytokine release. *Vaccine* **32,** 2882–95 (2014).

173. Behzad, H. *et al.* GLA-SE, a synthetic toll-like receptor 4 agonist, enhances T-cell responses to influenza vaccine in older adults. *J. Infect. Dis.* **205,** 466–73 (2012).

174. Parent, M. a *et al.* Gamma interferon, tumor necrosis factor alpha, and nitric oxide synthase 2, key elements of cellular immunity, perform critical protective functions during humoral defense against lethal pulmonary Yersinia pestis infection. *Infect. Immun.* **74,** 3381–6 (2006).

175. Teijaro, J. R. *et al.* Persistent LCMV infection is controlled by blockade of type I interferon signaling. *Science* **340,** 207–11 (2013).

176. Asselin-Paturel, C., Brizard, G., Pin, J.-J., Brière, F. & Trinchieri, G. Mouse Strain Differences in Plasmacytoid Dendritic Cell Frequency and Function Revealed by a Novel Monoclonal Antibody. *J. Immunol.* **171,** 6466–77 (2003).

177. Fletcher, A. L. *et al.* Reproducible isolation of lymph node stromal cells reveals site-dependent differences in fibroblastic reticular cells. *Front. Immunol.* **2,** 35 (2011).

178. Rose, S., Misharin, A. & Perlman, H. A novel Ly6C/Ly6G-based strategy to analyze the mouse splenic myeloid compartment. *Cytom. A.* **81,** 343–50 (2012).

179. Blume, G. & Cevc, G. Liposomes for the sustained drug release in vivo. *Biochim. Biophys. Acta* **1029,** 91–7 (1990).

180. Oussoren, C. & Storm, G. Lymphatic uptake and biodistribution of liposomes after subcutaneous injection: III. Influence of surface modification with poly(ethyleneglycol). *Pharm. Res.* **14,** 1479–1484 (1997).

181. Cai, S., Yang, Q., Bagby, T. R. & Forrest, M. L. Lymphatic drug delivery using engineered liposomes and solid lipid nanoparticles. *Adv. Drug Deliv. Rev.* **63,** 901–8 (2011).

182. Abdul-Sater, A. a *et al.* The overlapping host responses to bacterial cyclic dinucleotides. *Microbes Infect.* **14,** 188–97 (2012).

183. McWhirter, S. M. *et al.* A host type I interferon response is induced by cytosolic sensing of the bacterial second messenger cyclic-di-GMP. *J. Exp. Med.* **206,** 1899–911 (2009).

184. Crotty, S. Follicular helper CD4 T cells (TFH). *Annu. Rev. Immunol.* **29,** 621–63 (2011).

185. Alving, C. R. & Rao, M. Lipid A and liposomes containing lipid A as antigens and adjuvants. *Vaccine* **26,** 3036–45 (2008).

186. Garaude, J., Kent, A., van Rooijen, N. & Blander, J. M. Simultaneous targeting of toll- and nod-like receptors induces effective tumor-specific immune responses. *Sci. Transl. Med.* **4,** 120ra16 (2012).

187. Napolitani, G., Rinaldi, A., Bertoni, F., Sallusto, F. & Lanzavecchia, A. Selected Toll-like receptor agonist combinations synergistically trigger a T helper type 1-polarizing program in dendritic cells. *Nat. Immunol.* **6,** 769–76 (2005).

188. Cella, M. *et al.* Plasmacytoid monocytes migrate to inflamed lymph nodes and produce large amounts of type I interferon. *Nat. Med.* **5,** 919–23 (1999).

189. Siegal, F. P. The Nature of the Principal Type 1 Interferon-Producing Cells in Human Blood. *Science (80-.).* **284,** 1835–1837 (1999).

190. Swiecki, M. *et al.* Type I interferon negatively controls plasmacytoid dendritic cell numbers in vivo. *J. Exp. Med.* **208,** 2367–74 (2011).

191. Blaauboer, S. M., Gabrielle, V. D. & Jin, L. MPYS/STING-mediated TNF-α, not type I IFN, is essential for the mucosal adjuvant activity of (3'-5')-cyclic-di-guanosine-monophosphate in vivo. *J. Immunol.* **192,** 492–502 (2014).

192. Simon, A. *et al.* Concerted action of wild-type and mutant TNF receptors enhances inflammation in TNF receptor 1-associated periodic fever syndrome. *Proc. Natl. Acad. Sci. U. S. A.* **107,** 9801–6 (2010).

193. Ouyang, S. *et al.* Structural analysis of the STING adaptor protein reveals a hydrophobic dimer interface and mode of cyclic di-GMP binding. *Immunity* **36,** 1073–86 (2012).

194. Li, X.-D. *et al.* Pivotal roles of cGAS-cGAMP signaling in antiviral defense and immune adjuvant effects. *Science* **341,** 1390–4 (2013).

195. Ogunniyi, A. D. *et al.* c-di-GMP is an effective immunomodulator and vaccine adjuvant against pneumococcal infection. *Vaccine* **26,** 4676–85 (2008).

196. Ebensen, T. *et al.* Bis-(3',5')-cyclic dimeric adenosine monophosphate: strong Th1/Th2/Th17 promoting mucosal adjuvant. *Vaccine* **29,** 5210–20 (2011).

197. McLennan, D. N., Porter, C. J. H. & Charman, S. a. Subcutaneous drug delivery and the role of the lymphatics. *Drug Discov. Today. Technol.* **2,** 89–96 (2005).

198. Walder, P. *et al.* Pharmacokinetic profile of the immunomodulating compound adamantylamide dipeptide (AdDP), a muramyl dipeptide derivative in mice. *Immunopharmacol. Immunotoxicol.* **13,** 101–19 (1991).

199. Kulkarni, R. R. *et al.* Activation of RIG-I pathway during influenza vaccination enhances germinal center reactions, T follicular helper cell induction and, provides dose-sparing effect and protective immunity. *J. Virol.* (2014). doi:10.1128/JVI.02273-14

200. Smirnov, D., Schmidt, J. J., Capecchi, J. T. & Wightman, P. D. Vaccine adjuvant activity of 3M-052: An imidazoquinoline designed for local activity without systemic cytokine induction. *Vaccine* **29,** 5434–42 (2011).

201. Liu, H. *et al.* Structure-based programming of lymph-node targeting in molecular vaccines. *Nature* **507,** 519–22 (2014).

202. Křupka, M. *et al.* Enhancement of immune response towards non-lipidized Borrelia burgdorferi recombinant OspC antigen by binding onto the surface of metallochelating nanoliposomes with entrapped lipophilic derivatives of norAbuMDP. *J. Control. Release* **160,** 374–81 (2012).

203. Wu, C. C. N. *et al.* Immunotherapeutic activity of a conjugate of a Toll-like receptor 7 ligand. *Proc. Natl. Acad. Sci. U. S. A.* **104,** 3990–5 (2007).

204. Wille-Reece, U. *et al.* HIV Gag protein conjugated to a Toll-like receptor 7/8 agonist improves the magnitude and quality of Th1 and CD8+ T cell responses in nonhuman primates. *Proc. Natl. Acad. Sci. U. S. A.* **102,** 15190–4 (2005).

205. Barker, J. R. *et al.* STING-Dependent Recognition of Cyclic di-AMP Mediates Type I Interferon Responses during Chlamydia trachomatis Infection. *MBio* **4,** 1–11 (2013).

206. Spörri, R. & Reis e Sousa, C. Inflammatory mediators are insufficient for full dendritic cell activation and promote expansion of CD4+ T cell populations lacking helper function. *Nat. Immunol.* **6,** 163–70 (2005).

207. Desch, A. N. *et al.* Dendritic cell subsets require cis-activation for cytotoxic CD8 T-cell induction. *Nat. Commun.* **5,** 4674 (2014).

208. Cucak, H., Yrlid, U., Reizis, B., Kalinke, U. & Johansson-Lindbom, B. Type I interferon signaling in dendritic cells stimulates the development of lymph-node-resident T follicular helper cells. *Immunity* **31,** 491–501 (2009).

209. Bon, A. Le *et al.* Type I Interferons Potently Enhance Humoral Immunity and Can Promote Isotype Switching by Stimulating Dendritic Cells In Vivo. *Immunity* **14,** 461–470 (2001).

210. Pasparakis, M., Alexopoulou, L., Episkopou, V. & Kollias, G. Immune and inflammatory responses in TNF alpha-deficient mice: a critical requirement for TNF alpha in the formation of primary B cell follicles, follicular dendritic cell networks and germinal centers, and in the maturation of the humoral immune response. *J. Exp. Med.* **184,** 1397–411 (1996).

211. Waterhouse, D. N., Tardi, P. G., Mayer, L. D. & Bally, M. B. A Comparison of Liposomal Formulations of Doxorubicin with Drug Administered in Free Form Changing Toxicity Profiles. *Drug Saf.* **24,** 903–920 (2001).

212. Friede, M., Muller, S., Briand, J.-P., Van Regenmortel, M. H. V. & Schuber, F. Induction of immune response against a short synthetic peptide antigen coupled to small neutral liposomes containing monophosphoryl lipid a. *Mol. Immunol.* **30,** 539–547 (1993).

213. Tewari, K. *et al.* Poly(I:C) is an effective adjuvant for antibody and multi-functional CD4+ T cell responses to Plasmodium falciparum circumsporozoite protein (CSP) and αDEC-CSP in non human primates. *Vaccine* **28,** 7256–66 (2010).

214. Park, H. *et al.* Polyinosinic-polycytidylic acid is the most effective TLR adjuvant for SIV Gag protein-induced T cell responses in nonhuman primates. *J. Immunol.* **190,** 4103–15 (2013).

215. Caskey, M. *et al.* Synthetic double-stranded RNA induces innate immune responses similar to a live viral vaccine in humans. *J. Exp. Med.* **208,** 2357–66 (2011).

216. Shirota, H. & Klinman, D. M. Recent progress concerning CpG DNA and its use as a vaccine adjuvant. *Expert Rev. Vaccines* **13,** 299–312 (2014).

217. Purcell, A. W., McCluskey, J. & Rossjohn, J. More than one reason to rethink the use of peptides in vaccine design. *Nat. Rev. Drug Discov.* **6,** 404–14 (2007).

218. Chandra, D. *et al.* STING Ligand c-di-GMP Improves Cancer Vaccination against Metastatic Breast Cancer. *Cancer Immunol. Res.* **2,** 901–910 (2014).

219. Miyabe, H. *et al.* A new adjuvant delivery system "cyclic di-GMP/YSK05 liposome" for cancer immunotherapy. *J. Control. Release* **184,** 20–7 (2014).